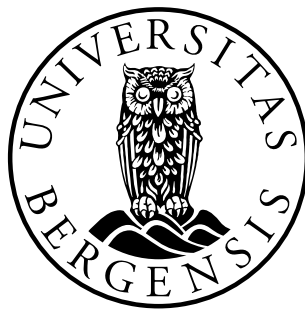


# A Golden-Channel Higgs Decay



Anders Haarr

Department of Physics and Technology

University of Bergen

Master's Thesis in Theoretical Particle Physics

June 2011

---

## Acknowledgements

First and foremost I would like to thank my supervisor Professor Per Osland. Your tolerance and patience with regards to proof-reading and my repeatedly naive questions is nothing short of astounding. I believe it is safe to say that this thesis would never have been finished without you. I also want to thank you for three wonderful courses, two good years and for sharing some of your vast knowledge in physics.

In addition I would like to thank Anders Kvellestad, Eivind Farestveit Larsen, Siri Fløgstad Svensson and Ørjan Dale for putting up with me for five years.

There are also a vast number of wonderful people at the physics institute in Bergen whom should be mentioned. Particuly the ones at the third floor. Thank you.

Lastly I would like to thank my family and friends for constant support and for knowing when to push me into doing anything worthwhile.

Anders Haarr

---

# Contents

<b>1</b>	<b>Introduction</b>	<b>1</b>
1.1	The Standard Model and Particle Physics Today . . . . .	1
<b>2</b>	<b>The experimental situation</b>	<b>3</b>
2.1	Decays . . . . .	3
2.2	Higgs Boson and my Thesis Approach . . . . .	4
2.3	Statistical fluctuation . . . . .	6
2.4	Possible explanations . . . . .	8
2.4.1	SM Higgs + new physics . . . . .	8
2.4.2	Other Higgs mechanism + new physics . . . . .	8
2.4.3	No Higgs . . . . .	8
2.5	A general restriction . . . . .	9
<b>3</b>	<b>The Standard Model</b>	<b>11</b>
3.1	Quantum fields and Lagrangians . . . . .	11
3.2	The gauge principle . . . . .	12
3.3	Mass and renormalizability . . . . .	18
3.4	Higgs mechanism . . . . .	19
3.4.1	Spontaneous Symmetry Breaking . . . . .	19
3.4.2	The Higgs Model . . . . .	22
3.4.3	Weinberg-Salam model . . . . .	25
<b>4</b>	<b>Electroweak Precision Tests</b>	<b>27</b>

## CONTENTS

---

<b>5</b>	<b>A New <math>Z'</math> Gauge Boson?</b>	<b>33</b>
5.1	A Neutral, Massive Gauge Boson $Z'$ . . . . .	33
5.2	Quark-parton model and deep-inelastic scattering . . . . .	34
5.3	Cross section at parton and proton level . . . . .	35
5.4	The amplitude for $Z'$ production . . . . .	38
5.5	Landau-Yang Theorem and its Generalization . . . . .	43
5.6	Amplitude for $ZZ$ production . . . . .	48
5.7	Production cross sections . . . . .	51
5.7.1	Production cross section for $Z'$ . . . . .	52
5.7.2	Production cross section for $ZZ$ . . . . .	55
5.8	Limits and experimental constraints . . . . .	57
<b>6</b>	<b>A Scalar Signature</b>	<b>61</b>
6.1	The SM Higgs in the Golden Channel . . . . .	61
6.2	The Two-Higgs-Doublet Model . . . . .	64
6.2.1	The 2HDM Potential . . . . .	65
6.2.2	Yukawa Couplings . . . . .	66
6.2.3	A 2HDM(II) Example . . . . .	67
6.3	Neutral Higgs Couplings and Higgs Production . . . . .	68
6.4	Experimental restrictions on $\tan\beta$ . . . . .	71
6.5	Enhancing $ZZ$ production . . . . .	75
6.6	Possible Limits . . . . .	77
<b>7</b>	<b>Kaluza-Klein Theories and the Graviton</b>	<b>81</b>
7.1	What are Kaluza-Klein Theories? . . . . .	82
7.2	ADD, Large Extra Dimensions . . . . .	85
7.3	RS, a warped geometry . . . . .	86
7.4	Phenomenology . . . . .	88
<b>8</b>	<b>Technicolor</b>	<b>91</b>
8.1	Hierarchy problem . . . . .	92
8.2	Composite Higgs and Dynamical Electroweak Symmetry Breaking . . . . .	94
8.2.1	Toy model . . . . .	95
8.2.2	Minimal Technicolor . . . . .	97

## CONTENTS

---

8.3	Beyond the minimal Technicolor . . . . .	99
8.3.1	Extended Technicolor . . . . .	100
8.3.2	Walking Technicolor . . . . .	102
8.3.3	Pseudo-Goldstone bosons . . . . .	104
8.4	Phenomenology . . . . .	105
<b>9</b>	<b>Conclusion</b>	<b>107</b>
	<b>References</b>	<b>109</b>

## CONTENTS

---

# Chapter 1

## Introduction

### 1.1 The Standard Model and Particle Physics Today

There are four known fundamental forces in nature: Electromagnetism, the weak and strong nuclear forces and gravity. The three first are described by the Standard Model of Particle Physics (SM), while the latter is described by the General Theory of Relativity (GR). GR is used to describe large-scale phenomena like the distribution of matter in a galaxy, or whether or not a supernova will collapse into a black hole. On the other hand we have the SM, which describes phenomena on the smallest scales. As accelerators reach higher energies and can probe smaller distances, one expects that something new will appear. Whether this will end up with a unification of the SM and GR, a revision of the standard model or something else entirely, still remains to be seen. In the framework of the SM there are also several reasons to suspect new physics at higher energy scales.

The thesis will concern itself with a hypothetical experimental observation. We will assume that the observation cannot be encompassed in the SM Higgs mechanism. This means that we have to look elsewhere for explanations. The objective throughout the thesis will be to look at theories beyond the Standard Model that can explain the experimental observation. Theories we will consider include a new neutral gauge boson,  $Z'$  [1], the 2HDM [2], Technicolor[3] and extra-dimensional theories like ADD [4] and Randall-Sundrum [5]. To state the objective of the thesis more clearly we need to go through the experimental situation in some detail. This is the purpose of the next

## 1. INTRODUCTION

---

chapter. The observation concerns an unknown state or particle decaying.

## Chapter 2

# The experimental situation

In this section the hypothetical experimental situation is described. The thesis is meant to be self-contained, so I will try to always describe the basic ideas and quantities I am using.

### 2.1 Decays

After a particle is created it can break up into other particles (i.e. decay). The type of particles that it can decay to is constrained by conservation laws. For instance, if the decaying particle is electrically neutral, the other particles must have a total charge of zero. If you specify which particles it decays to, it is called a decay mode or decay channel. A decay mode of the Higgs boson is  $H \rightarrow ZZ$ . This decay channel will be a main theme in this thesis.

For different values of the Higgs-boson mass, it decays to different particles with different rates. The quantity used to characterize this is called the decay rate. The way one does calculations in quantum field theory is by specifying initial and final states and then do a lot of maths. To calculate the total decay rate, one specifies the initial state as the decaying particle (e.g. Higgs) and sums over all possible decay products (e.g.  $ZZ$  or  $W^+ W^-$  etc.). More specifically:

The differential decay rate of a particle P with four-momentum  $p = (E, \mathbf{p})$  decaying to  $N$  particles with four-momenta  $p_f = (E_f, \mathbf{p}_f)$  is given by [6]:

## 2. THE EXPERIMENTAL SITUATION

---

$$d\Gamma = (2\pi)^4 \delta^{(4)}(\Sigma p_f - p) \frac{1}{2E} \left( \prod_l (2m_l) \right) \left( \prod_f \frac{d^3 \mathbf{p}_f}{(2\pi)^3 2E_f} \right) |\mathcal{M}|^2 \quad (2.1)$$

The index  $f$  stands for “final” and refers to the outgoing particles. The decay rate is then obtained by performing the phase-space integrals over the three-momenta. If we label each of the different final states by  $r$ , we can write the total decay rate as

$$\Gamma_{\text{tot}} = \sum_r \Gamma_r \quad (2.2)$$

Here, the index  $r$  must not be confused with the index  $f$  that labels the final particles for a given  $r$ . There are two other important quantities that are derived from the above ones. First off the lifetime of a particle is defined as:

$$\tau = \frac{1}{\Gamma_{\text{tot}}} \quad (2.3)$$

Secondly, there is a quantity called the branching ratio. The branching ratio describes how much one mode contributes to the total decay. It is defined as

$$B_r = \frac{\Gamma_r}{\Gamma_{\text{tot}}} \quad (2.4)$$

The branching ratio will also be denoted as  $BR(\text{initial state} \rightarrow \text{state } r)$

### 2.2 Higgs Boson and my Thesis Approach

If we knew the mass of the Higgs boson we would know all couplings in the Standard Model. Specifically, we would know the  $\lambda$  parameter which pops up in the quartic term of the Higgs potential, see (3.46). An observation of the Higgs particle should then, along with the assumption that the Standard Model is correct, enable us to calculate the physical observables for any process. As mentioned, different values of the Higgs mass would give different decay rates and branching ratios. In Figure 2.1 we see a plot of branching ratios for different values of the Higgs mass. The thesis will be mainly concerned with the region from 190-220 GeV, where decay to  $ZZ$  and  $W^+ W^-$  dominates. I will look at the specific decay channel.

$$H \rightarrow ZZ \rightarrow 4 \text{ leptons} \quad (2.5)$$

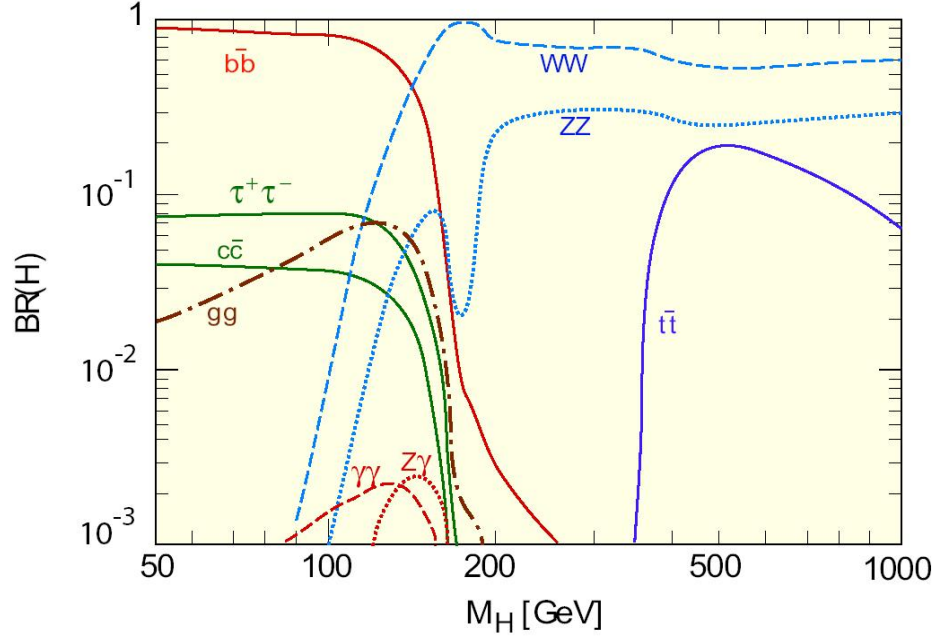


Figure 2.1: Higgs branching ratio, [7]

This channel is often called the golden channel for heavy (i.e.  $\geq 190$  GeV) Higgs detection. The reason is that it has a low background, meaning that a standard model Higgs boson would stand out. My thesis approach is roughly: We see some state or particle decaying but we see more than we would expect. What can it be? More precisely:

We observe 4 leptons out of which we reconstruct a  $ZZ$ -pair (i.e. each lepton pair came from a decaying  $Z$ ). The  $ZZ$ -pair originates from the same point, has an invariant mass round 200 GeV, but the production rate exceeds the theoretically expected value. Could such an observation be encompassed in any version of the Higgs mechanism? If not, what else could it be?

To be clear, theoretical expectations include:

1. Contributions from a Higgs with the mass equal to the  $ZZ$ -pair's invariant mass
2. Other SM diagrams with  $ZZ \rightarrow 4$  leptons final state

## 2. THE EXPERIMENTAL SITUATION

---

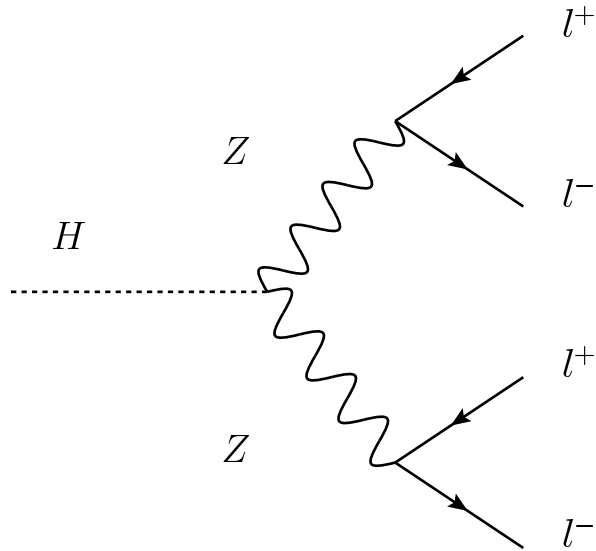


**Figure 2.2:** Higgs contribution to the process  $H \rightarrow ZZ \rightarrow 4$

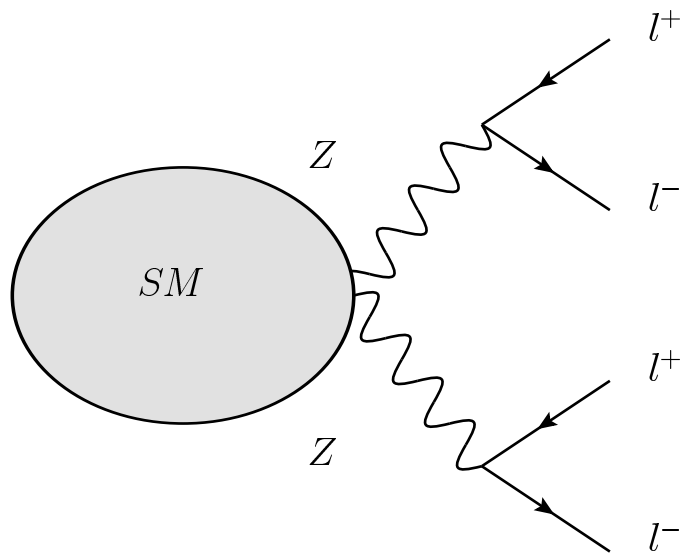


**Figure 2.3:** Other SM contributions to the process  $H \rightarrow ZZ \rightarrow 4$

The Feynman diagrams of the contributions are shown in Figures 2.2 and 2.3. Before categorizing possible explanations, we will go through a calculation of the probability that it's just a statistical fluctuation.

### 2.3 Statistical fluctuation

Before doing the calculation we need some basic definitions. The expected number of events from a particular process is the product of the luminosity and the cross section for that process,

$$\langle N \rangle = L\sigma_r \tag{2.6}$$

The cross section  $\sigma_r$  is a quantity describing the likelihood of an interaction taking place. The decay formula shown above is analogous to the cross section formula, but for decay calculations you only have one initial particle. The cross section is the product of two things: The phase-space factor and the dynamical factor (determined by the Feynman amplitude). The phase-space factor incorporates the different configurations the system can end up in, while the amplitude encodes the physics of the specific interaction. The amplitude is obtained after specifying initial and final states. The cross section has units of area.

On the other hand you have the luminosity, which is a machine-dependent quantity. It can be thought of as how many particles go through some unit area per second<sup>1</sup>. The product of the luminosity and the cross section is a number describing the expected number of events per second. There is also the concept of integrated luminosity. The luminosity is a time-dependent function and we usually need to know the time integral of this function. This tells us how many particles have had a chance to interact in the total time the experiment has been running.

To get the expected number of events we do the following: Integrate the luminosity from start of the experiment till end and then multiply it with the cross section for the initial and final states we specified. An easy example is: If one runs the accelerator for an hour with constant luminosity, the expected number of events will be 3600 as

---

<sup>1</sup>Particle flux

## 2. THE EXPERIMENTAL SITUATION

---

many as if you would run it for one second.

Under the assumptions that the parent particle is the Higgs boson and that the Standard Model is correct we can now calculate the cross section for any process. We then multiply it with the integrated luminosity and get the expected number of events. Let us denote the theoretically expected number of events for this process by  $N_{4l}^{\text{th}}$ . The next step is to recognise that we have an expected number of occurrences (events) in a fixed interval (dataset), making the Poisson distribution applicable. The probability distribution function for the Poisson distribution with  $x$  denoting the number of events is:

$$P(X = x) = \frac{N_{4l}^{\text{th}x}}{x!} e^{-N_{4l}^{\text{th}}} \quad (2.7)$$

Our situation is one observation in the dataset. So  $P(X = 1) = N_{4l}^{\text{th}} e^{-N_{4l}^{\text{th}}}$  is the probability for having one such observation in the dataset. The probability for observing one or more events (called p-value in statistics) is:

$$P(X \geq 1) = 1 - e^{-N_{4l}^{\text{th}}} \quad (2.8)$$

### 2.4 Possible explanations

For a low value of the probability, it is highly unlikely that our observation can be explained by the Standard Model alone. We will therefore assume that this probability is low in the remainder of the thesis. Different explanations can be divided into the three following categories

1. SM Higgs + New Physics
2. Other Higgs mechanism + New Physics
3. No Higgs

This is of course a rough categorization, but it will give us something to relate the different theories to. The key idea is that we somehow have to enhance the  $ZZ$  production rate. Here follows a short explanation of each category:

### 2.4.1 SM Higgs + new physics

Assume that the Higgs of the Standard Model is correct. We would now have to explain the excess in the cross section by some new physics. Examples that I will go through include: A new neutral gauge boson  $Z'$  coupling to the  $Z$  boson or a graviton decaying to  $ZZ$ . Both these mechanisms could enhance the production rate.

### 2.4.2 Other Higgs mechanism + new physics

A different version of the Higgs mechanism could give us larger freedom in adjusting the Higgs coupling to the  $Z$  boson. An example is the 2HDM where we have more free parameters to adjust in the Yukawa couplings [2]. In addition to this we could include the above-mentioned examples of a  $Z'$  or a graviton decaying.

### 2.4.3 No Higgs

There are theories that do not make use of the Higgs mechanism. An example of this is Technicolor which generates masses for the  $Z$  and  $W$  bosons by introducing new gauge interactions. The main problem with Technicolor is that Electroweak Precision Measurements easily come into conflict with the theory. The possible candidates to enhance the  $ZZ$  cross section are composite particles similar to ordinary vectormesons, called technivectormesons.

## 2.5 A general restriction

If we are to explain the observation by some new particle decaying, we can say something about its spin. Since the particle decays to two  $Z$  bosons with intrinsic spin 1, the parent particle can (by addition of angular momentum) have spin 0, 1 or 2. This gives us another way of thinking about the possible explanations. Spin 0 corresponds to the Higgs mechanism (e.g SM or 2HDM), spin 1 could be a new gauge boson or the technipions and technirhos, while spin 2 would be a graviton decaying.

Enhancing the cross section for  $ZZ$  production with a particle,  $X$  ( $M_X \sim 200$  GeV) of spin 0, 1 or 2 that decays, can be laid out as follows: The cross section is,

$$\sigma(pp \rightarrow X \rightarrow ZZ \rightarrow 4l) \tag{2.9}$$

## 2. THE EXPERIMENTAL SITUATION

---

which can be written

$$\sigma(pp \rightarrow X) \times BR(X \rightarrow ZZ) \times BR^2(Z \rightarrow 2l) \quad (2.10)$$

The branching ratio of  $Z \rightarrow 2l$  is well known, so the alternatives left are:

1. Increase the production cross section  $\sigma(pp \rightarrow X)$
2. Increase the branching ratio  $X \rightarrow ZZ$
3. Increase both of the above

Before discussing this any further, we go through some relevant SM theory.

## Chapter 3

# The Standard Model

Here I will go through the parts of the Standard Model that will be needed later on. I will assume that the reader is familiar with some quantum field theory and Lagrangian mechanics. First I will give a brief overview of the theoretical framework, then we will look at the gauge principle and finish with a discussion of the Higgs mechanism. The content of this section is largely based on [6], [8] and [9].

### 3.1 Quantum fields and Lagrangians

The Standard Model's basic quantities are called quantum fields. They are abstract quantities that we use to calculate physical observables. There are basically three different types of fields needed to describe fermions and bosons. The spin  $\frac{1}{2}$  field (Dirac field), the spin 1 field (vector field) and the spin 0 field (scalar field). We construct the quantum fields out of a procedure called "second quantization", where we start out with classical fields defined by their equations of motion. Each classical field is Fourier expanded. The coefficients in the expansion are turned into creation and annihilation operators by imposing commutation and anticommutation relations. The spin-half field carries with it spinors and the spin-1 field four vectors. For each point in spacetime we now have operators that create and annihilate particles.

We can compare the classical fields in field theory to our description of electricity and magnetism. For each point in space-time we associate either a number (scalar or spin 0), four-vector (spin 1) or spinor (spin  $\frac{1}{2}$ ). In electricity and magnetism we

### 3. THE STANDARD MODEL

---

associate a three-vector, which tells us about the strength and direction of the force a test particle would experience. Sadly we can not lay out iron filaments to get a better visualization of four vectors.

Lastly we write all the fields, appropriately combined, in the same function called the Lagrangian. It is from these fields and Lagrangians that we calculate physical observables.

Up until now we have not discussed how one decides which Lagrangian to write down. This is not an easy question to answer, because one basically has to take a guess. The Lagrangian you write down is of course checked against its experimental consequences. In modern physics there is a method of guessing Lagrangians that seems to work for several different types of theories. It's called the gauge principle. The gauge principle is interesting for two main reasons. Firstly it seems to be a unified way of guessing at interactions. Unified in the sense that one uses the same procedure for introducing interactions in QED, EW theory and the theory of the strong interactions. Secondly it is grounded in principles of symmetry which, if one looks at the history of physics, seem to be important.

In addition, there is the problem of renormalization. Physical quantities are calculated through a perturbative expansion involving the Lagrangian. When calculating to second order and more, divergent integrals appear. QED, Fermi's theory of weak interactions and EW theory are all examples of this. In QED and EW theory the divergences can be dealt with through the procedure of renormalization. In the Fermi theory this is not possible, so calculations beyond first order usually contain non-sensical infinities. We summarize this by saying that the Fermi Lagrangian is non-renormalizable. Before discussing renormalization any further, I will go through the gauge principle.

#### 3.2 The gauge principle

I will begin by showing how the gauge principle is used to get the Lagrangian density for QED. Afterwards we will see how one can implement it in EW theory. The total

QED Lagrangian is:

$$L_{QED} = \bar{\psi}(i\gamma_\mu\partial^\mu - m)\psi + e\bar{\psi}\partial_\mu A^\mu\psi - \frac{1}{4}F^{\mu\nu}F_{\mu\nu} \quad (3.1)$$

Written out explicitly the tensor in the kinetic term is:

$$F_{\mu\nu} = \partial_\nu A_\mu - A_\nu\partial_\mu \quad (3.2)$$

If we perform the coupled transformation:

$$\begin{aligned} A_\mu &\rightarrow A'_\mu(x) = A_\mu(x) + \partial_\mu f(x) \\ \psi(x) &\rightarrow \psi'(x) = \psi e^{-ief(x)} \\ \bar{\psi}(x) &\rightarrow \bar{\psi}'(x) = \bar{\psi} e^{ief(x)} \end{aligned} \quad (3.3)$$

the Lagrangian density is invariant (i.e. it looks the same before and after the transformation). This means that our adjustment of the fields  $A_\mu$  and  $\psi$  has not changed the physical content of the Lagrangian. This freedom is referred to as gauge freedom and the coupled transformation is called a  $U(1)$  gauge transformation. Above we essentially did two things: Postulated the Lagrangian and found the coupled transformation.

Now let us look at the alternate way of introducing the Lagrangian. I will illustrate the procedure with the explicit example of QED, but the steps are quite general. They are as follows:

1. Start with the free Lagrangian density

$$L_0 = \bar{\psi}(i\gamma_\mu\partial^\mu - m)\psi - \frac{1}{4}F^{\mu\nu}F_{\mu\nu}$$

2. Identify global transformations leaving  $L_0$  invariant

$$\psi(x) \rightarrow \psi'(x) = \psi e^{-ief}$$

$$\bar{\psi}(x) \rightarrow \bar{\psi}'(x) = \bar{\psi} e^{ief}$$

3. Make the global transformations local, i.e.  $f = f(x)$ . The Lagrangian is no longer invariant due to the  $\partial_\mu$  term

4. Introduce the covariant derivative (through  $\partial_\mu \rightarrow D_\mu$ ) and demand that the resulting Lagrangian is invariant under the local transformation

$$L = \bar{\psi}(i\gamma_\mu D^\mu - m)\psi$$

### 3. THE STANDARD MODEL

---

The demand that  $L$  be invariant under local transformations plus the requirement of renormalizability, makes the covariant derivative take a specific form

$$D_\mu = \partial_\mu - ieA_\mu \quad (3.4)$$

Here the introduced field transforms as

$$A'_\mu(x) = A_\mu(x) + \partial_\mu f(x) \quad (3.5)$$

under the local transformations. Finally if we write everything out:

$$L = \bar{\psi}(i\gamma_\mu D^\mu - m)\psi = \bar{\psi}(i\gamma_\mu \partial^\mu - m)\psi + e\bar{\psi}\partial_\mu A^\mu\psi = L_{QED} \quad (3.6)$$

Let us pause for a moment and summarize what has happened. Through demanding invariance of  $L$  under local transformations, we had to introduce a new field  $A_\mu$  which we call a gauge field. It is the photon field and it now couples to the Dirac field through the QED interaction term in just the right way. An interesting point here is that by enforcing invariance in the Lagrangian we had to introduce the interaction term. This was once referred to by the theoretical physicist C.N. Yang as “...The principle that symmetry dictates interaction.” [10]

When we introduce the gauge bosons of the EW theory we do it by the same procedure, but we rewrite the free Lagrangian density such that the global transformations are different. We now start with a free Lagrangian density of the form

$$L_0 = i(\bar{\psi}_l\gamma_\mu\partial^\mu\psi_l + \bar{\psi}_{\nu_l}\gamma_\mu\partial^\mu\psi_{\nu_l}) \quad (3.7)$$

The indices  $l$  and  $\nu_l$  refer to charged leptons and neutrinos respectively.  $l$  can be any one of the three generations ( $l = e, \mu, \text{ or } \tau$ ). If we define the doublet:

$$\Psi_l = \begin{pmatrix} \psi_{\nu_l} \\ \psi_l \end{pmatrix} \quad (3.8)$$

we can write the Lagrangian as

$$L_0 = \bar{\Psi}_l i\gamma_\mu \partial^\mu \Psi_l \quad (3.9)$$

We identify the global transformation leaving  $L_0$  invariant as:

$$\begin{aligned} \Psi_l(x) &\rightarrow \Psi'_l(x) = U\Psi_l(x) \\ \bar{\Psi}_l(x) &\rightarrow \bar{\Psi}'_l(x) = \bar{\Psi}_l(x)U^\dagger \\ U &= e^{\frac{-ig\sigma_j\alpha_j}{2}} \end{aligned} \quad (3.10)$$

with

$$[\sigma_i, \sigma_j] = 2i\epsilon_{ijk}\sigma_k \tag{3.11}$$

Here  $U$  is a two by two matrix with determinant 1. It is an  $SU(2)$  transformation. Since  $SU(2)$  is a simply connected group it is completely characterized by its Lie algebra. This means that every  $SU(2)$  transformation can be written as the exponential of an element of its Lie algebra. Each element of the Lie algebra can in turn be written as a linear combination of the three generators  $\sigma_j$ . An  $SU(N)$  transformation has  $N^2 - 1$  parameters needed to characterize the transformation. This will be important when we make the transformation local ( $U = U(x)$ ) and substitute the ordinary derivative for the covariant one. To enforce invariance on the Lagrangian we will need to introduce three gauge fields corresponding to the three free parameters in  $SU(2)$ . These three gauge fields are associated with the  $Z$  and  $W^\pm$ . This is also the reason for having 8 gauge fields with their associated gluons in the  $SU(3)_C$  theory of the strong interactions.

We now proceed as in the QED case:

1. Make the transformation local (i.e.  $U = U(x)$ )
2. Replacing the ordinary derivative with the covariant derivative and demanding invariance results in gauge fields

In EW theory the  $SU(2)$  transformation is implemented on such a doublet, but only with the left-handed part of the fields organized in a doublet. The total gauge group of EW theory is  $SU(2)_L \times U(1)$  which makes the total amount of gauge fields  $3 + 1 = 4$ . Two of the fields from  $SU(2)_L$  combine to give  $W^+$  and  $W^-$ , while the last  $SU(2)_L$  field and the  $U(1)$  field make up the  $Z$  and the  $\gamma$ . For the sake of completeness the mathematical steps just described will be given here and we will add the kinetic terms of the fields. If one is comfortable with these steps, feel free to skip down past (3.28) Fair warning has been given, without further ado:

We start with the free Lagrangian density

$$L_0 = \bar{\Psi}_l i\gamma_\mu \partial^\mu \Psi_l \tag{3.12}$$

### 3. THE STANDARD MODEL

---

We split the field into left and right-handed parts defined by the relations

$$\Psi_l^L = P_L \Psi_l = \frac{1}{2}(1 - \gamma_5)\Psi_l \quad (3.13)$$

$$\Psi_l^R = P_R \Psi_l = \frac{1}{2}(1 + \gamma_5)\Psi_l \quad (3.14)$$

Using the relation  $P_R + P_L = 1$  and the fact that  $\gamma_\mu$  and  $\gamma_5$  anticommute results in

$$L_0 = \overline{\Psi}_l^L i\gamma_\mu \partial^\mu \Psi_l^L + \overline{\Psi}_l^R i\gamma_\mu \partial^\mu \Psi_l^R \quad (3.15)$$

The right-handed doublet is treated differently from the left-handed one. The free Lagrangian density we will gauge is now:

$$L = \overline{\Psi}_l^L i\gamma_\mu \partial^\mu \Psi_l^L + \overline{\psi}_l^R i\gamma_\mu \partial^\mu \psi_l^R + \overline{\psi}_{\nu_l}^R i\gamma_\mu \partial^\mu \psi_{\nu_l}^R \quad (3.16)$$

The left-handed doublet is now invariant under a global  $SU(2)$  transformation (3.10). Both the doublet and singlets are invariant under a global  $U(1)$  transformation. Without further detail regarding transformation properties, here is the result of applying this procedure to (3.16).

$$L = \overline{\Psi}_l^L i\gamma_\mu D^\mu \Psi_l^L + \overline{\psi}_l^R i\gamma_\mu D^\mu \psi_l^R + \overline{\psi}_{\nu_l}^R i\gamma_\mu D^\mu \psi_{\nu_l}^R \quad (3.17)$$

The different covariant derivatives are:

$$D^\mu \Psi_l^L = [\partial^\mu - ig\sigma_j W_j^\mu / 2 + ig' B^\mu / 2] \Psi_l^L \quad (3.18)$$

$$D^\mu \psi_l^R = [\partial^\mu + ig' B^\mu] \psi_l^R \quad (3.19)$$

$$D^\mu \psi_{\nu_l}^R = \partial^\mu \psi_{\nu_l}^R \quad (3.20)$$

As mentioned the  $B$  field corresponds to the  $U(1)$  transformation and the three  $W_j$  fields to the  $SU(2)$ . Note that the Pauli matrices enter here as coefficients for the  $W_{j\mu}$  fields. The fields  $W_{3\mu}$  and  $B_\mu$  are combined in an appropriate way:

$$\begin{aligned} W_{3\mu}(x) &= \cos \theta_W Z_\mu + \sin \theta_W A_\mu \\ B_\mu(x) &= -\sin \theta_W Z_\mu + \cos \theta_W A_\mu \end{aligned} \quad (3.21)$$

Here, the fields  $A_\mu$  and  $Z_\mu$  are taken to be the photon field and  $Z$  boson field, respectively. The angle,  $\theta_W$ , is called the weak mixing (a.k.a. Weinberg angle). Similarly, the  $W_{1\mu}$  and  $W_{2\mu}$  fields are combined through:

$$\begin{aligned} W_\mu &= W_{1\mu} - iW_{2\mu} \\ W_\mu^\dagger &= W_{1\mu} + iW_{2\mu} \end{aligned} \quad (3.22)$$

### 3.2 The gauge principle

---

Note that these fields are not hermitian, indicating that they describe charged particles. In the interaction Lagrangian the fields will couple through the currents:

$$\begin{aligned}
 s^\mu(x) &= -e\bar{\psi}_l(x)\gamma^\mu\psi_l(x) \\
 J^\mu(x) &= \bar{\psi}_l(x)\gamma^\mu(1 - \gamma_5)\psi_{\nu_l}(x) \\
 J^{\mu\dagger}(x) &= \bar{\psi}_{\nu_l}(x)\gamma^\mu(1 - \gamma_5)\psi_l(x) \\
 J_3^\mu(x) &= \frac{1}{2} \left[ \bar{\psi}_{\nu_l}^L(x)\gamma^\mu\psi_{\nu_l}^L(x) - \bar{\psi}_l^L(x)\gamma^\mu\psi_l^L(x) \right]
 \end{aligned} \tag{3.23}$$

The last current,  $J_3^\mu$ , is a neutral current. That is, it only couples particles of no charge or particles of opposite charge, consequently the mediating particle is neutral. The second term in the bracket is similar to the electromagnetic current, which is also neutral (the photon has no charge). Demanding that the electromagnetic field only couples to charged particles in the ordinary way (i.e. through  $s^\mu A_\mu$ ) we need to put:

$$g \sin \theta_W = g' \cos \theta_W = e \tag{3.24}$$

The constants  $g$  and  $g'$  were introduced through the covariant derivative in (3.17). Writing the Lagrangian as a sum of the free part and an interaction part,

$$L_{EW} = L_{EW}^0 + L_{EW}^I \tag{3.25}$$

where the interaction part, written by the above currents is [6]:

$$\begin{aligned}
 L_{EW}^I &= -s^\mu(x)A_\mu(x) - \frac{g}{2\sqrt{2}} \left[ J^{\mu\dagger}(x)W_\mu(x) + J^\mu(x)W_\mu^\dagger(x) \right] \\
 &\quad - \frac{g}{\cos \theta_W} \left[ J_3^\mu(x) - \sin^2 \theta_W s^\mu(x)/e \right] Z_\mu(x)
 \end{aligned} \tag{3.26}$$

The above Lagrangian describes free, massless leptons and their interactions with the gauge bosons. We still need to add kinetic terms for the gauge bosons. The  $U(1)$  kinetic term for the  $B$  will be the same as for QED, but the  $W_j$  kinetic term is a bit different. Due to  $SU(2)$  transformation properties we get an extra term in the kinetic tensor  $G_i^{\mu\nu}$ . The kinetic terms are

$$\begin{aligned}
 & - \frac{1}{4} B_{\mu\nu} B^{\mu\nu} \\
 & - \frac{1}{4} G_{i\mu\nu} G_i^{\mu\nu}
 \end{aligned} \tag{3.27}$$

### 3. THE STANDARD MODEL

---

where the tensors above expressed in terms of the fields are

$$\begin{aligned}
 B^{\mu\nu} &= \partial^\nu B^\mu - \partial^\mu B^\nu \\
 G_i^{\mu\nu} &= F_i^{\mu\nu} + g\epsilon_{ijk}W_j^\mu W_k^\nu \\
 F_i^{\mu\nu} &= \partial^\nu W_i^\mu - \partial^\mu W_i^\nu
 \end{aligned} \tag{3.28}$$

The term  $g\epsilon_{ijk}W_j^\mu W_k^\nu$  will, when multiplied with  $G_i^{\mu\nu}$ , give new interaction terms. These interaction terms describe the self coupling of the gauge bosons.

This is not the whole story though. The attentive reader will notice that, in contrast to the QED example, we did not include mass terms for the leptons in the free Lagrangian density. The masses of the gauge bosons are not included either. This is closely related to the problem of divergent loop integrals and renormalization.

### 3.3 Mass and renormalizability

We now have an  $SU(2)_L \times U(1)$  invariant theory (gauge invariant), but all particles in it are massless. At this point we could simply add mass terms for the gauge-bosons and leptons. They look like:

$$m_W^2 W_\mu^\dagger W^\mu \tag{3.29}$$

$$\frac{1}{2}m_Z^2 Z^\mu Z_\mu \tag{3.30}$$

$$m_l \bar{\psi}_l \psi_l \tag{3.31}$$

These mass terms are not gauge invariant. This does not seem like a problem yet, because as long as the theory gives sensible results, gauge invariance is not needed. Unfortunately the resulting model (Glashow model) is non-renormalizable. The resolution of this problem is the Higgs mechanism. We will retain gauge invariance by adding a scalar field in an  $SU(2)_L \times U(1)$  invariant way. The scalar field will generate masses through the mechanism of spontaneous symmetry breaking. This will be the topic of the next section.

## 3.4 Higgs mechanism

The Higgs mechanism is most easily explained by first considering a simple model called the Goldstone model. The reason is that the Goldstone model is a good illustration of spontaneous symmetry breaking (SSB). We will go on to consider the Higgs model and briefly show its implementation in the Weinberg-Salam theory. The development will follow closely that of Mandl and Shaw [6]. We keep in mind that the problem we are trying to solve is how to add mass terms without spoiling the calculability of the theory.

### 3.4.1 Spontaneous Symmetry Breaking

The arguments for SSB are a bit abstract if one has not gone through some example first. I will first state the abstract arguments, then go through the Goldstone example and make the abstract a bit more concrete.

1. In field theory the lowest-energy state is the vacuum state
2. SSB is relevant if the vacuum state is non-unique
3. Non-uniqueness means that we have some way of distinguishing one vacuum state from another
4. In the quantum theory, we assume this distinguishing label to be a vacuum expectation value (VEV) of some field
5. Lorentz invariance ensures that it is the VEV of a scalar field
6. The assumption that the vacuum is the same everywhere (translational invariance) ensures that the VEV is constant

In the Goldstone model, we will look at the Lagrangian of a scalar field. It will possess a certain symmetry. The lowest-energy state of the system will not share the symmetry. This is what is called spontaneous symmetry breaking.

The Goldstone model is described by the Lagrangian

$$L = [\partial_\mu \phi^*][\partial^\mu \phi] - V(\phi) \tag{3.32}$$

$$V(\phi) = \mu^2 |\phi|^2 + \lambda |\phi|^4 \tag{3.33}$$

### 3. THE STANDARD MODEL

---

Here,  $\phi$  is to be considered as a classical, complex-valued, scalar field. The Hamiltonian of the system is:

$$H = [\partial_0 \phi^*][\partial^0 \phi] + [\nabla \phi^*][\nabla \phi] + V(\phi) \quad (3.34)$$

Minimizing the Hamiltonian w.r.t.  $\phi$ , means solving the equation

$$\frac{\partial H}{\partial \phi} = 0 \quad (3.35)$$

Since the derivative of  $\phi$  and  $\phi$  itself, are independent normal coordinates we get:

$$\frac{\partial H}{\partial \phi} = \frac{\partial V}{\partial \phi} = 0 \quad (3.36)$$

Minimizing  $H$  is therefore the same as minimizing  $V(\phi)$ .

We write  $\phi$  as the sum of two real-valued fields in the following way:

$$\phi = \frac{1}{\sqrt{2}}[\phi_1 + i\phi_2] \quad (3.37)$$

Before we attempt to quantize the field we will look at the potential part. The quartic term must have a positive constant to be bounded from below. For the quadratic term we have two situations:

1.  $\mu^2 > 0$
2.  $\mu^2 < 0$

In Figure 3.1 a plot for the case  $\mu^2 < 0$  in the  $\phi_1, \phi_2$  space is shown. In each case we have rotational invariance of the potential. This is reflected in the Lagrangian by the invariance under  $\phi' = e^{i\theta}\phi$  (Since multiplying by  $e^{i\theta}$  rotates by  $\theta$ ). An energy level will correspond to a point along the  $V$ -axis, while an energy state corresponds to a point in the  $\phi_1, \phi_2$  plane. One can think of a marble rolling around on the potential surface, the marble's position will define the energy state and the height is the energy level.

1. For the  $\mu^2 > 0$  case, we have a unique lowest-energy state and the energy state is also invariant under rotation.

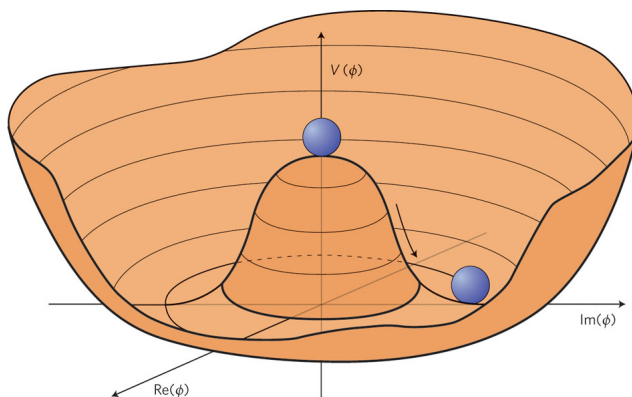


**Figure 3.1:** The Higgs potential for the case  $\mu^2 < 0$

2. In the  $\mu^2 < 0$  case, we have several lowest-energy states corresponding to the lowest-energy level. If we rotate the potential, a lowest-energy state will rotate into another state with the same energy. So the lowest-energy state does not share the symmetry of  $L$ .

More generally, if a Lagrangian possesses a particular symmetry, we have two possible situations that can occur when classifying energy levels. If an energy level is non-degenerate the corresponding energy state is unique and invariant under the symmetry transformations of  $L$ . If it is degenerate the energy eigenstates are not invariant, but transform linearly among themselves.

Now I will relate the above abstract concepts to the Goldstone example. We will choose  $\mu^2 < 0$  so that the vacuum state is non-unique. Each point on the circle of minima  $\phi_0 = \sqrt{\frac{-\mu^2}{2\lambda}} e^{i\theta}$  corresponds to a different vacuum state with the same energy.  $\theta$  is now our label to distinguish vacuum states. The idea is that once we choose a specific state (e.g.  $\theta = 0$ ) we have spontaneously broken the symmetry. This is because under the transformation  $\phi' = e^{i\theta}\phi$ , the Lagrangian is invariant, but the specific vacuum state is transformed into another vacuum state. We will now choose  $\theta = 0$  and define  $\frac{v}{\sqrt{2}} = \sqrt{\frac{-\mu^2}{2\lambda}}$  as the label of THE vacuum state. Just to be clear here: The specific value of  $\theta$  chosen is not important, but choosing one is.

So far we have been treating this as a classical field theory. We will now try relat-

### 3. THE STANDARD MODEL

---

ing this to the quantum theory by relating the VEV of  $\phi$  to the labelling quantity  $v$ . First we make a coordinate change

$$\phi = \frac{1}{\sqrt{2}}[v + \sigma(x) + i\eta(x)] \quad (3.38)$$

The quantum criterion for SSB is expressed in the relation of the VEV to  $v$ , which is:

$$\langle 0|\phi(x)|0\rangle = \frac{v}{\sqrt{2}} \quad (3.39)$$

We get a new Lagrangian density, which is equivalent to the Lagrangian density before the variable change (3.33)

$$\begin{aligned} L = & \frac{1}{2}[\partial_\mu\sigma][\partial^\mu\sigma] - \frac{1}{2}(2\lambda v^2)\sigma^2 \\ & + \frac{1}{2}[\partial_\mu\eta][\partial^\mu\eta] - \lambda v\sigma[\sigma^2 + \eta^2] \\ & - \frac{1}{4}\lambda[\sigma^2 + \eta^2]^2 + \text{const} \end{aligned} \quad (3.40)$$

The reason for making the variable change is, in short, because perturbation about  $\phi = 0$  gives non-sensical results.

We instead perturb about  $\frac{v}{\sqrt{2}}$  with the free Lagrangian density

$$L_0 = \frac{1}{2}[\partial_\mu\sigma][\partial^\mu\sigma] - \frac{1}{2}(2\lambda v^2)\sigma^2 + \frac{1}{2}[\partial_\mu\eta][\partial^\mu\eta] \quad (3.41)$$

Upon quantization the fields  $\eta$  and  $\sigma$  lead to spin-0 particles. The particle associated with  $\sigma$  has a mass  $\sqrt{2\lambda v^2}$ , while the  $\eta$  particle is massless (no  $\eta^2$  term). This can be interpreted by looking at small displacements from the equilibrium configuration. Small displacements along the  $\sigma$  direction correspond to climbing the potential valley, where  $V$  goes as  $\sigma^2$  (like the mass term) while small displacements in the  $\eta$  direction do not change the potential. The quantum excitations of  $\eta$  are consequently massless. These massless bosons pop up everywhere in theories with SSB and are called Goldstone bosons. In the next section we will get rid of these Goldstone bosons by retaining gauge invariance in the SSB model. This is the Higgs model.

### 3.4.2 The Higgs Model

The Lagrangian for the Higgs model is

$$L = [D^\mu \phi]^* [D_\mu \phi] - \mu^2 |\phi|^2 - \lambda |\phi|^4 - \frac{1}{4} F^{\mu\nu} F_{\mu\nu} \quad (3.42)$$

Here,  $\phi$  is again to be considered as a classical, complex-valued, scalar field. Comparing this to the Goldstone model the differences are:

1. We have made the substitution  $\partial_\mu \rightarrow D_\mu$ , where  $D_\mu = \partial_\mu + igA_\mu$
2. We have added the kinetic term of  $A_\mu$

This is similar to what we did when we obtained the Lagrangian density for QED by the gauge principle. The Lagrangian density is invariant under the  $U(1)$  gauge transformation (3.3).

We now proceed similarly as in the Goldstone case:

1. Classical field theory
2.  $\lambda > 0, \mu^2 < 0$
3. We obtain the circle of minima and choose  $\theta = 0$
4. Make the variable change (3.38)

Neglecting higher-order interaction terms, the Lagrangian density has the form:

$$L = \frac{1}{2} [\partial^\mu \sigma] [\partial_\mu \sigma] - \frac{1}{2} (2\lambda v^2) \sigma^2 - \frac{1}{4} F^{\mu\nu} F_{\mu\nu} + \frac{1}{2} (qv)^2 A_\mu A^\mu + \frac{1}{2} [\partial^\mu \eta] [\partial_\mu \eta] + qv A^\mu \partial_\mu \eta \quad (3.43)$$

By inspection the Lagrangian seems to describe a massive real scalar field  $\sigma$ , a real massless scalar field  $\eta$  and a massive vector field  $A_\mu$ . Upon counting degrees of freedom (d.o.f.) in the Lagrangian before and after the variable change (3.38) we find that they are different. Before changing variables (3.42) the d.o.f. are four. Two for the complex field  $\phi$  and two for the massless vector field  $A_\mu$ . Afterwards (3.43) the d.o.f. are five. One each for  $\eta$  and  $\sigma$  and three for the now massive vector field  $A_\mu$ .

### 3. THE STANDARD MODEL

---

Since the degrees of freedom cannot be changed by a change of variables, one concludes that something is amiss. We now use the gauge invariance we insisted on retaining for what it's worth. For every point in space-time we can choose the function  $f(x)$  in (3.3) such that the  $\phi$  field is real. In other words we use gauge invariance to get rid of  $\eta$  making  $\phi = \frac{1}{\sqrt{2}}[v + \sigma(x)]$ . This restriction on the function  $f(x)$  is called the unitary gauge.

The free Lagrangian density now takes the form

$$L_0 = \frac{1}{2}[\partial^\mu \sigma][\partial_\mu \sigma] - \frac{1}{2}(2\lambda v^2)\sigma^2 - \frac{1}{4}F^{\mu\nu}F_{\mu\nu} + \frac{1}{2}(qv)^2 A_\mu A^\mu \quad (3.44)$$

We now see that we have a free Lagrangian density describing a massive vector field and a massive spin-0 particle. There are also higher-order interaction terms coupling  $\sigma$  to itself and  $A_\mu$ . Let's summarize what we just did:

1. Started from (3.42), containing a complex field and a massless vector field
2. SSB
3. Unitary gauge
4. Ended up with (3.43), containing a massive scalar field and a massless vector field

This is often summarized as the vector field “eating” a d.o.f. from the complex field, becoming massive in the process.

Now we come back to the renormalizability of the theory, which was the problem we started with. An added bonus of retaining gauge invariance is being able to show that the theory is renormalizable. A renormalizable theory has the property that physical observables are finite and computable. Gauge-invariant theories have the same physical content no matter which gauge is chosen (unitary or otherwise). This means that if we can show that the theory is renormalizable in one gauge it will apply in every gauge. Fortunately, one can do this both for this theory and for the  $SU(2)_L \times U(1)$  invariant Weinberg-Salam theory. When Weinberg first published his theory he didn't prove that it was renormalizable. He talks about this in his Nobel lecture and it is related to the above:

“With hindsight, my main difficulty was that in quantizing the vector fields I adopted a gauge now known as the unitarity gauge [30]: this gauge has several wonderful advantages, it exhibits the true particle spectrum of the theory, but it has the disadvantage of making renormalizability totally obscure.”

### 3.4.3 Weinberg-Salam model

The Weinberg-Salam theory is the successful implementation of the Higgs mechanism to the  $SU(2)_L \times U(1)$  invariant theory. Since one wants to break an  $SU(2)$  symmetry, we must at least introduce a doublet field. It is of course possible to introduce more doublets as is done in the 2HDM. In the Standard Model, the mathematically simplest choice is made. One adds the doublet

$$\Phi = \begin{pmatrix} \phi_a \\ \phi_b \end{pmatrix} \quad (3.45)$$

through the Lagrangian

$$\begin{aligned} L^H &= [D_\mu \Phi]^\dagger [D^\mu \Phi] - \mu^2 \Phi^\dagger \Phi - \lambda [\Phi^\dagger \Phi]^2 \\ &= [D_\mu \Phi]^\dagger [D^\mu \Phi] - V(\Phi) \end{aligned} \quad (3.46)$$

The doublet transforms under both  $SU(2)$  and  $U(1)$  gauge transformations. The covariant derivative is

$$D^\mu \Phi = [\partial^\mu - ig\sigma_j W_j^\mu / 2 - ig' B^\mu / 2] \Phi \quad (3.47)$$

We repeat the procedure we used in the Higgs model. Taking  $\lambda > 0$ ,  $\mu^2 < 0$ , the classical field has a minimum for a constant value of  $\Phi$ . The SSB relations for the doublet become:

$$\begin{aligned} \langle \Phi_0^\dagger \Phi_0 \rangle &= |\phi_a^0|^2 + |\phi_b^0|^2 = \frac{-\mu^2}{2\lambda} \\ \langle \Phi_0 \rangle &= \begin{pmatrix} \phi_a^0 \\ \phi_b^0 \end{pmatrix} = \begin{pmatrix} 0 \\ \frac{v}{\sqrt{2}} \end{pmatrix} \\ v &= \sqrt{\frac{-\mu^2}{\lambda}} \quad (> 0) \end{aligned} \quad (3.48)$$

We make the coordinate change

$$\Phi = \frac{1}{\sqrt{2}} \begin{pmatrix} \eta_1 + i\eta_2 \\ v + \sigma + i\eta_3 \end{pmatrix} \quad (3.49)$$

### 3. THE STANDARD MODEL

---

Once again we can exploit the gauge invariance of the theory. We employ the unitary gauge and rid ourselves of the Goldstone bosons  $\eta_i$

$$\Phi = \frac{1}{\sqrt{2}} \begin{pmatrix} 0 \\ v + \sigma \end{pmatrix} \quad (3.50)$$

For future reference, this gauge will be employed when calculating amplitudes in chapter 5. The gauge bosons will acquire mass terms, when they are multiplied by the  $v$  term in the lower component of  $\Phi$ . This happens through the term  $[D_\mu \Phi]^\dagger [D_\mu \Phi]$  in (3.46). Doing this we obtain terms quadratic in the  $W$  and  $Z$  fields. Their coefficients give a mass for each of the bosons,

$$M_W = \frac{1}{2} g v M_Z = \frac{1}{2} \sqrt{g^2 + g'^2} v \quad (3.51)$$

This (3.24) leads to the relation,

$$M_W = M_Z \cos \theta_W \quad (3.52)$$

The last thing we have to consider is the mass of the leptons, they will be introduced through Yukawa couplings. A Yukawa coupling is a term containing a product of two spinors and a scalar. The Yukawa term for the charged leptons is gauge invariant and looks like

$$-g_l \left[ \bar{\Psi}_l^L \psi_l^R \Phi + \Phi^\dagger \bar{\psi}_l^R \Psi_l^L \right] \quad (3.53)$$

In the unitary gauge this reduces to

$$\begin{aligned} -\frac{g_l}{\sqrt{2}} \left[ \bar{\psi}_l^L \psi_l^R (v + \sigma) + \bar{\psi}_l^R \psi_l^L (v + \sigma) \right] &= -\frac{g_l}{\sqrt{2}} (v + \sigma) [\bar{\psi}_l \psi_l] \\ &= -\frac{g_l}{\sqrt{2}} v \bar{\psi}_l \psi_l - \frac{g_l}{\sqrt{2}} \sigma \bar{\psi}_l \psi_l \end{aligned} \quad (3.54)$$

This enables us to identify the mass of the charged leptons as  $m_l = \frac{g_l v}{\sqrt{2}}$ . Similar couplings can be added in the quark case.

## Chapter 4

# Electroweak Precision Tests

The main task of the thesis is to enhance the  $ZZ$  cross-section in accordance with our experimental observation (chapter 2). Before we look at theories beyond the Standard Model, we will look at the Electroweak Precision Tests (EWPT). The EWPT are high-precision measurements of the properties and parameters in the EW part of the Standard Model. The high accuracy of the EWPT makes them crucial for ruling out Beyond-SM theories (BSM). Any extension of the Standard Model must yield results that are compatible with these measurements. This section will follow [11] closely. The references [8], [9] and [6] will also be used.

Since the discovery of the massive gauge bosons 30 years ago, their properties have been extensively measured. To get a good idea of how they were measured, we will look at the reaction:  $e^+e^- \rightarrow \mu^+\mu^-$ , then generalize to  $e^+e^- \rightarrow f\bar{f}$ , where the  $f$  stands for fermion. We will end up with the total cross-section formula for any fermion final state. This formula together with measurements made at LEP (Large Electron Positron collider) was used to confirm predictions in the EW theory and set bounds on BSM theories.

Because of conservation of electric charge, the mediating particle must be neutral. Viable candidates are the photon,  $Z$  boson and Higgs boson. To lowest order we then have the diagrams (4.1) (4.2) and (4.3). The amplitude looks like:

$$\mathcal{M} = \mathcal{M}_\gamma + \mathcal{M}_Z + \mathcal{M}_H \tag{4.1}$$

#### 4. ELECTROWEAK PRECISION TESTS

---

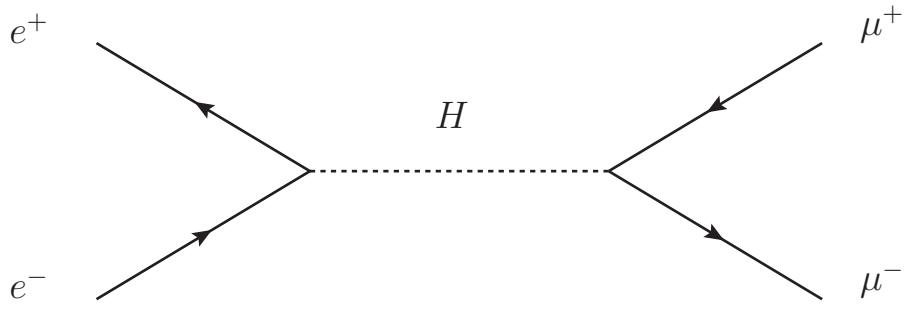


**Figure 4.1:** Higgs contribution

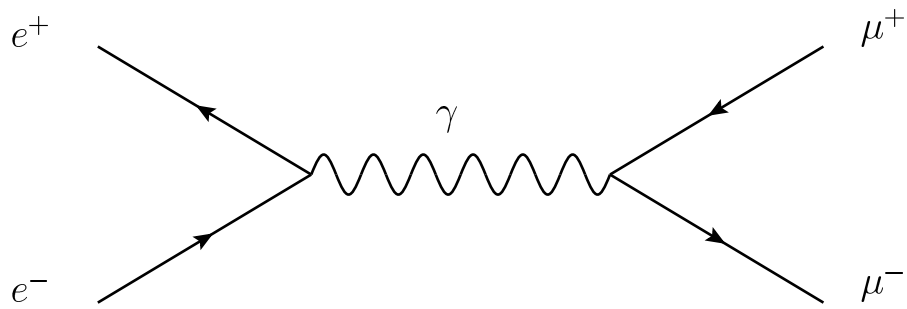


**Figure 4.2:** Photon contribution

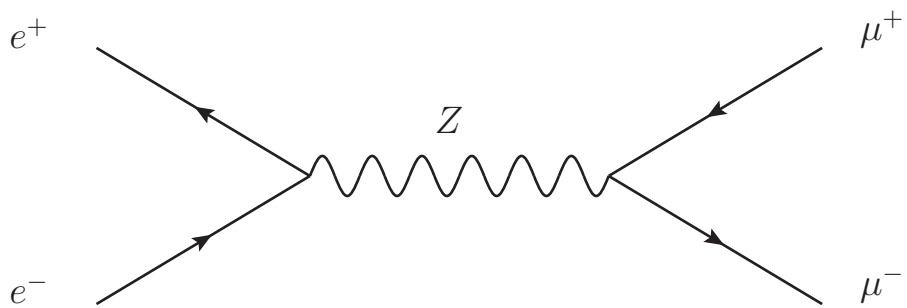


**Figure 4.3:**  $Z$  contribution

---

where [6]

$$\mathcal{M}_\gamma = ie^2 [\bar{u}_\mu \gamma^\alpha v_\mu] \frac{1}{k^2 + i\epsilon} [\bar{v}_e \gamma_\alpha u_e] \quad (4.2)$$

$$\mathcal{M}_Z = \frac{ig^2}{4 \cos^2 \theta_W} [\bar{u}_\mu \gamma^\alpha (v_l - a_l \gamma_5) v_\mu] \frac{1}{k^2 - M_Z^2 + i\epsilon} [\bar{v}_e \gamma_\alpha (v_l - a_l \gamma_5) u_e] \quad (4.3)$$

$$\mathcal{M}_H = \frac{-i}{v^2} m_e m_\mu [\bar{u}_\mu v_\mu] \frac{1}{k^2 - M_H^2 + i\epsilon} [\bar{v}_e u_e] \quad (4.4)$$

$$v_l = t_l^3 - 2Q_l \sin^2 \theta_W \quad (4.5)$$

$$a_l = t_l^3 \quad (4.6)$$

Here,  $t_l^3$  is the lepton's third component of isospin. We observe that  $\mathcal{M}_H/\mathcal{M}_Z$  is of the order:

$$\frac{m_e m_\mu}{m_Z^2} \frac{k^2 - M_Z^2}{k^2 - M_H^2} \quad (4.7)$$

The lepton masses make this contribution vanishingly small unless  $k^2 \approx M_H^2$ . The amplitude then becomes:

$$\mathcal{M} = \mathcal{M}_\gamma + \mathcal{M}_Z \quad (4.8)$$

Based on this we end up with a cross section of the form [11]:

$$\sigma = \frac{4\pi\alpha^2}{3s} [1 + a_1] \quad (4.9)$$

where  $a_1$  and  $f_Z$  are given by

$$\begin{aligned} a_1 &= 2v_l^2 f_Z + (v_l^2 + a_l^2)^2 f_Z^2 \\ f_Z &= \frac{s}{s - M_Z^2} \frac{1}{\sin^2 2\theta_W} \end{aligned} \quad (4.10)$$

We note the following points:

1. If  $a_1 = 0$ , we have the QED case and the only mediator is the photon, Feynman diagram shown in Figure 4.2
2. The term proportional to  $f_Z^2$  is the pure  $Z$  contribution, Feynman diagram shown in Figure 4.3
3. The term proportional to  $f_Z$  is due to interference between the photon 4.2 and the  $Z$  4.3

#### 4. ELECTROWEAK PRECISION TESTS

---

For charged leptons  $v_l = \frac{1}{2}(1 - 4\sin^2\theta_W)$ , which is close to zero. In this limit, the interference term vanishes and we have:

$$\sigma(e^+e^- \xrightarrow{\gamma,Z} \mu^+\mu^-) \simeq \frac{4\pi\alpha^2}{3s} \left[ 1 + \frac{1}{16\sin^4 2\theta_W} \frac{s^2}{(s - M_Z^2)^2} \right] \quad (4.11)$$

We see that the cross section diverges at  $\sqrt{s} = M_Z$ , but this is not really what happens. The  $Z$  has a finite decay width, this is accounted for by the propagator substitution:

$$\frac{1}{(s - M_Z^2)} \rightarrow \frac{1}{(s - M_Z^2) + iM_Z\Gamma_Z} \quad (4.12)$$

This is an ad hoc way of taking into account higher order effects on the propagator. (Ad hoc in the sense that one skips all the formalism and calculations involved in taking higher orders.) The cross section after the substitution will have its maximum value at  $s = M_Z^2$  and looks like:

$$\sigma(e^+e^- \rightarrow \mu^+\mu^-) \simeq \frac{4\pi\alpha^2}{3s} \left[ 1 + \frac{1}{16\sin^4 2\theta_W} \frac{s^2}{(s - M_Z^2)^2 + \Gamma_Z^2 M_Z^2} \right] \quad (4.13)$$

Now we make the promised generalizations to  $e^+e^- \rightarrow f\bar{f}$ . Substituting:

$$(v_l^2 + a_l^2)^2 \rightarrow (v_l^2 + a_l^2)(v_f^2 + a_f^2) \quad (4.14)$$

The values of the coefficients are computed by means of (4.5) and (4.6), with  $f$  substituted for  $l$ . Observe that  $v_f$  is non-zero for quarks (fractional charge). Our integrated cross section evaluated at the  $Z$  mass is now:

$$\sigma_{\max} \simeq \frac{4\pi\alpha^2}{3M_Z^2} \left[ 1 + \frac{(v_e^2 + a_e^2)(v_f^2 + a_f^2) M_Z^2}{\sin^4 2\theta_W \Gamma_Z^2} \right] \quad (4.15)$$

With the substitution [11]

$$\Gamma_{Z \rightarrow f\bar{f}} \equiv \Gamma_f = \alpha M_Z^2 \frac{v_f^2 + a_f^2}{3\sin^2 2\theta_W} \quad (4.16)$$

we get

$$\sigma_{\max}(e^+e^- \rightarrow f\bar{f}) \simeq \frac{4\pi\alpha^2}{3M_Z^2} \left[ 1 + \frac{9\Gamma_e\Gamma_f}{\alpha^2\Gamma_Z^2} \right] \quad (4.17)$$

The numerical value of the parenthesis in (4.17) is  $\gg 1$ . Neglecting the 1 in the parenthesis we arrive at the formula used to confirm the predictions of the SM.

$$\sigma_{\max}^f \simeq \frac{12\pi}{M_Z^2} \frac{\Gamma_e\Gamma_f}{\Gamma_Z^2} \quad (4.18)$$

Here are some comments concerning what we can measure from this formula and the LEP data. They are adapted from the article [11].

- 
1. If we plot the cross-section against the C.O.M. energy, we will have a Breit-Wigner resonance with peak around  $s = M_Z^2$  for any final state. This means that we can determine the mass of the  $Z$  by measuring any final state.
  2. The half-width at the maximum of the Breit-Wigner shape gives the total width  $\Gamma_Z$  for any final state
  3. By measuring the Bhabha scattering (i.e  $f\bar{f} = e^+e^-$ ) cross section, we have  $\sigma_{\max}^f \simeq \frac{12\pi}{M_Z^2} \frac{\Gamma_e^2}{\Gamma_Z^2}$  and can calculate  $\Gamma_e$ , since we know  $\sigma_{\max}^f$  and  $\Gamma_Z$
  4. By measuring the peak of the cross-section for other final states we can now determine  $\Gamma_f$
  5. The neutrinos are not detected in experiments, but their decay width can be inferred from the total width  $\Gamma_Z$  and the rest of the visible decay widths.  $\Gamma_{\text{invis}} = \Gamma_Z - \Gamma_{\text{vis}}$
  6. The Standard Model prediction of three neutrinos can then be confirmed by noticing that the number of neutrinos should be  $\frac{\Gamma_{\text{invis}}}{\Gamma_\nu}$ , where  $\Gamma_\nu$  is the SM prediction. This number is measured to be  $2.984 \pm 0.008$  [11]

Other measurements involve the differential cross section (C.O.M.) of the process  $e^+e^- \xrightarrow{\gamma, Z} l^+l^-$ , where  $l = \mu, \tau$ . The differential cross section can be written as a sum of two terms, one proportional to  $\cos\theta$  and one proportional to  $(1 + \cos^2\theta)$ . The term proportional to  $\cos\theta$  gives rise to forward-backward asymmetries (i.e. there is an excess production in one direction). From experiments such as above<sup>1</sup> the value of the parameters of the electroweak theory are accurately measured. For instance [8],

$$\begin{aligned}
M_Z &= 91.1875 \pm 0.0021 \text{ GeV} \\
M_W &= 80.396 \pm 0.029 \text{ GeV} \\
\sin^2 \theta_W &= 0.23150 \pm 0.00016
\end{aligned}
\tag{4.19}$$

Since these values are so accurately known one defines the parameter  $\rho$  through:

$$\rho = \frac{M_W^2}{M_Z^2 \cos^2 \theta_W}
\tag{4.20}$$

---

<sup>1</sup>Other experiments of course also perform these measurements. The mass of the  $W$ , given below, is an average over measurements from LEP II and the Tevatron at Fermilab [8]

#### 4. ELECTROWEAK PRECISION TESTS

---

At the tree level, the Standard model predicts  $\rho = 1$ . The parameter describes how much the difference in self energy of the W and Z can deviate from the SM value. Measurements from LEP give the restriction [12]:

$$\rho = 1.005 \pm 0.001 \tag{4.21}$$

It is a very useful parameter, when looking for new physics. For instance if we choose to add more more scalar particles through multiplets, the demand that  $\rho$  is equal to 1 at tree level sets restrictions on the allowed quantum numbers (weak isospin and hypercharge) of the multiplet [8]. The parameter  $\rho$  is modified through loop diagrams when calculating beyond first order in perturbation theory. Within the Standard Model, the parameter  $\rho$  receives a correction from the top-bottom mass splitting [11]. The corrections to  $\rho$  are an effective way of probing for new physics. If a theory predicts new particles, they would typically contribute to the  $\rho$  parameter through loops. If the contribution is too large compared to the measured value, something is wrong with the theory.

More generally these corrections are often parametrized by the three quantities  $S$ ,  $U$  and  $T$ , introduced by Peskin [13]<sup>1</sup>. The variable  $T$  is essentially the same as the corrections to the parameter  $\rho$ , described above. They differ only by the fine structure constant,  $\Delta\rho = \alpha T$  [11]. These parameters both form an obstacle and provide guidance when guessing at new theories.

---

<sup>1</sup>In this paper, only the S parameter is introduced

## Chapter 5

# A New $Z'$ Gauge Boson?

### 5.1 A Neutral, Massive Gauge Boson $Z'$

Ever since the prediction and discovery of the  $W$  and  $Z$  gauge bosons of EW theory, speculations on the existence of other massive gauge bosons have been abundant. Many theories beyond the Standard Model predict such bosons (e.g.  $E_6$ , Kaluza-Klein theories etc.). The different gauge bosons differ by how they are introduced into the theories. One introduces them by means of the gauge principle and uses the mechanism of spontaneous symmetry breaking to generate masses. More technically, it is done in the following way:

First one enlarges the SM gauge group from  $SU(3)_C \times SU(2)_L \times U(1)_Y$  to  $SU(3)_C \times SU(2)_L \times U(1)_Y \times G$ , where  $G$  is the new gauge group. The form of the couplings and the number of fields to be introduced is decided by the gauge group. Now we have to decide which particles we associate with which field. A typical example is where the group  $G$  is  $U(1)$  (not to be confused with the  $U(1)_Y$  from electroweak theory). The  $U(1)$  introduces 1 new field, which is associated with the  $Z'$  boson.

Other theories predicting  $Z'$  bosons already have an enlarged gauge sector, which is broken at some scale. The resulting theory can be broken again at another scale and so on. This procedure continues all the way down to the Standard Model and the Electroweak symmetry breaking. Diagrammatically we can represent it by:

1.  $G_1 \longrightarrow G_2$  at scale  $\Lambda_1$

## 5. A NEW $Z'$ GAUGE BOSON?

---

2.  $G_2 \longrightarrow G_3$  at scale  $\Lambda_2$
3. ...
4.  $G_k \longrightarrow SU(3)_C \times SU(2)_L \times U(1)_Y$  at scale  $\Lambda_{\text{new physics}} (\sim 1 \text{ TeV?})$

In this sense one can imagine the enlargement described in the above paragraph as a bottom to top approach. That is, without knowing the governing theory one can take a guess at how it breaks to the SM gauge group at the scale  $\Lambda_{\text{new physics}}$ . If the LHC reaches such energies, we could develop an effective-field description beyond the SM one and perhaps get some pointers for which theory describes nature.

Following the philosophy outlined at the end of chapter 2, we will calculate an estimate on the cross section for  $Z'$  production at the LHC. Such an estimate involves using the quark-parton model and parton distribution functions.

### 5.2 Quark-parton model and deep-inelastic scattering

The proton is normally said to be composed of three quarks, namely two up quarks and one down quark. This is only an approximate picture. A more accurate description would be that the proton is a swarming sea of point-like gluons and quarks (also called partons), continuously changing because of the interactions between them. In the quark-parton model, we imagine the proton as being in a superposition of these point-like states. We use what is called parton distribution functions (p.d.f.) to describe this. A parton distribution function  $f_i$  tells you how often you can find particle  $i$  carrying a fraction  $x_i$  of the protons momentum ( $P$ ), when a collision happens at momentum transfer  $Q^2$ . In other words, it is a function of the momentum fraction and the momentum transfer,  $f_i(x_i, Q^2)$ . The analytical form of the p.d.f.s are not known, but are obtained through numerically analysing data from high-energy scattering experiments <sup>1</sup>.

When we probe hadrons at high enough energies (small distances), we observe point-like interactions between the constituents. This is interpreted as interactions involving

---

<sup>1</sup>There are collaborations devoted to measuring these p.d.f.s. Two of them are CTEQ, mainly based in U.S.A. and MRST, based in England.

---

### 5.3 Cross section at parton and proton level

quarks [14]. The amplitudes we calculate from theory describe *free* quarks coming together to interact for a short time, producing new particles that exit. Quarks are confined in the proton due to their strong interactions and are not free. Treating the quarks as free is justified by the following argument which is borrowed from [15]: Imagine the proton dissociating into virtual states of free partons where one parton carries the momentum  $xP$  and the others carry the momentum  $(1-x)P$ . The lifetime of these states can by the uncertainty principle be expressed as  $\tau_{\text{lifetime}} \sim \frac{1}{\Delta E}$ , where  $\Delta E$  is the difference in energy of the virtual state and the physical proton. The collision time can be estimated by  $\tau_{\text{collision}} \sim \frac{1}{\Delta E_t}$ , where  $\Delta E_t$  is the energy transferred during the collision. If we are in a Lorentz frame where  $\tau_{\text{collision}} \ll \tau_{\text{lifetime}}$  we can treat the quarks as free. This is a typical situation in high-energy physics. A more intuitive way of thinking about it is:

If we are in a Lorentz frame where the proton clock runs slowly enough, the relative motions of the partons will be become effectively frozen. This means that the internal strong interactions, which are the cause of the relative motion, can be neglected. This is called the “impulse approximation”.

The objective of this chapter is to calculate a production cross section and we need to use the quark-parton model. In the next section we will consider how to calculate proton-proton cross sections at the LHC.

### 5.3 Cross section at parton and proton level

We now assume that a parton-level cross section has been calculated and show how to turn it into a measurable cross section. The cross section for the quarks (or partons) is denoted by  $\hat{\sigma}(\hat{s})$  and the cross section for protons by  $\sigma$ . The relationship between them is [15].

$$\sigma = \sum_{ab} C_{ab} \int dx_a dx_b F(x_a, x_b, Q^2) \hat{\sigma}(\hat{s}) \quad (5.1)$$

This is called a convolution integral. The  $C_{ab}$  are color-averaging factors, but we will only be interested in the  $q\bar{q}$  case where  $C_{q\bar{q}} = \frac{1}{9}$ . Summing over colours in the cross

## 5. A NEW $Z'$ GAUGE BOSON?

---

section gives a factor three, since each type of incoming quark (red, green, blue) can annihilate. The overall factor is then  $\frac{1}{3}$ , which gives:

$$\sigma = \frac{1}{3} \int dx_q dx_{\bar{q}} F(x_q, x_{\bar{q}}, Q^2) \hat{\sigma}(\hat{s}) \quad (5.2)$$

Here,  $F$  is a weight function involving the p.d.f.s and in our case looks like:

$$F(x_q, x_{\bar{q}}, Q^2) = f_{qP_1}(x_q) f_{\bar{q}P_2}(x_{\bar{q}}) + f_{qP_2}(x_q) f_{\bar{q}P_1}(x_{\bar{q}}) \quad (5.3)$$

The first term represents the probability of a quark from the first proton carrying the momentum fraction  $x_q$  annihilating with an antiquark carrying the momentum fraction  $x_{\bar{q}}$  from the second proton. The second term represents the probability of a quark from proton 2 carrying a momentum fraction  $x_q$ , annihilating with an antiquark carrying a momentum fraction  $x_{\bar{q}}$  from proton 1. Since the quark and antiquark distributions are equal for each proton we denote them by:  $q(x) = f_{qP_1}(x) = f_{qP_2}(x)$  and  $\bar{q}(x) = f_{\bar{q}P_1}(x) = f_{\bar{q}P_2}(x)$ . We then sum over up and down quark flavours and evaluate the functions at the momentum transfer  $Q^2 = M^2$ . The weight function,  $F$ , is then of the form:

$$F(x_q, x_{\bar{q}}, M^2) = 2u(x_q)\bar{u}(x_{\bar{q}}) + 2d(x_q)\bar{d}(x_{\bar{q}}) \quad (5.4)$$

The symbols  $s$  and  $\hat{s}$  denote the square of the C.O.M. energy of the protons and partons respectively. They are defined by:

$$s \equiv (P_1 + P_2)^2 \quad (5.5)$$

$$\hat{s} \equiv (p_1 + p_2)^2 \quad (5.6)$$

See Figure 5.1 for notation. Forgetting about the integral in (5.2) for a while, we write the convolution integrand as:

$$\frac{d^2\sigma}{dx_q dx_{\bar{q}}} = \frac{1}{3} F(x_q, x_{\bar{q}}, M^2) \hat{\sigma}(\hat{s}) \quad (5.7)$$

We will evaluate the parton-level cross section  $\hat{\sigma}(\hat{s})$  in the C.O.M. frame of the  $Z'$ . Since it is invariant, we can then look at everything from the proton-proton C.O.M. frame. In the latter frame the four-momenta of the particles are related by:

$$p_1 = x_q P_1 \quad (5.8)$$

$$p_2 = x_{\bar{q}} P_2 \quad (5.9)$$

### 5.3 Cross section at parton and proton level

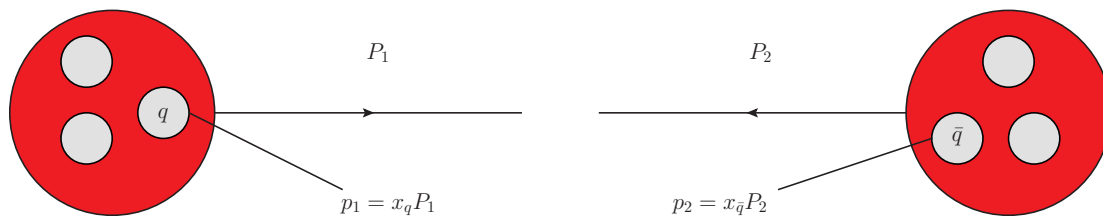


**Figure 5.1:** Quarks carry part of proton momentum

This is illustrated in Figure 5.1. In a frame where the masses of the particles can be neglected we have:

$$\begin{aligned} s &\simeq 2(P_1 \cdot P_2) \\ &\simeq \frac{1}{x_q x_{\bar{q}}} \hat{s} \end{aligned} \quad (5.10)$$

Now we make a change of variables from  $(x_q, x_{\bar{q}})$  to  $(\tau, y)$ . The variable  $\tau$  is the product of the momentum fractions and  $y$  is a quantity called rapidity. The rapidity of a system can be related to a Lorentz boost along the beam axis.<sup>1</sup> The change of variables is defined by:

$$\begin{aligned} \tau &= x_q x_{\bar{q}} \\ x_q &= \sqrt{\tau} e^{+y} \\ x_{\bar{q}} &= \sqrt{\tau} e^{-y} \end{aligned} \quad (5.11)$$

In our case we look at the rapidity of the  $q\bar{q}$  system. Its definition is [15]:

$$y = \frac{1}{2} \ln \left[ \frac{E_{q\bar{q}} + |\mathbf{P}_{q\bar{q}}|_L}{E_{q\bar{q}} - |\mathbf{P}_{q\bar{q}}|_L} \right] \quad (5.12)$$

$$E_{q\bar{q}} = E_q + E_{\bar{q}} \quad (5.13)$$

$$\mathbf{P}_{q\bar{q}} = \mathbf{P}_q + \mathbf{P}_{\bar{q}} \quad (5.14)$$

The  $L$  stands for the longitudinal component of the vector (i.e. along the beam axis). In the proton-proton C.O.M. frame it reduces to:

$$y = \frac{1}{2} \ln \left[ \frac{2E_q}{2E_{\bar{q}}} \right] = \frac{1}{2} \ln \left[ \frac{x_q}{x_{\bar{q}}} \right] \quad (5.15)$$

Notice that a high absolute value of rapidity corresponds to a situation where the quarks carry widely different fractions of their respective protons momentum<sup>2</sup>. A nice thing

<sup>1</sup> The original reason for defining rapidity was that it is additive also when  $v$  is close to  $c$ .

<sup>2</sup> A high rapidity of the  $q\bar{q}$  system translates into the system moving with a high velocity along the beam axis. We will come back to this when discussing the limits on the integral over rapidity

## 5. A NEW $Z'$ GAUGE BOSON?

---

about the variable change  $(x_q, x_{\bar{q}})$  to  $(\tau, y)$  is that the Jacobian of the transformation is 1. That is [15]:

$$\frac{d^2\sigma}{dx_q dx_{\bar{q}}} = \frac{d^2\sigma}{d\tau dy} = \frac{1}{3} F(\tau, y, M^2) \hat{\sigma}(\hat{s}) \quad (5.16)$$

Our relationship between the proton C.O.M. energy  $(\sqrt{s})$  and the parton C.O.M. energy  $(\sqrt{\hat{s}})$  is now:

$$\hat{s} = \tau s \quad (5.17)$$

Proton-proton collisions at the LHC occur at  $s = 7$  TeV presently. Exploiting that this is constant for our purposes we multiply each side of (5.16) by  $\frac{1}{s}$  and obtain

$$\frac{1}{s} \frac{d^2\sigma}{d\tau dy} = \frac{d^2\sigma}{d\hat{s} dy} = \frac{1}{3s} F(\tau, y, M^2) \hat{\sigma}(\hat{s}) \quad (5.18)$$

Before we go on to calculate production cross sections we need to calculate the parton cross sections. For that we need amplitudes. We will evaluate two different amplitudes in the next two sections and then go on to calculate their cross sections. The first amplitude is for the  $q\bar{q} \rightarrow Z'$  process, while the second is for the  $q\bar{q} \rightarrow Z' \rightarrow ZZ$  for on-shell  $Z$  bosons.

### 5.4 The amplitude for $Z'$ production

In this section we calculate the amplitude for the process  $q\bar{q} \rightarrow Z'$ . The tree-level Feynman diagram for this is shown in Figure 5.2.

The most general coupling between two fermions and a spin-1 particle can be written:

$$(q\bar{q}Z')_{\text{coupling}} = \gamma_\alpha (g_V - g_A \gamma_5) \quad (5.19)$$

Here,  $g_V$  and  $g_A$  are constants characterizing the magnitude of the vector and axial coupling strength, respectively. These coupling constants are dimensionless. This is an important point, since a coupling constant with dimensions would indicate a characteristic interaction energy. Let us discuss this some more, before writing down the amplitude and doing spin sums.

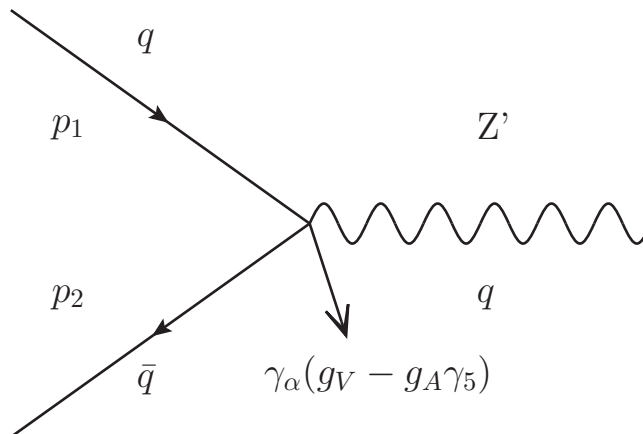


**Figure 5.2:** Feynman diagram for the process  $q\bar{q} \rightarrow Z'$

The dimension of the coupling constants  $g_V$  and  $g_A$  are derived by counting powers of the fields involved in the coupling. Each coupling comes from a term in the Lagrangian density. By doing some dimensional analysis we can find the dimension of the Lagrangian density and of each type of field (fermion, vector, scalar). We utilize the action,  $S$ , to find this.

The action is the time integral of the Lagrangian, which is in turn a three-dimensional integral of the Lagrangian density. The action is just a number and consequently has no dimension. Time and length have the same dimensions in natural units. This means that the Lagrangian density should have dimensions of inverse length to the power 4 ( $l^{-4}$ ). Length is inversely proportional to mass and the Lagrangian density therefore has dimensions of mass to the power 4 (mass dimension 4).

We can find the dimension of each type of field by looking at known terms from the Lagrangian density. As an example consider the fermion mass term  $m\bar{\Psi}\Psi$ . This term appears in the Lagrangian density and should have a mass dimension of 4. There is already a mass factor there, which means that  $\bar{\Psi}\Psi$  should have mass dimension 3. This implies that the fermion field,  $\Psi$ , has mass dimension  $\frac{3}{2}$ . Applying this procedure to

## 5. A NEW $Z'$ GAUGE BOSON?

---

the other fields results in:

$$\begin{aligned}\text{Dim}(\Psi) &= M^{\frac{3}{2}} \text{ (fermion)} \\ \text{Dim}(Z'^{\mu}) &= M^1 \text{ (vector)} \\ \text{Dim}(\Phi) &= M^1 \text{ (scalar)}\end{aligned}\tag{5.20}$$

We have a coupling between two fermion fields and a vector field, which give a mass dimension of  $\frac{3}{2} + \frac{3}{2} + 1 = 4$ . The gamma matrices in the coupling (5.19) have no dimension. To ensure that the Lagrangian density has the correct dimension, the coupling constants must also be dimensionless.

It was mentioned above that a coupling constant with dimensions implies a characteristic interaction energy. An example of this is Fermi's theory of beta decay. He wrote down a Lagrangian which had an overall coupling constant  $G_F$ . By power counting as above one finds that  $G_F$  has mass dimension  $-2$ . The value of the constant was known from experiment. Taking the inverse square root of this number one obtains,

$$G_F^{-\frac{1}{2}} \sim 300 \text{ GeV}\tag{5.21}$$

which is termed the ‘‘Fermi scale’’ and is around the electroweak scale. We end our discussion of coupling-constant dimension here and go on to consider the process  $q\bar{q} \rightarrow Z'$  as promised. If one is not interested in the calculation, the amplitude evaluated in the C.O.M. frame of the  $Z'$ , is given in (5.39). The Feynman amplitude for this process is:

$$\mathcal{M}_{q\bar{q}\rightarrow Z'} \equiv \mathcal{M} = [\bar{v}_r \gamma_{\alpha} (g_V - g_A \gamma_5) u_s] \varepsilon_k^{\alpha}\tag{5.22}$$

where  $u, v$  are the spinors corresponding to  $p_1, p_2$ , respectively, and  $\varepsilon_k^{\alpha}$  is the polarization vector of the  $Z'$ . Squaring the amplitude yields:

$$|\mathcal{M}|^2 = \varepsilon_k^{\alpha} \varepsilon_k^{\beta} [\bar{v}_r \gamma_{\alpha} (g_V - g_A \gamma_5) u_s] [\bar{u}_s \gamma_{\beta} (g_V - g_A \gamma_5) v_r]\tag{5.23}$$

Next, we label the spinors with indices and average over the incoming particle spins,

$$X = \left( \frac{1}{2} \sum_r \right) \left( \frac{1}{2} \sum_s \right) |\mathcal{M}|^2\tag{5.24}$$

$$= \frac{1}{4} \varepsilon_k^{\alpha} \varepsilon_k^{\beta} C_{\alpha\beta}\tag{5.25}$$

## 5.4 The amplitude for Z' production

---

with

$$C_{\alpha\beta} = \text{Tr}[(\not{p}_2 - m)\gamma_\alpha(g_V - g_A\gamma_5)(\not{p}_1 + m)\gamma_\beta(g_V - g_A\gamma_5)] \quad (5.26)$$

Note that each of the energy projection operators is missing a factor  $\frac{1}{2m}$ . In the cross section calculation we compensate for this by omitting the factor  $2m$  which accompanies each external fermion. To calculate the trace we first use the identities

$$\text{Tr}[\text{odd \# of gamma matrices}] = 0 \quad (5.27)$$

$$\text{Tr}[(\text{odd \# of gamma matrices})\gamma_5] = 0 \quad (5.28)$$

$$\{\gamma_\alpha, \gamma_5\} = 0 \quad (5.29)$$

which simplify the trace to:

$$C_{\alpha\beta} = \text{Tr}[\not{p}_2\gamma_\alpha(g_V - g_A\gamma_5)\not{p}_1\gamma_\beta(g_V - g_A\gamma_5)] - m^2\text{Tr}[\gamma_\alpha(g_V - g_A\gamma_5)\gamma_\beta(g_V - g_A\gamma_5)] \quad (5.30)$$

By using the identities

$$\text{Tr}[\not{p}_2\gamma_\alpha\not{p}_1\gamma_\beta] = 4(p_{1\alpha}p_{2\beta} + p_{1\beta}p_{2\alpha} - (p_1 \cdot p_2)g_{\alpha\beta}) \quad (5.31)$$

$$\text{Tr}[\not{p}_2\gamma_\alpha\not{p}_1\gamma_\beta\gamma_5] = -4ip_1^\mu p_2^\nu \epsilon_{\nu\alpha\mu\beta} \quad (5.32)$$

we end up with the final result:

$$C_{\alpha\beta} = 4(g_V^2 + g_A^2)(p_{1\alpha}p_{2\beta} + p_{1\beta}p_{2\alpha} - (p_1 \cdot p_2)g_{\alpha\beta}) + 8ig_A g_V p_1^\mu p_2^\nu \epsilon_{\nu\alpha\mu\beta} - 4m^2(g_V^2 - g_A^2)g_{\alpha\beta} \quad (5.33)$$

Two comments should be made here. Firstly the symbol  $\epsilon_{\nu\alpha\mu\beta}$  (the Levi-Cevita tensor density) is defined by

$$\begin{aligned} \epsilon^{\nu\alpha\mu\beta} &= +1, (\nu, \alpha, \mu, \beta) = \text{even permutation of } (0, 1, 2, 3) \\ &= -1, (\nu, \alpha, \mu, \beta) = \text{odd permutation of } (0, 1, 2, 3) \\ &= 0, \text{ otherwise} \end{aligned} \quad (5.34)$$

Secondly the factor  $i$  that appears is rather unnerving. This is after all something that appears when we square an amplitude and should be real-valued. The term only contributes if one looks at other types of polarization (e.g. circular) where the polarization vectors are complex. We will not worry about this at all since we will sum over

## 5. A NEW $Z'$ GAUGE BOSON?

---

outgoing polarizations. This means that we will only consider calculations where we contract the Levi-Cevita tensor with rank-two symmetric (rank = number of indices) tensors. This contraction makes the term vanish:

$$\begin{aligned}
& \text{If } s^{\alpha\beta} = s^{\beta\alpha} \text{ (s is symmetric in } \alpha \beta) \\
& \text{then } s^{\alpha\beta} \epsilon_{\mu\nu\alpha\beta} = s^{\beta\alpha} \epsilon_{\mu\nu\beta\alpha} \text{ (changed dummy indices)} \\
& \quad = s^{\alpha\beta} \epsilon_{\mu\nu\beta\alpha} \text{ (changed indices of s)} \\
& \quad = -s^{\alpha\beta} \epsilon_{\mu\nu\alpha\beta} \text{ (changed } \alpha \text{ and } \beta \text{ in } \epsilon)
\end{aligned} \tag{5.35}$$

Now we use the relation

$$\sum_k = \epsilon_k^\alpha \epsilon_k^\beta = -g^{\alpha\beta} + \frac{q^\alpha q^\beta}{M^2} \tag{5.36}$$

and sum over the polarization of the  $Z'$ . The  $M$  will denote the mass of the  $Z'$  throughout this chapter. Note that the above expression is symmetric in the indices and will make the epsilon term vanish.  $X'$  is now:

$$\begin{aligned}
X' &\equiv \sum_k X = \frac{1}{4} \left( -g^{\alpha\beta} + \frac{q^\alpha q^\beta}{M^2} \right) C_{\alpha\beta} \\
&= \left[ \frac{2(g_V^2 + g_V'^2)}{M^2} (p_1 \cdot q)(p_2 \cdot q) + (g_V^2 + g_A^2)(p_1 \cdot p_2) + 12m^2(g_V^2 - g_A^2) \right]
\end{aligned} \tag{5.37}$$

In the  $Z'$  C.O.M. system with the fermions approximated as massless ( $E_q = |\mathbf{p}_q|$ ) and the  $+z$ -axis along the quark direction, the four-vectors can be expressed:

$$\begin{aligned}
p_1 &= (E_q, 0, 0, E_q) \\
p_2 &= (E_q, 0, 0, -E_q) \\
q &= (M, 0, 0, 0)
\end{aligned} \tag{5.38}$$

The four-vector identities reduce the amplitude to:

$$X' = 4(g_V^2 + g_A^2)E_q^2 \tag{5.39}$$

Before calculating production cross sections we take a detour to obtain a coupling between three spin-1 particles, needed to calculate the  $q\bar{q} \rightarrow Z' \rightarrow ZZ$  amplitude. This involves looking at the ‘‘Landau-Yang theorem’’ and its generalization. The original theorem was obtained independently by Lev Landau and C.N. Yang [16] in 1948-1949 and the paper generalizing it is from 2008 [1].

## 5.5 Landau-Yang Theorem and its Generalization

In 1949 C.N. Yang wrote a paper called “Selection Rules for the Dematerialization of a Particle into Two Photons”. It was motivated by an observation made by John Archibald Wheeler that positronium in the S-triplet state can not decay into two photons. Positronium is a bound state of an electron and a positron, the S refers to the fact that they have no relative orbital angular momentum and the triplet state means that they have their intrinsic spins aligned. It is therefore a state with total angular momentum  $J = 1$ . We will see that such a decay ( $J = 1$  initial particle) is forbidden by selection rules. The selection rules are derived from principles of invariance under rotations in space and inversion (parity).

Yang starts the paper with saying “Consider two photons of equal wavelength  $\lambda_0$  traveling in opposite directions along a  $z$ -axis”. This is the same physical situation as if a particle  $X$  decayed into two photons. The different two-particle states of the system are denoted by  $\Psi^{\lambda_1\lambda_2}$ , where  $\lambda_{1,2}$  takes the values  $R$  and  $L$ . The first index refers to the photon propagating in the  $+z$  direction and the second to the photon propagating along the  $-z$  direction.  $R$  means that the photon has polarization along its direction of motion, while  $L$  means polarization opposite the direction of motion. There are four different states to be considered, namely  $\Psi^{RR}$ ,  $\Psi^{RL}$ ,  $\Psi^{LR}$  and  $\Psi^{LL}$ . Figure 5.3 illustrates this. Yang goes on to see how these states are changed under the following operations:

1.  $R_\theta$ , rotation by  $\theta$  around  $z$ -axis
2.  $R_\phi$  180 degrees rotation around  $x$ -axis
3.  $P$ , reflection

Remembering that states are transformed by unitary operators under symmetry operations, we take a look at the result. It is summarized in table 5.1, which is reproduced from the original paper. In the C.O.M. frame the following arguments for the selection rules are made:

1. For an odd initial state (- under parity), the initial particle must decay to  $\Psi^{RR} - \Psi^{LL}$ , since it is the only odd final state

## 5. A NEW $Z'$ GAUGE BOSON?

---

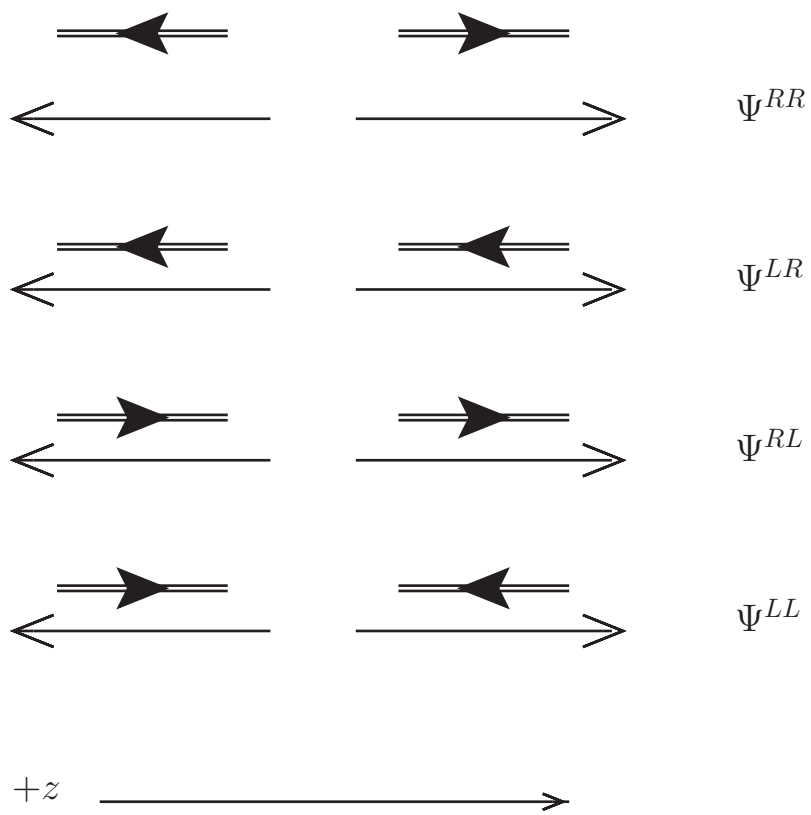


**Figure 5.3:** Two-photon helicity states

## 5.5 Landau-Yang Theorem and its Generalization

	$\Psi^{RR} + \Psi^{LL}$	$\Psi^{RR} - \Psi^{LL}$	$\Psi^{RL}$	$\Psi^{LR}$
$R_\theta$ rotation by $\theta$ around $z$ -axis	1	1	$e^{2i\theta}$	$e^{-2i\theta}$
$R_\phi$ 180 degrees rotation around $x$ -axis	1	1		
$P$ , reflection	1	-1	1	1

**Table 5.1:** Eigenvalues of symmetry operators on two-photon helicity states

Parity( $\nabla$ ) J( $\triangleright$ )	0	1	2,4,6 ...	3,5,7 ...
even	$\Psi^{RR} + \Psi^{LL}$	forbidden	$\Psi^{RR} + \Psi^{LL}, \Psi^{RL}, \Psi^{LR}$	$\Psi^{RL}, \Psi^{LR}$
odd	$\Psi^{RR} - \Psi^{LL}$	forbidden	$\Psi^{RR} - \Psi^{LL}$	forbidden

**Table 5.2:** Selection rules for two-photon helicity states

2. An even initial state must go into one of the three final states  $\Psi^{RL}$ ,  $\Psi^{LR}$  or  $\Psi^{RR} + \Psi^{LL}$
3. For an initial state with angular momentum  $J = 1, 3, 5, \dots$ , the only possible final states are  $\Psi^{RL}$  and  $\Psi^{LR}$ . We can rule out the other two because:  $\Psi^{RR} + \Psi^{LL}$  and  $\Psi^{RR} - \Psi^{LL}$  are simultaneous eigenstates of  $R_\theta$  and  $R_\phi$  with eigenvalue 1, while an initial state with eigenvalue 1 under  $R_\theta$  will have eigenvalue -1 under  $R_\phi$ <sup>1</sup>
4. For an initial state with  $J = 0, 1$  the only possible final states are  $\Psi^{RR} + \Psi^{LL}$  and  $\Psi^{RR} - \Psi^{LL}$ . This is because the other two states have angular momentum  $J = \pm 2\hbar$ , which is too large for  $J = 0$  or  $J = 1$

Looking at the  $J = 1$  case, argument 3 rules out  $\Psi^{RR} + \Psi^{LL}$  and  $\Psi^{RR} - \Psi^{LL}$  as final states, while argument 4 rules out  $\Psi^{RL}$  and  $\Psi^{LR}$  as final states. Therefore no such decays should take place. These results are summarized here as table 5.2.

In the paper written in 2008, a similar analysis is made, but with two  $Z$  bosons instead of photons. The difference now is that massive particles have one extra degree

---

<sup>1</sup>Yang mentions that such a state has the rotational properties of the spherical harmonics. The spherical harmonics of odd powers of angular momentum, have a factor  $e^{im\phi}$ , where  $\phi$  is the azimuthal angle and  $m$  is the projection of spin along the  $z$ -axis (odd number). Rotating about the  $x$ -axis means  $\phi' \rightarrow \phi + \pi$ , which gives a factor of -1

## 5. A NEW $Z'$ GAUGE BOSON?

---

Parity( $\nabla$ ) J( $\triangleright$ )	0	1
even	$\Psi^{++} + \Psi^{--}, \Psi^{00}$	$\Psi^{+0} - \Psi^{0-}, \Psi^{0+} - \Psi^{-0}$
odd	$\Psi^{++} - \Psi^{--}$	$\Psi^{+0} + \Psi^{0-}, \Psi^{0+} + \Psi^{-0}$

**Table 5.3:** Selection rules for two- $Z$  helicity states

of freedom in terms of longitudinal polarization. Instead of  $R, L$  we have  $(-, 0, +)$  denoting the polarization states of the final particles. Decay of a spin-1 parent particle can now result in two spin-1 final states. The symmetry of the situation does however limit the possible couplings. Their result is reproduced here as table 5.3. A result obtained in the paper is that if the three particles involved ( $Z'$  and  $ZZ$ ) are on-shell, they have a momentum-space vertex factor of the form:

$$i\Gamma_{Z' \rightarrow ZZ}^{\nu\alpha\beta} = if_4(q_3^\alpha g^{\nu\beta} + q_2^\beta g^{\nu\alpha}) - if_5 \epsilon^{\nu\alpha\beta\rho} (q_3 - q_2)_\rho \quad (5.40)$$

Here,  $q_2$  and  $q_3$  denote the  $Z$  boson momenta, the indices  $\alpha$  and  $\beta$  are related to the polarization vector of the  $Z$  boson with four momentum  $q_3$  and  $q_2$ , respectively. By power counting we have a mass dimension of three from the spin-1 fields. In the vertex-factor we have an additional mass dimension from the momentum factors. Therefore  $f_4$  and  $f_5$  are dimensionless coupling constants. Another interesting point is that the coupling does not change if we make the substitutions:

$$(\alpha, 2) \rightarrow (\beta, 3) \quad (5.41)$$

These substitutions are the same as switching the two  $Z$  bosons and reflects the fact that they are bosons. From the spin-statistics theorem such a switch should yield no change<sup>1</sup>.

This vertex factor will be used when obtaining the amplitude and polarization sum in the next section. Before we go on to consider polarization sums, it's instructive to calculate some helicity amplitudes to see how this coupling relates to the generalized Landau-Yang theorem. In particular the theorem states that for the spin-1 case only polarization states from column two in table 5.3 contribute. We will now use the part of the coupling proportional to  $f_4$  to illustrate this.

---

<sup>1</sup>In contrast to switching two fermions which gives a minus sign.

## 5.5 Landau-Yang Theorem and its Generalization

---

Consider the process  $q\bar{q} \rightarrow Z' \rightarrow ZZ$ . The Feynman diagram is shown in Figure 5.4. The amplitude looks like,

$$\mathcal{M} = [\text{spinor factor}][Z' \text{ propagator}]\varepsilon_k^{*\alpha}\varepsilon_l^{*\beta}i\Gamma_{\nu\alpha\beta} \quad (5.42)$$

where  $i\Gamma^{\nu\alpha\beta}$  is temporarily set to

$$i\Gamma^{\nu\alpha\beta} = if_4(q_3^\alpha g^{\nu\beta} + q_2^\beta g^{\nu\alpha}) \quad (5.43)$$

The polarization vectors are complex since we do not look at linear polarization. Let us ignore the spinor and  $Z'$  parts of the amplitude for a moment and look at the  $ZZ$  part:

$$\begin{aligned} P_\nu &\equiv \varepsilon_k^{*\alpha}\varepsilon_l^{*\beta}(q_{3\alpha}g_{\nu\beta} + q_{2\beta}g_{\nu\alpha}) \\ &= [\varepsilon_{l\nu}^*(\varepsilon_k^* \cdot q_3) + \varepsilon_{k\nu}^*(\varepsilon_l^* \cdot q_2)] \end{aligned} \quad (5.44)$$

In the C.O.M. frame with  $+z$ -direction pointing along  $Z(q_2)$  we have the four vector relations:

$$\begin{aligned} q_1 &= (M, 0, 0, 0) \\ q_2 &= (E, 0, 0, +p) \\ q_3 &= (E, 0, 0, -p) \end{aligned} \quad (5.45)$$

There are nine different helicity states for the two  $Z$ s, they can each have  $+$ ,  $-$  and  $0$ . For the helicity states of interest ( $+$ ,  $-$  and  $0$ ) the polarization vectors can be written [1]:

$$\begin{aligned} \varepsilon_{(k=0)} &= \gamma(\beta, 0, 0, 1) = \frac{M_{Z'}}{2M_Z}(\beta, 0, 0, 1) \\ \varepsilon_{(l=0)} &= \gamma(-\beta, 0, 0, 1) = \frac{M_{Z'}}{2M_Z}(-\beta, 0, 0, 1) \\ \varepsilon_{(k=\pm)} &= \frac{1}{\sqrt{2}}(0, \mp 1, -i, 0) = \varepsilon_{(l=\mp)} \end{aligned} \quad (5.46)$$

For the case where *both*  $Z$ s are transversely polarized (i.e.  $l = \pm$  and  $k = \pm$ ), both dot-products in (5.44) vanish since  $q_2$  and  $q_3$  do not have  $x$ - $y$  components. This eliminates four cases, namely  $+-$ ,  $-+$ ,  $++$  and  $--$ .

This means that we are left with the cases  $00$ ,  $0+$ ,  $+0$ ,  $0-$  and  $-0$ . The  $00$  amplitude vanishes when we contract with the  $Z'$  propagator: The propagator of a massive

## 5. A NEW $Z'$ GAUGE BOSON?

---

particle in the unitary gauge is:

$$D_F^{\mu\nu} = \frac{-g^{\mu\nu} + \frac{q_1^\mu q_1^\nu}{M^2}}{q_1^2 - M^2 + iM\Gamma_{Z'}} \quad (5.47)$$

When  $k$  and  $l$  are zero, we have the following dot-products:

$$\begin{aligned} (\varepsilon_{(k=0)} \cdot q_3) &= 2\gamma\beta E \equiv A \\ (\varepsilon_{(l=0)} \cdot q_2) &= -2\gamma\beta E = -A \end{aligned} \quad (5.48)$$

Ignoring the denominator of the propagator we calculate for the 00 case:

$$\left(-g^{\mu\nu} + \frac{q_1^\mu q_1^\nu}{M^2}\right) [A\varepsilon_{(l=0)\nu}^* - A\varepsilon_{(k=0)\nu}^*] = A(\varepsilon_{(k=0)}^{*\mu} - \varepsilon_{(l=0)}^{*\mu}) - \frac{2A\gamma\beta}{M}q_1^\mu = 0 \quad (5.49)$$

To see that the last expression is zero, look at the four-vector relations above.

Now we are left with  $0+$ ,  $+0$ ,  $0-$  and  $-0$ , which do not vanish, but contribute. A similar analysis can be made for the  $f_5$  term. We can see more clearly how the coupling ( $f_4$  and  $f_5$  part) is related to the generalised Landau-Yang theorem. It picks out the polarization states that contribute (compare with table 5.3). Now we move on to the next section where we find the polarization sum of the squared amplitude.

## 5.6 Amplitude for ZZ production

Here we calculate the amplitude for the process  $q\bar{q} \rightarrow Z' \rightarrow ZZ$ . The Feynman diagram is shown in Figure 5.4. The amplitude is given by:

$$\mathcal{M} = [\bar{v}_r \gamma_\mu (g_V - g_A \gamma_5) u_s] i D_F^{\mu\nu} i \Gamma_{\nu\alpha\beta} \varepsilon_k^\alpha \varepsilon_l^\beta \quad (5.50)$$

The propagator of the massive gauge boson,  $D_F^{\mu\nu}$ , is taken to be in the unitary gauge as in (5.47), where  $\Gamma_{Z'}$  is the decay rate of the  $Z'$  boson and will be discussed later on. Squaring the amplitude gives:

$$|\mathcal{M}|^2 = D_F^{\mu\nu} D_F^{*\rho\sigma} \Gamma_{\nu\alpha\beta} \Gamma_{\sigma\theta\xi}^* \varepsilon_k^\alpha \varepsilon_k^\theta \varepsilon_l^\beta \varepsilon_l^\xi [\bar{v}_r \gamma_\mu (g_V - g_A \gamma_5) u_s] [\bar{u}_s \gamma_\rho (g_V - g_A \gamma_5) v_r] \quad (5.51)$$

Averaging over initial spins yields the same trace as before (5.33) :

$$\begin{aligned} X &= \frac{1}{4} \sum_{s,r} |\mathcal{M}|^2 \\ &= \frac{1}{4} C_{\mu\rho} D_F^{\mu\nu} D_F^{*\rho\sigma} \varepsilon_k^\alpha \varepsilon_k^\theta \varepsilon_l^\beta \varepsilon_l^\xi \Gamma_{\nu\alpha\beta} \Gamma_{\sigma\theta\xi}^* \end{aligned} \quad (5.52)$$

## 5.6 Amplitude for ZZ production

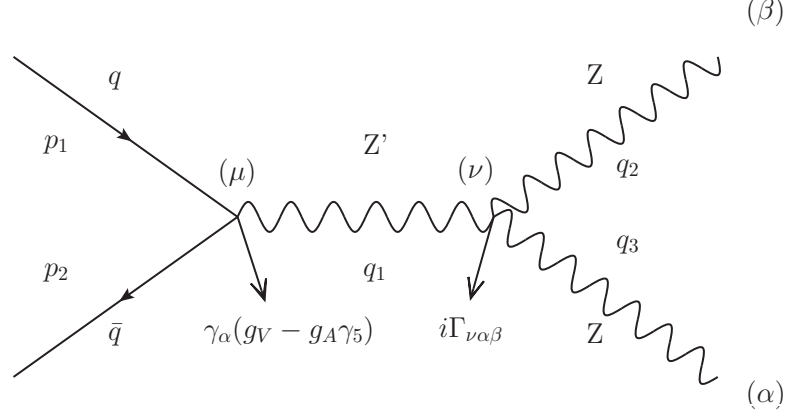


**Figure 5.4:** Feynman diagram for the process  $q\bar{q} \rightarrow Z' \rightarrow ZZ$

Summing over final polarization gives:

$$\begin{aligned}
 X' &= \sum_k \sum_l X \\
 &= \frac{1}{4} C_{\mu\rho} D_F^{\mu\nu} D_F^{*\rho\sigma} \left(-g^{\alpha\theta} + \frac{q_3^\alpha q_3^\theta}{M_Z^2}\right) \left(-g^{\beta\xi} + \frac{q_2^\beta q_2^\xi}{M_Z^2}\right) \Gamma_{\nu\alpha\beta} \Gamma_{\sigma\theta\xi}^*
 \end{aligned} \tag{5.53}$$

Writing out the propagator and gathering all terms to be contracted with  $\Gamma_{\nu\alpha\beta} \Gamma_{\sigma\theta\xi}^*$  we have:

$$X' = \frac{1}{4} \frac{1}{(q_1^2 - M^2)^2 + \Gamma_{Z'}^2 M^2} C_{\mu\rho} H^{\mu\rho} \tag{5.54}$$

The tensor  $H^{\mu\rho}$  is short for

$$\begin{aligned}
 H^{\mu\rho} &= \left[ \left(-g^{\mu\nu} + \frac{q_1^\mu q_1^\nu}{M^2}\right) \left(-g^{\rho\sigma} + \frac{q_1^\rho q_1^\sigma}{M^2}\right) \left(-g^{\alpha\theta} + \frac{q_3^\alpha q_3^\theta}{M_Z^2}\right) \left(-g^{\beta\xi} + \frac{q_2^\beta q_2^\xi}{M_Z^2}\right) \right] \\
 &\quad \times \Gamma_{\nu\alpha\beta} \Gamma_{\sigma\theta\xi}^*
 \end{aligned} \tag{5.55}$$

The vertex factor becomes:

$$\begin{aligned}
 \Gamma_{\nu\alpha\beta} \Gamma_{\sigma\theta\xi}^* &= f_4^2 (q_{3\theta} g_{\sigma\xi} + q_{2\xi} g_{\sigma\theta}) (q_{3\alpha} g_{\nu\beta} + q_{2\beta} g_{\nu\alpha}) \\
 &\quad - f_4 f_5 (q_{3\theta} g_{\sigma\xi} + q_{2\xi} g_{\sigma\theta}) \epsilon_{\nu\alpha\beta\gamma} (q_3 - q_2)^\gamma \\
 &\quad - f_4 f_5 (q_{3\alpha} g_{\nu\beta} + q_{2\beta} g_{\nu\alpha}) \epsilon_{\sigma\theta\xi\phi} (q_3 - q_2)^\phi \\
 &\quad + f_5^2 \epsilon_{\nu\alpha\beta\gamma} \epsilon_{\sigma\theta\xi\phi} (q_3 - q_2)^\gamma (q_3 - q_2)^\phi
 \end{aligned} \tag{5.56}$$

In evaluating the spin sum, the program REDUCE is used. It is a program which manipulates algebraic expressions (and can apparently contract 30 hours of work into 3).

## 5. A NEW $Z'$ GAUGE BOSON?

---

REDUCE typically gives a list of terms that are not fully factored. After doing some algebra with these terms, the result was:

$$H^{\mu\rho} = \frac{M^2}{2M_Z^2} [f_4^2 + \beta^2 f_5^2] I^{\mu\rho} \quad (5.57)$$

with

$$\begin{aligned} I^{\mu\rho} &= (\beta^2 + 1) [(q_2^\mu q_3^\rho + q_2^\rho q_3^\mu)] \\ &+ (\beta^2 - 1) [(q_2^\mu q_2^\rho + q_3^\rho q_3^\mu)] \\ &- \beta^2 g^{\mu\rho} M^2 \end{aligned} \quad (5.58)$$

and

$$\beta^2 = \left(1 - \frac{4M_Z^2}{M^2}\right) \quad (5.59)$$

Note that  $H^{\mu\rho}$  is symmetric in the indices so when we contract it with  $C_{\mu\rho}$  the anti-symmetric part of  $C_{\mu\rho}$  (the scary  $i$  term) vanishes. Neglecting the term proportional to  $m^2$  in  $C_{\mu\rho}$  and contracting gives:

$$\begin{aligned} C_{\mu\rho} H^{\mu\rho} &= \frac{4M^2}{M_Z^2} (g_V^2 + g_A^2) [f_4^2 + \beta^2 f_5^2] \\ &\times \left\{ [(p_1 \cdot q_2)(p_2 \cdot q_3) + (p_1 \cdot q_3)(p_2 \cdot q_2) - (p_1 \cdot p_2)(q_2 \cdot q_3)](\beta^2 + 1) \right. \\ &+ [(p_1 \cdot q_2)(p_2 \cdot q_2) + (p_1 \cdot q_3)(p_2 \cdot q_3) - M_Z^2(p_1 \cdot p_2)](\beta^2 - 1) \\ &\left. + M^2(p_1 \cdot p_2)\beta^2 \right\} \end{aligned} \quad (5.60)$$

In the C.O.M. system with massless quarks (i.e.  $E_q = |\mathbf{p}_q|$ ) we have the following relations:

$$\begin{aligned} q_1 &= (M, 0, 0, 0) \\ q_2 &= (E_Z, \mathbf{q}_2) \\ q_3 &= (E_Z, -\mathbf{q}_2) \\ p_1 &= (E_q, \mathbf{p}_q) \\ p_2 &= (E_q, -\mathbf{p}_q) \end{aligned} \quad (5.61)$$

Substituting these relations in 5.60 and manipulating the result we get:

$$\begin{aligned} C_{\mu\rho} H^{\mu\rho} &= \frac{4M^2}{M_Z^2} (g_V^2 + g_A^2) [f_4^2 + \beta^2 f_5^2] \\ &\times 2E_q^2 \left\{ [|\mathbf{q}_2|^2 (\cos^2 \theta - 1)] (\beta^2 + 1) \right. \\ &\left. + [|\mathbf{q}_2|^2 (1 - \cos^2 \theta)] (\beta^2 - 1) + M^2 \beta^2 \right\} \end{aligned} \quad (5.62)$$

Using the relation

$$\begin{aligned}
|\mathbf{q}_2|^2 &= E_Z^2 - M_Z^2 \\
&= \frac{M^2}{4} - M_Z^2 \\
&= \frac{M^2}{4} \beta^2
\end{aligned} \tag{5.63}$$

we get the result:

$$C_{\mu\rho} H^{\mu\rho} = \frac{4M^4\beta^2}{M_Z^2} (g_V^2 + g_A^2) [f_4^2 + \beta^2 f_5^2] [1 + \cos^2 \theta] \tag{5.64}$$

The squared amplitude summed over polarization (5.54) is now

$$X' = \frac{M^4\beta^2}{M_Z^2} \frac{[f_4^2 + \beta^2 f_5^2] (g_V^2 + g_A^2)}{(q_1^2 - M^2)^2 + \Gamma_{Z'}^2 M^2} E_q^2 [1 + \cos^2 \theta] \tag{5.65}$$

Here,  $\theta$  is the angle between the direction of motion of the quarks and the  $Z$  bosons in the  $Z'$  C.O.M. frame. For later convenience we define the quantity

$$A_{ZZ}(q_1) = \frac{M^4\beta^2}{M_Z^2} \frac{[f_4^2 + \beta^2 f_5^2] (g_V^2 + g_A^2)}{(q_1^2 - M^2)^2 + \Gamma_{Z'}^2 M^2} \tag{5.66}$$

and write the polarization sum as:

$$X' = A_{ZZ}(q_1) E_q^2 [1 + \cos^2 \theta] \tag{5.67}$$

## 5.7 Production cross sections

This section includes two subsections, one for each of the amplitudes calculated above. Although varying in calculational detail, the purpose of each section is the same:

1. Calculate total parton-level cross section  $\hat{\sigma}(\hat{s})$  from the polarization sums  $X'$
2. Express the total proton-level cross section  $\sigma$  in terms of the parton-level one
3. Write  $\sigma$  as an integral, which is to be numerically integrated.

Before we begin, we need the formula for the differential cross section in a frame where the colliding particles are moving collinearly:

$$d\hat{\sigma} = (2\pi)^4 \delta^{(4)} \left( \sum_i p_i - \sum_f p_f \right) \frac{1}{4E_1 E_2 v_{rel}} \left( \prod_f \frac{d^3 \mathbf{p}_f}{(2\pi)^3 2E_f} \right) X' \tag{5.68}$$

## 5. A NEW $Z'$ GAUGE BOSON?

---

In the C.O.M. frame of the quarks, where  $v_{rel} = 2$  and  $E_1 = E_2 = E_q$ , it reduces to:

$$d\hat{\sigma} = (2\pi)^4 \delta^{(4)} \left( p_1 + p_2 - \sum_f p_f \right) \frac{1}{8E_q^2} \left( \prod_f \frac{d^3 \mathbf{p}_f}{(2\pi)^3 2E_f} \right) X' \quad (5.69)$$

### 5.7.1 Production cross section for $Z'$

We here make use of the amplitude (5.39) substituted into (5.69). Here we have only one final particle, which gives the result:

$$d\hat{\sigma}(\hat{s}) = \frac{(g_V^2 + g_A^2)\pi}{2M} \delta^{(4)}(p_1 + p_2 - q) d^3 \mathbf{q} \quad (5.70)$$

Integrating and exploiting three of the delta functions we get:

$$\hat{\sigma}(\hat{s}) = \frac{(g_V^2 + g_A^2)\pi}{2M} \delta(2E_q - M) \quad (5.71)$$

The C.O.M. energy squared in this frame is  $\hat{s} = (p_1 + p_2)^2 = 4E_q^2$ . Now we have the parton-level cross section.

$$\hat{\sigma}(\hat{s}) = \frac{(g_V^2 + g_A^2)\pi}{2M} \delta(\sqrt{\hat{s}} - M) \quad (5.72)$$

We utilize (5.18) from the discussion of cross sections and convolution,

$$\frac{d^2 \sigma}{d\hat{s} dy} = \frac{(g_V^2 + g_A^2)\pi}{6Ms} F(\tau, y, Q^2) \delta(\sqrt{\hat{s}} - M) \quad (5.73)$$

For the integration over  $\hat{s}$  we need to transform the delta-function:

$$\delta(f(x)) = \sum_i \frac{1}{|f'(x_i)|} \delta(x - x_i), \text{ where } x_i \text{ are the values where } f(x_i) = 0 \quad (5.74)$$

In our case this means:

$$\delta(\sqrt{\hat{s}} - M) = 2M \delta(\hat{s} - M^2) \quad (5.75)$$

Integrating over  $\hat{s}$  yields:

$$\frac{d\sigma}{dy} = \frac{(g_V^2 + g_A^2)\pi}{3s} F\left(\tau = \frac{M^2}{s}, y, Q^2\right) \quad (5.76)$$

As mentioned before, the p.d.f.s are not analytically known so we have to do the last integral over rapidity numerically. The limits on the integral are decided in the following way:

$$y = \frac{1}{2} \ln \left[ \frac{x_q^2}{\tau} \right] \quad (5.77)$$

Here,  $\tau$  is held constant throughout the integration, with a value determined by the C.O.M. energies  $s$  and  $\hat{s}$ :

$$\tau = \frac{\hat{s}}{s} = \frac{200^2}{7000^2} = \frac{1}{35^2} \quad (5.78)$$

The maximum value of the variables are  $x_{q\max} = 1$ , therefore:

$$a \equiv y_{\max} = -y_{\min} \equiv -b = \frac{1}{2} \ln \left[ \frac{x_{q\max}^2}{\tau} \right] = \frac{1}{2} \ln \left[ \frac{1}{\tau} \right] \quad (5.79)$$

This gives limits on the rapidity between

$$-a = 3.55 = b \quad (5.80)$$

Having introduced the limits we will now modify them based on the following argument:

We are considering the rapidity of the  $q\bar{q}$  system in the proton-proton C.O.M. frame. Keeping  $\tau$  constant corresponds to fixing the C.O.M. energy of the colliding quarks  $\sqrt{\hat{s}}$ . Let us, with  $\tau$  constant, define the term ‘‘quark configuration’’ to mean that each quark carries a definite fraction of their respective proton’s momentum, but the quark energies still sum to  $\sqrt{\hat{s}}$ . For instance the situation where quark  $a$  has  $|\mathbf{p}_a| = 250$  GeV along  $+z$  and quark<sup>1</sup>  $b$  has  $|\mathbf{p}_b| = 50$  GeV along  $-z$  is one quark configuration. Using this terminology, the integral over rapidity corresponds to integrating over all different quark configurations. Remembering that a high absolute value for rapidity corresponds to a situation where the quarks have widely different fractions<sup>2</sup> of their respective proton’s momentum, we see the following: For a high value of the rapidity the  $q\bar{q}$  C.O.M. system tends to go with a sizable momentum in either the  $+z$  or  $-z$  direction. This means that the scattering products tend to align with the beam axis for high values of rapidity. Detectors, although extremely well built, have a hard time

---

<sup>1</sup>Strictly speaking, they are massless in this example and one should be an antiquark

<sup>2</sup>For example  $|\mathbf{p}_a| = 1$  GeV  $|\mathbf{p}_b| = 201$  GeV

## 5. A NEW $Z'$ GAUGE BOSON?

---

covering small angles<sup>1</sup>. This means that we do not detect the cases of high rapidity and so should subtract it from our proton-level cross section. We do this by using the so-called pseudorapidity. The pseudorapidity is a measure of the angle between the beam axis and particle momentum direction. For highly energetic collisions the numerical value of the rapidity is nearly equal to the numerical value of the pseudorapidity,  $\eta$ . A high value of  $\eta$  corresponds to a small angle (i.e. close to the beam axis). A good rule of thumb is  $\eta \sim 2.45 \rightarrow \theta \sim 10^\circ$ . Typical values of pseudorapidity that can be detected are  $|\eta| \leq 2.5$ . The inner detector at ATLAS at the LHC has this kind of limit on detection [17]. We therefore modify our limits to be

$$a = -2.5 = -b \quad (5.81)$$

and go on to evaluate the integral.

The integral is done in C++ with a program provided by my supervisor Per Osland. It was made by Alan Martin, who is a member of the MRST collaboration and a professor of physics at Durham University. With some small modifications it could be used to evaluate the integral over rapidity. The integral to be evaluated is:

$$\sigma = \frac{(g_V^2 + g_A^2)\pi}{3s} \int_a^b F\left(\frac{M^2}{s}, y, Q^2\right) dy \quad (5.82)$$

Using the weight function (5.4), we obtain the final expression for the production cross section:

$$\sigma = \frac{(g_V^2 + g_A^2)\pi}{3s} \int_a^b [2u(y)\bar{u}(y) + 2d(y)\bar{d}(y)] dy \quad (5.83)$$

This integral will come up again when we evaluate the other cross section. We will therefore give the value of the expression

$$\begin{aligned} I &= \frac{1}{s} \int_a^b F\left(\frac{M^2}{s}, y, Q^2\right) dy = \frac{1}{s} \int_a^b [2u(y)\bar{u}(y) + 2d(y)\bar{d}(y)] dy \\ &= 6.233 \times 10^{-5} \frac{1}{\text{GeV}^2} \end{aligned} \quad (5.84)$$

This is given in natural units. The conversion to  $\text{cm}^2$  is given by multiplying by appropriate factors of  $\hbar c$ . Given a number  $a$  of dimension  $\frac{1}{\text{GeV}^2}$  we do the following:

$$\begin{aligned} \hbar c &= 1.97 \times 10^{-11} \text{ MeV cm} \\ &= 1.97 \times 10^{-14} \text{ GeV cm} \end{aligned} \quad (5.85)$$

---

<sup>1</sup>There must be room for the beam pipe!

and so

$$\begin{aligned}
 a \left[ \frac{1}{\text{GeV}^2} \right] &= a(1.97 \times 10^{-14})^2 \text{ cm}^2 \\
 &= a \times 3.8910^{-28} \text{ cm}^2 \\
 &= a \times 3.8910^{-4} \text{ barn}
 \end{aligned} \tag{5.86}$$

The value of the integral in units of nanobarn is then:

$$I = 6.23 \times 10^{-5} \times 3.89 \times 10^{-4} \sim 24 \text{ nb} \tag{5.87}$$

### 5.7.2 Production cross section for ZZ

We here make use of the amplitude (5.67) substituted in (5.69). There are two final particles which gives:

$$\begin{aligned}
 d\hat{\sigma}(\hat{s}) &= A_{ZZ}(q_1) \frac{(2\pi)^4}{8} \delta^{(4)}(p_1 + p_2 - q_2 - q_3) \\
 &\times [1 + \cos^2 \theta] \frac{d^3 \mathbf{q}_2}{(2\pi)^3 2E_Z} \frac{d^3 \mathbf{q}_3}{(2\pi)^3 2E_Z}
 \end{aligned} \tag{5.88}$$

Arranging factors and using three of the four-delta functions we get:

$$d\hat{\sigma}(\hat{s}) = A_{ZZ}(q_1) \frac{1}{32(2\pi)^2} \delta(2E_q - 2E_Z) \frac{1}{E_Z^2} [1 + \cos^2 \theta] d^3 \mathbf{q}_2 \tag{5.89}$$

To use the final delta function we need to express the differential in an appropriate way. This will be done in spherical coordinates where the differential can be expressed:

$$\begin{aligned}
 d^3 \mathbf{q}_2 &= |\mathbf{q}_2|^2 d|\mathbf{q}_2| d(\cos \theta) d\varphi \\
 &= \frac{1}{2} |\mathbf{q}_2| d(|\mathbf{q}_2|^2) d(\cos \theta) d\varphi \\
 &= \frac{1}{2} |\mathbf{q}_2| d(E_Z^2 - M_Z^2) d(\cos \theta) d\varphi \\
 &= \frac{1}{2} |\mathbf{q}_2| E_Z d(2E_Z) d(\cos \theta) d\varphi
 \end{aligned} \tag{5.90}$$

Substituting this for the differential and integrating out the last delta function yields:

$$d\hat{\sigma}(\hat{s}) = A_{ZZ}(q_1) \frac{1}{64(2\pi)^2} \frac{|\mathbf{q}_2|}{E_Z} [1 + \cos^2 \theta] d(\cos \theta) d\varphi \tag{5.91}$$

Using the identity

$$\int_{-1}^1 dx (1 + x^2) = \frac{8}{3} \tag{5.92}$$

## 5. A NEW $Z'$ GAUGE BOSON?

---

and integrating out  $\theta$  and  $\varphi$  we obtain:

$$\begin{aligned}\hat{\sigma}(\hat{s}) &= A_{ZZ}(q_1) \frac{1}{48\pi} \frac{|\mathbf{q}_2|}{E_Z} \\ &= A_{ZZ}(q_1) \frac{1}{48\pi} \beta\end{aligned}\tag{5.93}$$

The relations for the squared C.O.M. energy in this frame are:

$$\begin{aligned}\hat{s} &= (p_1 + p_2)^2 \\ &= q_1^2\end{aligned}\tag{5.94}$$

We then have:

$$\hat{\sigma}(\hat{s}) = A_{ZZ}(\hat{s}) \frac{1}{48\pi} \beta\tag{5.95}$$

Collecting the function,  $A_{ZZ}(\hat{s})$ , from (5.65), gives the parton-level cross section:

$$\hat{\sigma}(\hat{s}) = \frac{M^4 \beta^3}{48\pi M_Z^2} \frac{[f_4^2 + \beta^2 f_5^2] (g_V^2 + g_A^2)}{(\hat{s} - M^2)^2 + \Gamma_{Z'}^2 M^2}\tag{5.96}$$

If we had used this function in our numerical integration of rapidity, we would have a function of  $\hat{s}$ . This function would have the characteristic Breit-Wigner shape (a peak indicating a resonance) for values around  $\hat{s} = M^2$ . We are interested in a production cross section, meaning a number equal (approximately) to the area under this peak. If we assume the  $Z$ -peak to be narrow, we can use the so-called the narrow-width approximation. It involves substituting the factor which comes from the propagator for a delta-function multiplied by a number. The delta function collapses the integral over  $\hat{s}$ , while the number is the correct area in the limit of an infinitely narrow peak. Mathematically we make the substitution:

$$\frac{1}{(\hat{s} - M^2)^2 + \Gamma_{Z'}^2 M^2} \longrightarrow \frac{\pi}{M\Gamma_{Z'}} \delta(\hat{s} - M^2)\tag{5.97}$$

The error in the approximation is usually assumed to be of order  $\sim \frac{\Gamma}{M}$ , although this is a topic of debate in the literature [18]. Using the narrow-width approximation we get:

$$\hat{\sigma}(\hat{s}) = \frac{M^3 \beta^3 [f_4^2 + \beta^2 f_5^2] (g_V^2 + g_A^2)}{48M_Z^2 \Gamma_{Z'}} \delta(\hat{s} - M^2)\tag{5.98}$$

Now we go on to consider the convolution integrand which takes the form:

$$\frac{d^2\sigma}{d\hat{s}dy} = \frac{M^3 \beta^3 [f_4^2 + \beta^2 f_5^2] (g_V^2 + g_A^2)}{48M_Z^2 \Gamma_{Z'}} \frac{1}{s} F(\tau, y, Q^2) \delta(\hat{s} - M^2)\tag{5.99}$$

Integrating out  $\hat{s}$  and writing this as an integral over rapidity we obtain.

$$\sigma = \frac{M^3 \beta^3 [f_4^2 + \beta^2 f_5^2] (g_V^2 + g_A^2)}{48 M_Z^2 \Gamma_{Z'}} \frac{1}{s} \int_a^b F\left(\tau = \frac{M^2}{s}, y, Q^2\right) dy \quad (5.100)$$

Observe that this is the same integral as we evaluated in the previous section.

## 5.8 Limits and experimental constraints

For this section we denote the production cross sections of  $Z'$  and  $ZZ$  by  $\sigma_{q\bar{q} \rightarrow Z'}$  and  $\sigma_{q\bar{q} \rightarrow Z' \rightarrow ZZ}$ , respectively. We will also compare the production cross section with the production cross section of a Higgs with mass 200 GeV. This cross section is of the order 10-20 fb (see section 6.1). To state something about the production cross sections and related quantities we need to have an overview of input versus output. Looking at the formulas (5.83) and (5.100) we see the following:

1. For given values of  $g_V$  and  $g_A$ , we know  $\sigma_{q\bar{q} \rightarrow Z'}$
2. For given values of  $g_V$ ,  $g_A$ ,  $f_5$ ,  $f_4$  and  $\Gamma_{Z'}$  we know  $\sigma_{q\bar{q} \rightarrow Z' \rightarrow ZZ}$

There is also another quantity that we can look at, which is the ratio of the two production cross sections:

$$BR(Z' \rightarrow ZZ) = \frac{\sigma_{q\bar{q} \rightarrow Z' \rightarrow ZZ}}{\sigma_{q\bar{q} \rightarrow Z'}} = \frac{\Gamma_{Z' \rightarrow ZZ}}{\Gamma_{Z'}} \quad (5.101)$$

Inserting the expressions for the production cross sections (5.99) and (5.82) in (5.101) we see that all the information needed to obtain  $BR(Z' \rightarrow ZZ)$  are the values of  $f_4$  and  $f_5$ .

$$BR(Z' \rightarrow ZZ) = \frac{[f_4^2 + \beta^2 f_5^2] M^3 \beta^3}{16\pi M_Z^2 \Gamma_{Z'}} \quad (5.102)$$

We find the production cross section for  $q\bar{q} \rightarrow Z' \rightarrow ZZ \rightarrow 4l$  by multiplying  $\sigma_{q\bar{q} \rightarrow Z'}$  by the branching ratio for  $Z' \rightarrow ZZ$  and the square of the branching ratio for  $Z \rightarrow ZZ$ :

$$\sigma_{q\bar{q} \rightarrow Z' \rightarrow ZZ \rightarrow 4l} = \sigma_{q\bar{q} \rightarrow Z'} \times BR(Z' \rightarrow ZZ) \times BR^2(Z \rightarrow 2l) \quad (5.103)$$

The branching ratio for  $Z \rightarrow 2l$  is universal (i.e. equal for all generations) and has the value  $BR(Z \rightarrow 2l) \sim 0.034$  [19]. One should note here that all leptons are equal in our case. We now want to estimate an upper limit on this cross-section derived from

## 5. A NEW $Z'$ GAUGE BOSON?

---

experimental constraints.

We start with the branching ratio  $BR(Z' \rightarrow ZZ)$ . Plugging the masses

$$\begin{aligned} M &= 200 \text{ GeV} \\ M_Z &= 91 \text{ GeV} \end{aligned} \tag{5.104}$$

into (5.102) results in

$$BR(Z' \rightarrow ZZ) \sim 1.37 \frac{[f_4^2 + 0.172f_5^2]}{\Gamma_{Z'}} \tag{5.105}$$

We do not know much about the total decay width of the  $Z'$  and so will use a result from the paper on the Landau-Yang theorem [1]. Simulations are done using MAD-EVENT<sup>1</sup>, followed by hadronization and showering in PYTHIA. Using a  $Z'$  mass of 240 GeV, they estimate the decay-width to be around 12 GeV. We will assume the decay width to be in this neighbourhood, but lower. Looking back to (2.1) we see that the total decay width of a particle depends on both its interactions with other particles (Feynman amplitude) and its mass (phase-space factor). If two particles have the same interactions, but different mass, the one with the highest mass has the largest width. Based on this and the fact that we want to overestimate the cross section, we set the decay width to  $\Gamma_{Z'} = 4 \text{ GeV}$ .

We will also consider another assumption, namely that the constants  $f_4$  and  $f_5$  are constrained from analysing LEP data by the so-called anomalous Triple Gauge Boson (TGB) couplings.<sup>2</sup> The TGB couplings have the same Lorentz structure as our couplings, on account of it being three spin-1 particles, but they differ in that they are multiplied by a factor dependent on the C.O.M. energy. This factor makes the coupling disappear for on-shell particles on account of Bose symmetry (i.e. all three particles are  $Z$ s). The constraints are [20]<sup>3</sup>:

$$\begin{aligned} |f_4| &\leq 0.30 \\ |f_5| &\leq 0.38 \end{aligned} \tag{5.106}$$

---

<sup>1</sup>A program that produces parton-level events in accordance with SM and BSM theories and interfaces with PYTHIA

<sup>2</sup>Warning: This is not necessarily a valid assumption!

<sup>3</sup> In [20] they estimate expected bounds from Atlas on  $f_4$  and  $f_5$  to be  $\sim 0.01$  at  $1 \text{ fb}^{-1}$ .

## 5.8 Limits and experimental constraints

---

Letting these values be maximal and using the decay width above we get:

$$BR(Z' \rightarrow ZZ) \leq 0.04 \quad (5.107)$$

If we now insert the value of the convolution integral (5.84) of 24.3 nb into (5.83) and collect everything with (5.103) and the known branching ratios, we get the final production cross section as a function of  $g_V$  and  $g_A$ :

$$\sigma_{q\bar{q} \rightarrow Z' \rightarrow ZZ \rightarrow 4l} \leq (g_V^2 + g_A^2) \times 0.7 \text{ fb} \quad (5.108)$$

For comparison: If we do the same procedure, but assume that the LEP II constraints are not valid for the TGBs and that the coupling constants  $f_4, f_5$  are of order 1, we get:

$$\sigma_{q\bar{q} \rightarrow Z' \rightarrow ZZ \rightarrow 4l} \leq (g_V^2 + g_A^2) 11.2 \times \text{fb} \quad (5.109)$$

Considering for a moment, the case of a  $Z'$  that mixes with the  $Z$  there are additional constraints from the EWPT measurements at LEP. This is because the mixing distorts the  $Z$  properties, which are well measured. In general constraints on  $Z'$  from EWPT at electron-positron colliders fall into two categories: Precision measurements at the  $Z$ -pole and measurements of  $e^+e^- \rightarrow f\bar{f}$  at C.O.M. energies up to  $s = 209$  GeV (LEP II)[21] (see chapter 4).

Now we come to the question of the strength of the fermion couplings. If these were sizable, the  $Z'$  would couple strongly to all fermions<sup>1</sup>. This would mean that it could be produced in significant amounts at electron-positron colliders. Consequently it would be easy to detect for instance at LEP II, which had a C.O.M. energy of about 209 GeV. If we assume it to act as the SM  $Z$  boson with regards to fermions, the mass limit as given in [19] exceeds 1 TeV, which is not good for our case. So we further assume that the couplings cannot be of the SM type.

In [22], they estimate the LEP II bounds on a  $Z'$  from a  $U(1)$ -type model with slightly larger couplings to leptons than quarks. Their result is that the lepton coupling is at most of the order  $10^{-2}$  for  $Z'$  masses between  $M_Z = 91$  GeV and 213 GeV. Adopting this attitude results in a negligible cross section compared to the Higgs one and is

---

<sup>1</sup>Assuming universality of couplings as in SM

## 5. A NEW $Z'$ GAUGE BOSON?

---

therefore not desirable.

There are some  $U(1)$  theories that yield what is referred to as a leptophobic  $Z'$ , which couples weakly to leptons, but not quarks [23]. In such theories we could set the coupling constants higher and blame non-observation on the fact that it could not be produced at electron-positron colliders. This type of theory falls under the more general case where the  $Z'$  couples non-universally to fermions. In [22], they comment on the fact that it is possible to have a zero coupling between  $Z'$  and the electron<sup>1</sup>. This would invalidate the LEP-II bounds since the electron does not couple to  $Z'$ . Here we could in principle adjust the couplings to larger values for the other fermions and enhance the cross section. This could again be constrained by the fact that there would be an excess of jets at hadron colliders<sup>2</sup>. This, because the stronger ( $Z'q\bar{q}$ ) coupling both increases the production and decay of  $Z'$ s from and to  $q\bar{q}$ .

In summary we see that SM-like  $Z'$ s are unlikely, while leptophobic or non-universal  $Z'$ s could in principle enhance the cross section. If we assume that the ( $Zq\bar{q}$ ) coupling constants can be made to be of order  $\sim 1$  and make an order-of-magnitude comparison between the  $Z'$  and Higgs production cross sections we get:

1. If LEP-II bounds on  $f_4, f_5$  apply, they imply a negligible cross section,  $\frac{\sigma}{\sigma_H} \sim 0.1$
2. If  $f_4, f_5$  are  $\approx 1$ , they are of the same order,  $\frac{\sigma}{\sigma_H} \sim 1$

As a last option, we could consider the case where  $f_4$  and  $f_5$  are stronger. To increase the production by one order of magnitude compared to the Higgs cross section they would have to be  $\approx 3$ . This would probably modify the  $Z$  pole measurements at LEP by a large amount, since the numerical value of the couplings are quite high.

---

<sup>1</sup>They consider a Minimal Supersymmetric Model in this case

<sup>2</sup>A comment, with regards to the “bump” reported at 150 GeV at the Tevatron: This could be such an excess of jet signals. The measurement concerns an excess in the total amount of states decaying to one W boson and two jets. An example of a leptophobic explanation for this can be found in [24]

## Chapter 6

# A Scalar Signature

We will now consider the process  $S \rightarrow ZZ \rightarrow 4l$ , where  $S$  is some scalar particle, but we will not calculate a production cross section. Instead we will look at how a Two-Higgs-Doublet-Model (2HDM) could enhance the total production cross section. In the SM we have only one such scalar particle, namely the Higgs boson. First we will go through the SM Higgs, then consider the 2HDM enhancement of our “golden cross section”.

### 6.1 The SM Higgs in the Golden Channel

Considering a SM Higgs in the golden channel with the Higgs mass set to 200 GeV, we have three quantities, besides  $BR(Z \rightarrow 2l)$ , that are known:

1. The branching ratio of the Higgs,  $BR(H \rightarrow ZZ)$
2. The total production cross section of the Higgs,  $\sigma(pp \rightarrow H)$
3. The total decay width of the Higgs,  $\Gamma_H$

The above branching ratio can be found from Figure 2.1 and is approximately  $\sim \frac{1}{3}$ . One should note that this branching fraction does not vary significantly as the Higgs mass increases.

Higgs-fermion-fermion couplings are important when considering the production of

## 6. A SCALAR SIGNATURE

---

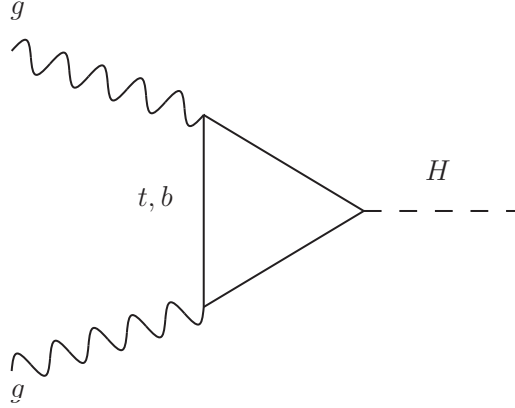


**Figure 6.1:** Gluon fusion, the dominant contribution to Higgs production at the LHC [25]

the Higgs at the LHC. The  $(Hf\bar{f})$  couplings are proportional to the fermion mass. Specifically their vertex factor is given by [6]

$$(Hf\bar{f}) = \frac{-i}{v}m_f \quad (f = l, q) \quad (6.1)$$

Naively, this suggests that the dominant contribution to Higgs production from fermion couplings should come from the top quark, since it is the heaviest fermion ( $m_t = 172 \text{ GeV}$  [19]). This is what happens, but not via a direct coupling<sup>1</sup> as one might assume. The p.d.f.s described in chapter 5 give a negligible top-quark content for protons and so the direct production from top quarks is vanishingly small. This means that the lighter quarks should produce more Higgs bosons directly than the top quark. The dominance of the top-quark contribution comes from a so-called triangle diagram for gluon fusion. Figure 6.1<sup>2</sup> shows the Feynman diagram for gluon fusion. . Even though such 1-loop diagrams usually contribute less than the tree level diagrams, the top mass is a factor 40000 larger than the light quarks The top-quark therefore provides the dominant contribution to Higgs production. In fact, for Higgs production at the LHC, the dominant production mechanism for all Higgs masses is through the gluon fusion diagram with a top triangle loop [6].

---

<sup>1</sup>Direct coupling here meaning coupling between colliding quarks and produced Higgs

<sup>2</sup>Had to use photon lines for gluons, due to a bug in jaxodraw

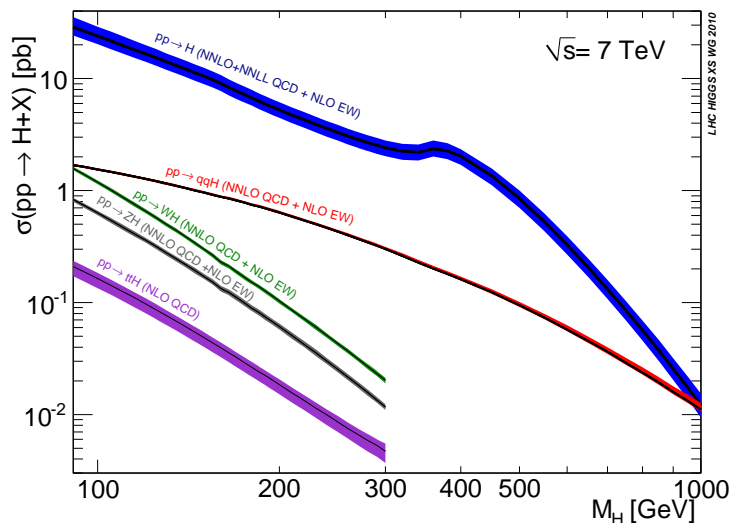


**Figure 6.2:** The total production cross section for  $p\bar{p} \rightarrow H + X$  at the LHC [25]

The total production cross section of the Higgs at the LHC, stems from reactions of the type,

$$p + p \longrightarrow H + X \quad (6.2)$$

where  $X$  is some hadron final state that satisfies appropriate conservation laws [6]. Calculations of the total production cross sections as a function of the Higgs mass results in plots as in Figure 6.2.

The Higgs boson can in principle decay into both fermions and gauge bosons. As mentioned in chapter 2 though, the mass region we are interested in ( $190 \text{ GeV} \leq M_H \leq 300 \text{ GeV}$ ) is completely dominated by the  $W^+W^-$  and  $ZZ$  modes (compare Figure 2.1). The total decay width is therefore to a good approximation,  $\Gamma(H \rightarrow ZZ) + \Gamma(H \rightarrow W^+W^-)$ . In Figure 6.3 the total decay width as a function of the Higgs mass is shown.

Using these plots we can read off values that enable us to estimate the SM cross section in the golden channel for a 200 GeV Higgs. We estimate it by the expression:

$$\sigma = \sigma(pp \rightarrow H) \times BR(H \rightarrow ZZ) \times BR^2(Z \rightarrow 2l) \quad (6.3)$$

## 6. A SCALAR SIGNATURE

---

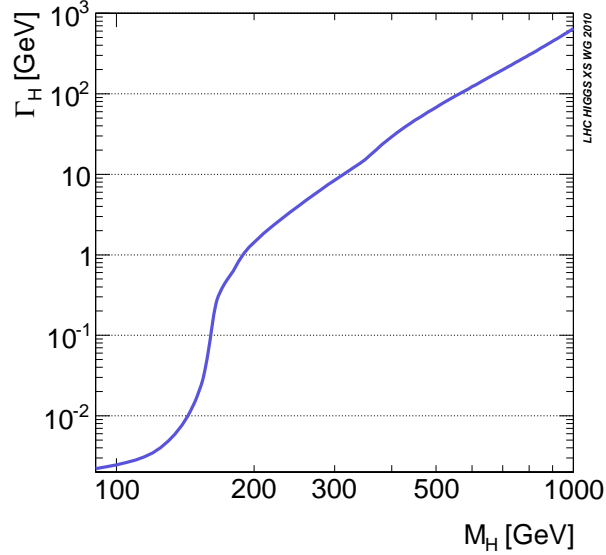


**Figure 6.3:** The total decay rate as a function of the Higgs mass [25]

The values

$$\begin{aligned}
 \sigma(pp \rightarrow H) &= 4.5 \pm 1 \text{ pb} \\
 BR(H \rightarrow ZZ) &= \frac{1}{3} \pm 0.05 \\
 BR(Z \rightarrow 2l) &= 0.034
 \end{aligned}
 \tag{6.4}$$

result in

$$\sim 11 \text{ fb} \leq \sigma \leq 24 \text{ fb}
 \tag{6.5}$$

Now that we have a rough understanding of how the SM Higgs behaves in the golden channel, we take a look at the 2HDM and possibilities for enhancing this cross section.

### 6.2 The Two-Higgs-Doublet Model

The Two-Higgs-Doublet model (2HDM) is an extension of the SM Higgs sector. As the name implies one adds a second complex scalar doublet in the Weinberg-Salam potential (3.46). A feature of theories with electroweak Higgs singlets or doublets is that the parameter  $\rho$ , discussed in chapter 4, is equal to 1 at tree level [26]. This makes the relationship between the 2HDM and the EWPT somewhat less strained. In addition to this property, some theoretical motivation can be found in the following consideration.

One can compare the 2HDM to the Minimal Supersymmetric Standard Model (MSSM), which also has a Higgs sector with two complex scalar doublets [12]. One of the differences is that at tree level, the MSSM Higgs sector can be parametrized by two independent quantities, while the 2HDM has more free parameters. In MSSM though, Supersymmetry leads to relations between Higgs masses and couplings. However, due to the fact that Supersymmetry (if valid) must be broken, these relations can change. Beyond tree level there are effects of Supersymmetry breaking that can enter through loop corrections and modify these relations [27]. The philosophy could therefore be that the 2HDM is an effective way of parametrizing the MSSM.<sup>1</sup>

### 6.2.1 The 2HDM Potential

To get a grip on the 2HDM potential, we will write down the most general potential possible for two scalar doublets and make some comments. The justification for doing it this way is that in the literature, different parametrizations arise and one is easily distracted by thinking about where these parametrizations come from. The constants  $\lambda_i$  and  $m_{ij}$   $i, j = 1, 2$ , which are typically used, often differ slightly. This means that the comments regarding the terms made below, should be thought of as a comment of the specific term, not including the constant. The most general gauge-invariant potential for two scalar doublets is [26]:

$$\begin{aligned}
 V(\Phi_1, \Phi_2) = & m_{11}^2 \Phi_1^\dagger \Phi_1 + m_{22}^2 \Phi_2^\dagger \Phi_2 - [m_{12}^2 \Phi_1^\dagger \Phi_2 + \text{H.c.}] \\
 & + \frac{\lambda_1}{2} (\Phi_1^\dagger \Phi_1)^2 + \frac{\lambda_2}{2} (\Phi_2^\dagger \Phi_2)^2 + \lambda_3 (\Phi_1^\dagger \Phi_1) (\Phi_2^\dagger \Phi_2) \\
 & + \lambda_4 (\Phi_1^\dagger \Phi_2) (\Phi_2^\dagger \Phi_1) \\
 & + \left\{ \frac{\lambda_5}{2} (\Phi_1^\dagger \Phi_2)^2 + [\lambda_6 \Phi_1^\dagger \Phi_1 + \lambda_7 \Phi_2^\dagger \Phi_2] \Phi_1^\dagger \Phi_2 + \text{H.c.} \right\}
 \end{aligned} \tag{6.6}$$

In general the parameters  $m_{12}^2$ ,  $\lambda_5$ ,  $\lambda_6$  and  $\lambda_7$  can be complex, while the rest are real. Some remarks regarding the different terms in the potential will now be made:

1. The terms proportional to  $\lambda_6$  and  $\lambda_7$  cause Flavour Changing Neutral Currents (FCNC). FCNCs change fermion flavour, without changing the electric charge.

---

<sup>1</sup> It does not have to be, the 2HDM does well enough on its own

## 6. A SCALAR SIGNATURE

---

They are severely constrained by experiment and consequently  $\lambda_6$  and  $\lambda_7$  must be small enough to incorporate this [12]<sup>1</sup>.

2. Demanding that the potential be bounded from below (since we need a lowest-energy state), one extracts a number of inequalities the parameters must satisfy [26], thereby constraining the parameters of the model.
3. Explicit and spontaneous<sup>2</sup> CP violation can be avoided by constraining parameters. For instance, a sufficient condition for not having explicit CP violation is taking all coefficients to be real [26].

These constraints are typically applied in different ways, depending on what properties one wants in the model (e.g. CP violating, small FCNC etc.). The literature therefore often contains a wide variety of different potentials. Before moving on, we should mention one more thing: Sometimes, the parameters in the potential are exchanged with a set of more physical parameters like the mass of a Higgs particle or the ratio of the VEVs of the two fields (named  $\tan\beta$ ). This will be the case, when we look at an example of a 2HDM. Having gained a few insights into the 2HDM-potential and its appearance, we now move on to the Yukawa couplings.

### 6.2.2 Yukawa Couplings

There are several ways Yukawa couplings enter in the literature. The most popular are quite nondescriptively referred to as model I, II and III. Model III contains the most general Yukawa couplings for two complex scalar doublets. [27]. The distinction between model I and II lies in how quarks acquire mass. In model I, the quarks of up and down type couple to only one of the Higgs doublets. In model II, the quarks of up type couple to one doublet and the quarks of down type to the other. Additionally the model II reproduces the Higgs-fermion coupling structure in the MSSM [2].

These different choices of models are related to the Flavour Changing Neutral Currents. It has been shown that FCNCs do not appear in the Yukawa couplings if the

---

<sup>1</sup> Introducing a discrete symmetry in the potential  $\Phi_1 \rightarrow -\Phi_1$  makes these terms and the  $m_{12}$  term vanish. The  $m_{12}$  term can be allowed under certain conditions [26].

<sup>2</sup>One has a formal definition of a CP transformation. If the Lagrangian is not invariant under this transformation we have explicit symmetry breaking. The idea of spontaneous CP-violation is analogous to SSB in EW theory, namely that the solution is not invariant under this transformation.

following condition is satisfied [28]: Quarks of one flavour couple at most to one of the Higgs doublets. This is automatically satisfied by models of type I and II. The more general type-III model have such FCNC terms and consequently one must be careful to keep the contributions small enough [27]. Now we will look at a specific 2HDM(II) and its phenomenology.

### 6.2.3 A 2HDM(II) Example

If we let the Higgs potential have real parameters, no FCNC terms and the type-II Yukawa couplings, the following phenomenological<sup>1</sup>, picture arises. There are five physical particles associated with the Higgs field. Two charged  $H^\pm$ , two neutral  $h^0, H^0$  (CP even) and another neutral  $A^0$  (CP odd), called a pseudoscalar. The charged pair has the same mass, while the neutral pair has a mass hierarchy  $M_{h^0} \leq M_{H^0}$ . The model has six independent parameters, they are:

1. Light, neutral Higgs mass,  $M_{h^0}$
2. Heavy, neutral Higgs mass,  $M_{H^0}$
3. Pseudoscalar mass,  $M_{A^0}$
4. Charged Higgs mass,  $M_{H^\pm}$
5. The ratio of the VEV's of the two fields  $\tan \beta = \frac{v_2}{v_1}$
6. A Higgs mixing angle,  $\alpha$

In general, having more free parameters than these does not change the amount of particles associated with the Higgs fields. The reason is that two complex scalar doublets has 8 degrees of freedom before SSB. After SSB, three of these are eaten by the gauge bosons. This leaves five scalar particles to be associated with the doublet. Two must be charged, for consistency with EW charge assignment. The remaining three are neutral.

We here make some notes regarding  $\tan \beta$ . Before choosing Yukawa couplings it is a physically meaningless quantity. This is because it does not appear in any couplings and therefore does not affect particle interactions. On the other hand, when one chooses

---

<sup>1</sup>All the facts presented in this paragraph can be found in [2]

## 6. A SCALAR SIGNATURE

---

the type-II Yukawa couplings one picks out a preferred direction in  $\Phi_1, \Phi_2$  space, which makes  $\tan \beta$  appear in the couplings [27]. Another important fact is that the parameter is equal to the ratio of the two VEVs of each Higgs doublet, but the expression

$$v = \sqrt{v_1^2 + v_2^2} = 246 \text{ GeV} \quad (6.7)$$

is fixed and equal to the usual SM VEV. This means that we can in principle, take  $\tan \beta$  as large ( $v_2 \gg v_1$ ) or small ( $v_1 \gg v_2$ ) as we like. We can also write this as,

$$\begin{aligned} v_1 &= v \cos \beta \\ v_2 &= v \sin \beta \end{aligned} \quad (6.8)$$

where the effects on  $\sin \beta$  and  $\cos \beta$  in the limits described above, are easier to see. Explicitly they are:

$$\begin{aligned} \sin \beta &\approx 1, \cos \beta \approx 0, & \text{for } \tan \beta \gg 1 \\ \sin \beta &\approx 0, \cos \beta \approx 1, & \text{for } \tan \beta \ll 1 \end{aligned} \quad (6.9)$$

The choice of  $\tan \beta$  is also constrained by experimental measurements, an issue we will return to later on. We will now pick the next-to lightest, neutral Higgs boson as the golden channel candidate and investigate its couplings to quarks in a type II model.

### 6.3 Neutral Higgs Couplings and Higgs Production

In a 2HDM(II) the neutral Higgses can couple with different strengths to fermions in a way that depends on the parameter  $\tan \beta$  and some mixing angles. The example we will use is from [12, 29], where a 2HDM of type II is considered. In these papers, the Higgses (denoted as  $H_i$ ) couple to the top and bottom quarks through:

$$(H_i t \bar{t}) = \frac{1}{\sin \beta} [R_{i2} - i\gamma_5 \cos \beta R_{i3}] \quad (6.10)$$

$$(H_i b \bar{b}) = \frac{1}{\cos \beta} [R_{i1} - i\gamma_5 \sin \beta R_{i3}] \quad (6.11)$$

Here, the couplings are given relative to the SM ones. The  $R_{ij}$  are the  $i$ 'th and  $j$ 'th component of a rotation matrix  $R$ , responsible for diagonalizing the mass-squared matrix of the neutral sector. More explicitly, the neutral sector contains the three fields  $\eta_1, \eta_2$  and  $\eta_3$ . The rotation matrix  $R$  transform the basis of weak eigenbasis  $(\eta_1, \eta_2, \eta_3)^T$  into the basis of mass eigenstates  $(H_1, H_2, H_3)^T$ . We see that the top-quark coupling (ignoring the mixing angles for now) is inversely proportional to  $\tan \beta$ , while the bottom-quark

### 6.3 Neutral Higgs Couplings and Higgs Production

---

coupling is proportional to it.

At first glance this seems like a neat way of increasing the Higgs-production cross section in the golden channel. The idea is simply that the SM vertex between quarks and Higgs in the gluon-fusion diagram shown in 6.1 gets multiplied by the above couplings. For the top-triangle case the factor varies as  $\cot \beta$ , while the bottom-quark varies as  $\tan \beta$ . We could now make  $\tan \beta$  small (large) and thereby enhance the top(bottom)-quarks production of the light Higgs. Let us investigate this more closely:

Since the coupling  $Hf\bar{f}$  is proportional to the fermion mass in the SM, the cross section for Higgs production through gluon fusion is proportional to the square of the fermion mass. In our case we have the modified couplings (6.10) and (6.11). Introducing these couplings in the  $(Hq\bar{q})$  vertex of Figure 6.1 changes the spinor structure of the amplitude because of  $\gamma_5$ . Making an estimate on the enhancement of the cross section is therefore a tricky job, since it involves the spinor structure of the triangle diagrams. We will therefore make a simplifying assumption with regards to the mixing angles. The assumption will make the spinor structure “factorizable”, meaning that the 2HDM(II) amplitude will just be a complex number times the SM amplitude. We will choose the heaviest of the CP even Higgses,  $H_2$  as our candidate for enhancing the cross section. As a simple choice of mixing angles that makes the coupling factorizable we choose the mixing angle constraint  $\sin \alpha_3 = 0$  (which implies  $\cos \alpha_3 = 1$ ). We are also interested in the  $H_2$ s coupling to the  $Z$  as this will be needed to estimate the enhancement. Taking  $\alpha_3 = 0$ , the relevant couplings of  $H_2$  become:

$$(H_2 t\bar{t}) = \frac{1}{\sin \beta} \cos \alpha_1 \equiv \frac{c_1}{s_\beta} \quad (6.12)$$

$$(H_2 b\bar{b}) = -\frac{1}{\cos \beta} \sin \alpha_1 \equiv -\frac{s_1}{c_\beta} \quad (6.13)$$

$$(H_2 ZZ) = [-\cos \beta \sin \alpha_1 + \sin \beta \cos \alpha_1] \equiv [s_\beta c_1 - c_\beta s_1] \quad (6.14)$$

Equipped with a set of new and more managable couplings we go on to consider the top and bottom contributions to gluon fusion.

In the SM, couplings between Higgs and fermion are, as mentioned before, proportional to the mass of the fermions. Within the SM, the top-quark triangle diagram is

## 6. A SCALAR SIGNATURE

---

the dominant contribution to Higgs production through gluon fusion. In our scenario this is not necessarily so. For instance, a large value of  $\tan\beta$  (i.e.  $\cos\beta \rightarrow 0$ ) makes the down type quarks couple more strongly than the up type. One could then imagine that as  $\tan\beta$  is increased, the bottom contribution will at some point be comparable to the top contribution. In fact, for a large enough value of  $\tan\beta$  even the light down type quarks could contribute more than the top (it would have to be *very* large for this to occur<sup>1</sup>). If the two amplitudes (top and bottom) are comparable in magnitude, the interference terms will give a significant contribution. Therefore we would like to introduce some measure, which would enable us to estimate the relative contribution of the top and bottom quarks. The ratio of the top and bottom squared amplitudes for gluon fusion should do. It is equal to:

$$\begin{aligned}
 \frac{|\mathcal{M}_{\text{top}}|^2}{|\mathcal{M}_{\text{bottom}}|^2} &= \frac{|H_1 t\bar{t}|^2 m_t^2}{|H_1 b\bar{b}|^2 m_b^2} \\
 &\sim 1600 \frac{|H_1 t\bar{t}|^2}{|H_1 b\bar{b}|^2} \\
 &= \frac{1600 \cos^2 \alpha_1}{\tan^2 \beta \sin^2 \alpha_1} \\
 &\equiv 1600 \frac{c_1^2}{t_\beta^2 s_1^2}
 \end{aligned} \tag{6.15}$$

Some comments on this expression are in order:

1. The expression (6.15) only measures the *relative* contribution of the top and bottom Higgs production from gluon fusion<sup>2</sup>.
2. If (6.15)  $\sim 1600$ , we adopt the same attitude as in the SM, which is that the top-quark contribution dominates
3. If (6.15) is of order  $\sim 1$ , interference effects between the two triangle diagrams become important in calculating the total production cross section from gluon fusion

---

<sup>1</sup>In this case  $\tan\beta$  must enhance the couplings by a factor  $\frac{m_t^2}{m_{\text{down-quark}}^2}$ , to make triangle contributions of light quarks comparable to the top ones. The larger p.d.f. contribution of light quarks would lower this  $\tan\beta$  value because of direct production. In any case the bottom quark would probably dominate through gluon fusion.

<sup>2</sup>For instance the case  $t_\beta = 1$ ,  $s_1 = c_1$ , gives the same ratio as in the standard model, but the couplings are clearly not the SM ones.

4. In the limit  $t_\beta \gg 1$ , the bottom-quark production dominates
5. In the limit  $t_\beta \ll 1$ , the top-quark production dominates
6. The choice of mixing angles that make  $\tan\alpha_1 \rightarrow \infty$  and  $\tan\alpha_1 = 0$ , just reflects the fact that the couplings to one of the quarks are turned off and our measure is not very useful in these limits.

The third comment is related to the fact alluded to above: We can no longer assume the dominant contribution to come from the top quark, because the bottom quark might very well couple more strongly to  $H_2$  than the top in this framework. The two limiting results above is what one would expect as the two cases correspond to enhancing one of the couplings in (6.13) or (6.12), while simultaneously decreasing the other. Armed with these facts we go on to investigate the charged Higgs and some limitations on  $\tan\beta$ .

## 6.4 Experimental restrictions on $\tan\beta$

Restrictions on the 2HDM can be divided into three categories [30]:

1. Theoretical consistency constraints
2. Experimental restrictions on the charged section
3. Experimental restrictions on the neutral sector

We will here go through the experimental restrictions on the charged and neutral sector.

The charged Higgs has couplings to the heavy quarks given by<sup>1</sup>:

$$\begin{aligned} (H^+ b\bar{t}) &= \frac{ig}{2\sqrt{2}m_W} [m_b(1 - \gamma_5) \tan\beta + m_t(1 + \gamma_5) \cot\beta] \\ (H^- t\bar{b}) &= \frac{ig}{2\sqrt{2}m_W} [m_b(1 + \gamma_5) \tan\beta + m_t(1 - \gamma_5) \cot\beta] \end{aligned} \tag{6.16}$$

Note that the charged sector contains no mixing angles since these are associated with the neutral sector. On the other hand, the sector does contain factors of  $\tan\beta$  and  $\cot\beta$ . For small or large  $\tan\beta$  the charged Higgs's couplings are enhanced. This contributes

---

<sup>1</sup>Couplings in (6.16) and (6.14) are still from [12]a [29]

## 6. A SCALAR SIGNATURE

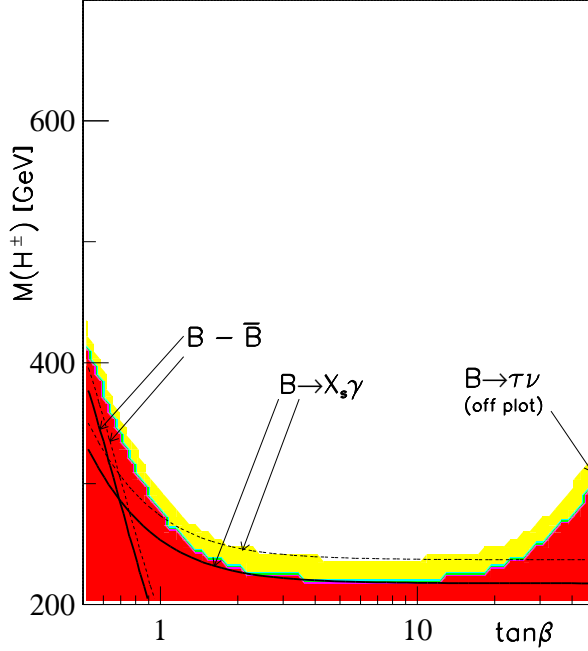


**Figure 6.4:** Experimental constraints on the charged Higgs sector, from [30]. The white areas are not excluded. Solid lines: 95% C.L., Dashed lines: 90% C.L., Colored: Joint exclusion at 90% and 95% C.L. Figure from [30]

to effects that are well measured in experiments. They therefore provide constraints for the 2HDM(II). All constraints on the charged sector come from  $B$  physics. In particular, contributions from:

1.  $B_d^0 - \bar{B}_d^0$  mixing
2. The process  $B \rightarrow \tau\nu$
3. The process  $B \rightarrow X_s\gamma$ , where  $X_s$  is a meson containing an  $s$  quark

constrain the charged sector of the theory. These constraints can typically be relaxed if we choose the charged Higgs to have a large mass [12]. Also, they depend on the parameter  $\tan\beta$ , which decides the quark couplings to the charged Higgs. The Figure 6.4 shows a plot of  $\tan\beta$  versus the charged Higgs mass, with excluded regions. As one can see, the data for  $B$  mixing and  $B \rightarrow X_s\gamma$ , typically constrain the theory at low

$\tan\beta$ , while  $B \rightarrow \tau\nu$  constrain it at high  $\tan\beta$ <sup>1</sup>.

In [28] a global fit of parameters was made for such a 2HDM(II). The model seemed to prefer rather low values for the two lightest Higgs. Based on this we want to pick the next to lightest neutral Higgs as our 200 GeV resonance and keep the lightest Higgs around 100 GeV. We now take into account neutral sector constraints and deal with them in due order. These constraints come from:

1. Lack of discovery at LEP II
2. Decay width of  $Z \rightarrow b\bar{b}$ , measured by the branching ratio often denoted  $R_b$
3.  $\Delta\rho$
4. The muon anomalous magnetic moment,  $(g-2)_\mu$

If we want to have a small mass for the lightest neutral Higgs we have to explain the non-discovery of this at LEP. Which means that we must look at its couplings to  $Z$ . Also the common decay channel  $H_1 \rightarrow b\bar{b}$  must be taken into account. In [12], the expression

$$\sigma_{Z(h \rightarrow X)} = \sigma_{Zh}^{ew} \times C_{Z(h \rightarrow X)}^2 \quad (6.17)$$

is used to exclude or allow values for different parameters. Here,  $\sigma_{Zh}^{ew}$  is the SM cross section for Higgs-Strahlung<sup>2</sup> for a particular value of the Higgs mass, while  $C_{Z(h \rightarrow X)}^2$  is a dilution<sup>3</sup> factor, that can account for the wanted reduction of the Higgs-Strahlung cross section. The effects described above are effectively parametrized by this dilution factor. It is defined as [12]:

$$C_{Z(h \rightarrow X)}^2 = [c_\beta R_{11} + s_\beta R_{12}]^2 \frac{1}{c_\beta^2} [R_{11}^2 + s_\beta^2 R_{13}^2] \quad (6.18)$$

For us this reduces to:

$$C_{Z(h \rightarrow X)}^2 = [c_\beta c_1 c_2 + s_\beta s_1 c_2]^2 \frac{1}{c_\beta^2} [c_1^2 c_2^2 + s_\beta^2 s_2^2] \quad (6.19)$$

<sup>1</sup>Even though this curve is off the particular plot

<sup>2</sup>Alongside  $W^+W^-$  fusion, the most important channel for potential Higgs discovery at LEP II [31]

<sup>3</sup>Since it, for the right choice of mixing angles and  $\tan\beta$ , can dilute the 2HDM Higgs-Strahlung cross section compared with the SM one.

## 6. A SCALAR SIGNATURE

---

This expression will be used to incorporate the LEP measurements. In [12] a rough estimate gives:

$$\begin{aligned} C_{Z(h \rightarrow X)}^2 &\sim 0.2 \text{ at } M_{H_1} = 100 \text{ GeV} \\ C_{Z(h \rightarrow X)}^2 &\sim 0.1 \text{ at } M_{H_1} = 80 \text{ GeV} \end{aligned} \quad (6.20)$$

We adopt their philosophy and exclude parameters which do not satisfy this constraint. Furthermore, we will look at three limits, namely  $\tan \beta \gg 1$ ,  $\tan \beta \ll 1$  and  $\tan \beta = 1$ . In these limits the above expression reduces to [12]:

1. For  $\tan \beta \ll 1$

$$C_{Z(h \rightarrow X)}^2 = c_1^4 c_2^4 \ll 1 \quad (6.21)$$

which requires that one of the angles be close to  $\pm \frac{\pi}{2}$

2. For  $\tan \beta \gg 1$

$$C_{Z(h \rightarrow X)}^2 = t_\beta^2 s_1^2 c_2^2 [c_1^2 c_2^2 + s_\beta^2 c_2] \ll 1 \quad (6.22)$$

which requires  $\alpha_1/\alpha_2 \rightarrow 0$  and  $\alpha_2/\alpha_1 \rightarrow \pm \frac{\pi}{2}$

3.  $\tan \beta = 1$

$$C_{Z(h \rightarrow X)}^2 = [(c_1 + s_1)c_2]^2 \left[ c_1^2 c_2^2 + \frac{1}{2} s_2^2 \right] \ll 1 \quad (6.23)$$

which requires that  $\alpha_2$  be close to  $\pm \frac{\pi}{2}$  or  $\alpha_1$  close to  $-\frac{\pi}{4}$

Lastly there are constraints related to corrections to the  $\rho$  parameter<sup>1</sup> (see end of chapter 4) and the muon anomalous magnetic moment, which we will effectively ignore. A word on their effects is nevertheless instructive. The additional contributions to  $\rho$  within the 2HDM come from the Higgses coupling to  $W$  and  $Z$  and the mass splitting in the Higgs sector (i.e. difference in mass of Higgses). It typically prefers a low mass splitting of the neutral Higgses. For the muon magnetic moment, the situation can be succinctly summarized by saying that new physics effects can either be used to obtain better agreement between theory and experiment or made to be non-negligible.

We now go on to look at  $ZZ$  production and enhancement of the “golden cross section”

---

<sup>1</sup>For the  $\rho$  parameter, they are not necessarily very precise because an assumption on the SM Higgs must be made to use EW fits. In [12], they of course comment on this.

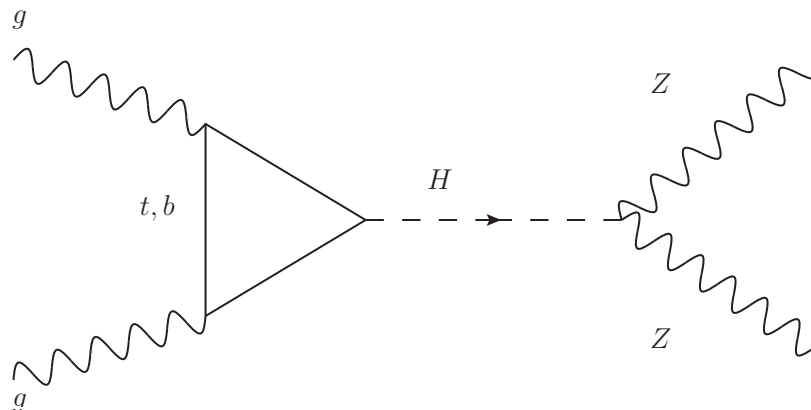


**Figure 6.5:** Feynmandiagram for ZZ production from H, where  $H = H_{SM}, H_1$

## 6.5 Enhancing ZZ production

We will now look at the process  $gg \rightarrow H_1 \rightarrow ZZ$  relative to  $gg \rightarrow H_{SM} \rightarrow ZZ$ . The Feynman diagram of this process is shown in Figure (6.5) Let us first write down the cross section for the pure top and bottom contributions to gluon fusion:

$$\begin{aligned} \sigma(gg \rightarrow H_1 \rightarrow ZZ)_{\text{top}} &= |(H_1 t\bar{t})|^2 |(H_1 ZZ)|^2 \sigma(gg \rightarrow H_{SM} \rightarrow ZZ)_{\text{top}} \\ \sigma(gg \rightarrow H_1 \rightarrow ZZ)_{\text{bottom}} &= |(H_1 b\bar{b})|^2 |(H_1 ZZ)|^2 \sigma(gg \rightarrow H_{SM} \rightarrow ZZ)_{\text{bottom}} \end{aligned} \quad (6.24)$$

When we insert the expressions (6.12), (6.13) and (6.14) we get

$$\sigma_{\text{top}} \equiv \sigma(gg \rightarrow H_1 \rightarrow ZZ)_{\text{top}} = [c_\beta^2 s_1^2 - 2c_\beta s_\beta c_1 s_1 + s_\beta^2 c_1^2] \frac{c_1^2}{s_\beta^2} \times \sigma_{\text{SM-top}} \quad (6.25)$$

and

$$\sigma_{\text{bot}} \equiv \sigma(gg \rightarrow H_1 \rightarrow ZZ)_{\text{bottom}} = [c_\beta^2 s_1^2 - 2c_\beta s_\beta c_1 s_1 + s_\beta^2 c_1^2] \frac{s_1^2}{c_\beta^2} \times \sigma_{\text{SM-bot}} \quad (6.26)$$

First we look at the small  $\tan \beta$  limit. Here the top cross section dominates completely. This because it, in addition to having a much greater mass<sup>1</sup>, couples more strongly than the bottom quark. The top contribution becomes:

$$\sigma_{\text{top}} = \frac{c_1^2 s_1^2}{t_\beta^2} \times \sigma_{\text{SM-top}} = \frac{1}{4} \frac{1}{t_\beta^2} [1 - \cos^4 2\alpha_1] \times \sigma_{\text{SM-top}} \quad (6.27)$$

<sup>1</sup>Which already makes it dominant in the SM case.

## 6. A SCALAR SIGNATURE

---

We see that small values of  $\tan \beta$  can indeed enhance the cross section considerably. Let us look at the mixing angle dependence of this expression. With the choice of mixing angles  $\alpha_1 = 0, \pm \frac{\pi}{2}$  the bottom cross section vanish. On the other hand a mixing angle choice of  $\alpha_1 = \pm \frac{\pi}{4}$  maximizes the cross section. Looking back to the expressions of the couplings (6.12), (6.13) and (6.14), we can understand these results as follows:

1. In the case  $\alpha_1 \rightarrow 0$ , the  $(H_2ZZ)$  coupling vanishes<sup>1</sup> and kills the cross section in the process.
2. In the case  $\alpha_1 \rightarrow \pm \frac{\pi}{2}$  the  $(H_2t\bar{t})$  coupling vanishes and the cross section disappears.
3. The cases of maximum cross section (i.e.  $\alpha_1 \rightarrow \pm \frac{\pi}{4}$ ) are in-between these three extremes.

In the large  $\tan \beta$  limit (i.e.  $s_\beta \sim 1, c_\beta \sim 0$ ). The cross section can be dominated by bottom or top production from gluon fusion. Alternatively they can be of comparable magnitude and interfere. The cross sections become:

$$\begin{aligned}\sigma_{bot} &= t_\beta^2 s_1^2 c_1^2 \times \sigma_{\text{SM-bot}} \\ &= \frac{1}{4} t_\beta^2 [1 - \cos^4 2\alpha_1] \times \sigma_{\text{SM-bot}}\end{aligned}\tag{6.28}$$

and

$$\sigma_{top} = c_1^4 \times \sigma_{\text{SM-top}}\tag{6.29}$$

Some comments on the mixing angle dependence are in order:

1. As  $\alpha_1 \rightarrow 0$ , the  $H_2b\bar{b}$  coupling vanishes and only  $\sigma_{top} = \sigma_{\text{SM-top}}$  contributes, which is not of interest for our analysis
2. As  $\alpha_1 \rightarrow \pm \frac{\pi}{4}$ , the bottom cross section is maximized  $\sigma_{bot} = \frac{1}{4} \times \sigma_{\text{SM-top}}$

The second case here could be of interest. In this case interference can be non-negligible. This could lead, in the case of maximum interference, to an additional factor 4. Checking with our measure (6.15) we find that the ratio of the amplitudes is  $\sim \frac{1600}{t_\beta^2}$  and the value of  $\tan \beta$  would have to be somewhat high for this to happen. We will return to

---

<sup>1</sup>Remember that  $s_\beta \sim 0$

these two cross sections and see how much we can enhance them with respect to experimental constraints in the next section. Before we do that we check the intermediate case, namely  $\tan \beta = 1$ .

In the  $\tan \beta = 1$  case we have

$$\sin \beta = \cos \beta = \frac{1}{\sqrt{2}} \quad (6.30)$$

The two cross sections for pure top and bottom contributions become:

$$\begin{aligned} \sigma_{top} &= (c_1 - s_1)^2 c_1^2 \times \sigma_{\text{SM-top}} \\ \sigma_{bot} &= (c_1 - s_1)^2 s_1^2 \times \sigma_{\text{SM-bot}} \end{aligned} \quad (6.31)$$

Let us make our usual mixing angle comments:

1. The case  $\alpha_1 \rightarrow \frac{\pi}{4}$  the  $H_2ZZ$  coupling vanishes, which is not interesting
2. The case  $\alpha_1 \rightarrow 0$  makes the bottom coupling vanish and is therefore not interesting
3. In the case  $\alpha_1 \rightarrow -\frac{\pi}{4}$  the  $H_2ZZ$  is maximized and the bottom and top couplings are equal. This is not interesting as the cross sections become the SM ones.

If we look at our measure for the case  $\alpha_1 \rightarrow -\frac{\pi}{4}$  it is clear that the top-quark contribution still dominates and interference cannot enhance this any further. Given the above results we restrict our discussion to the cases  $\tan \beta \ll 1$  and  $\tan \beta \gg 1$ .

## 6.6 Possible Limits

We now look at the limits discussed in the previous section and compare them with experimental constraints. Our goal is to constrain the maximal possible theoretical enhancement. We divide our discussion into the two limiting cases, namely

1. The case  $\tan \beta \ll 1$
2. The case  $\tan \beta \gg 1$

The relevant formulas will, for the reader's convenience, be reproduced in this section<sup>1</sup>

---

<sup>1</sup>To avoid the undesirable activity of page flipping!

## 6. A SCALAR SIGNATURE

---

For the  $\tan\beta \ll 1$ , the relevant equations are:

$$\begin{aligned}\sigma_{\text{top}} &= \frac{1}{4} \frac{1}{t_\beta^2} [1 - \cos^4 2\alpha_1] \times \sigma_{\text{SM-top}} \\ C_{Z(h \rightarrow X)}^2 &= c_1^4 c_2^4 \ll 1\end{aligned}\tag{6.32}$$

We are interested in maximizing this cross section, which corresponds to putting  $\alpha_1 \rightarrow \pm \frac{\pi}{4}$ . We then get

$$\sigma_{\text{top}} = \frac{1}{4} \frac{1}{t_\beta^2} \times \sigma_{\text{SM-top}}\tag{6.33}$$

For the constraint to be satisfied we need

$$C_{Z(h \rightarrow X)}^2 = \frac{1}{4} c_2^4 \ll 1\tag{6.34}$$

To increase the cross section by an order of magnitude we need  $\tan\beta \sim 0.16$ . The mixing angle is free to vary as long as it satisfies the constraint. We note that in [12] a mixing angle  $\alpha_2 \rightarrow 0$  corresponds to no CP violation, which makes this easier to satisfy if there is more CP violation.

For the  $\tan\beta \gg 1$ , the relevant equations are:

$$\begin{aligned}\sigma_{\text{bot}} &= \frac{1}{4} t_\beta^2 [1 - \cos^4 2\alpha_1] \times \sigma_{\text{SM-bot}} \\ \sigma_{\text{top}} &= c_1^4 \times \sigma_{\text{SM-top}} \\ C_{Z(h \rightarrow X)}^2 &= t_\beta^2 s_1^2 c_2^2 [c_1^2 c_2^2 + s_\beta^2 s_2] \ll 1\end{aligned}\tag{6.35}$$

We note, once again, that in order for the constraints to be satisfied we need  $\alpha_1/\alpha_2 \rightarrow 0$  and  $\alpha_2/\alpha_1 \rightarrow \pm \frac{\pi}{2}$ . These demands make our cross section vanish. If we let the mixing angles be close enough to these points so that they satisfy the constraints,  $\tan\beta$  would have to be enormously large to enhance the cross section. Here, the constraints from  $B \rightarrow \tau\nu$  would probably restrict it somewhat. We also note that if  $\tan\beta$  is enormously large, the bottom production would probably dominate. But just in case it does not, the case of maximal interference could provide us with an enhancement factor four.

In summary, we have tried to maximize the “golden cross section” for a next to lightest Higgs within the 2HDM(II). Constraints on the lightest Higgs from LEP II direct searches were applied. For the case of small  $\tan\beta$ , the top-quark triangle loop diagram provides the dominant contribution. In fact, it dominates even more than in the

standard model, because the coupling ( $H_2 t \bar{t}$ ) is enhanced by  $\tan \beta$ . At low  $\tan \beta$ , the constraints from  $B_d^0 - \bar{B}_d^0$  mixing,  $B \rightarrow X_s \gamma$  and the effective  $Z b \bar{b}$  vertex ( $R_b$  in [28]) must be taken into account. On the other hand for the large  $\tan \beta$  limit, where bottom-quark contribution dominates, it seems harder to obtain a sizable enhancement. This is because of the  $B \rightarrow \tau \nu$  constraint. For both cases we could always push the charged Higgs mass up to avoid the constraint. The top-quark enhancement does not require as high a value for the charged Higgs as the bottom-quark enhancement an easier mechanism to enhance the cross section. We conclude with saying that enhancement of the “golden cross section” seems most feasible at small values of  $\tan \beta$  with the top-quark providing the dominant contribution.

We end our discussion of the 2HDM here and move on to the chapters that deal with extra dimensions and Technicolor. These chapters are of a somewhat different nature than the preceding ones. More precisely, they do not contain explicit calculations as in the  $Z'$  and 2HDM case. Rather, they aim to introduce enough concepts to understand where the different phenomenological signatures come from. Phenomenological signatures relevant to our experimental situation (and some others) are summarized in a section contained at the very end of each chapter.

## 6. A SCALAR SIGNATURE

---

## Chapter 7

# Kaluza-Klein Theories and the Graviton

Out of the different theories of physics that exist, there are none more sacred to physicist than the unifying ones. Newton was one of the first to create such a theory. He identified the everyday forces we experience with the ones governing celestial motion of planets and stars. Boltzmann drew attention to the fact that the laws of thermodynamics can be understood through a statistical analysis of atoms and molecules moving about. Maxwell and Faraday unified the electric and magnetic forces through the electromagnetic field and Dirac arranged his “wedding” of Special Relativity and Quantum Mechanics. Today we have four known forces, namely Electromagnetic, Weak and Strong nuclear forces and Gravity. Unification of the three first have seen great progress during the last part of the twentieth century and are described by the Standard Model of particle physics. Many attempts have been made to unify Gravity with the three forces of the SM, but it has eluded every attempt so far. Most of the unifying theories include the introduction of extra spatial dimensions. In this chapter we’ll see how extra-dimensional theories were first contrived and end up with some modern theories and their phenomenological consequences.

## 7.1 What are Kaluza-Klein Theories?

The story starts in 1914 with Gunnar Nordström, who looked at a five-dimensional vector potential  $A_{\hat{\mu}}$ . The potential can be written in  $4 + 1$  dimensions as [32]:

$$A_{\hat{\mu}} = A_{\mu} + \phi \quad (7.1)$$

Here,  $A_{\mu}$  is the four-dimensional electromagnetic field and  $\phi$  is a scalar potential describing gravity. However in 1915 Einstein came with his extraordinarily successful tensor theory of gravity (general relativity). As a consequence Nordström abandoned his scalar theory of gravity, but the idea of an extra spatial dimension stuck.

In 1921 Theodor Franz Eduard Kaluza tried to unite general relativity (GR) and electromagnetism. By the introduction of a fifth spatial dimension, he could show that the fields describing GR and electromagnetism came from the same tensor. With  $y$  denoting the extra spatial dimensions the five-dimensional line element becomes<sup>1</sup>:

$$d\hat{s}^2 = \hat{g}_{\hat{\mu}\hat{\nu}}(x^{\mu}, y) d\hat{x}^{\hat{\mu}} d\hat{x}^{\hat{\nu}} \quad (7.2)$$

To reproduce the equations of general relativity Kaluza had to make an additional assumption. That the fields should not vary in the extra dimension or that their variation was small. This assumption is called the cylindrical condition. Once a spacetime metric is obtained, one can construct the other quantities appearing in general relativity. For a more thorough, but pedagogical review of this theory see [32].

Although Kaluza's theory neatly unifies GR and EM, it had some issues. Most prominently<sup>2</sup>

1. Where was the extra dimension?
2. Why should the ordinary fields not vary in the extra dimension?
3. The electric charge of a particle was explained by its velocity in the fifth dimension. This description worked only in the small velocity approximation.

---

<sup>1</sup>The hat over the symbols indicates that there are 5 dimensions to consider, consequently the indices such as  $\hat{u}$  can have values 0, 1, 2, 3, 4

<sup>2</sup>Adapted from [32]

## 7.1 What are Kaluza-Klein Theories?

---

Five years after Kaluza's theory, Oscar Klein came up with an explanation for the cylindrical condition. He suggested that the extra dimension was curled up. The new dimension has circular topology. Physically it means that at each spacetime point (4D) there is a circle. Particle motion in this dimension does not change the position in four-dimensional space-time. The topology of the space is expressed mathematically as  $R^4 \times S^1$ , where  $R^4$  denotes the usual Minkowski space. A cylinder has the topology  $R \times S^1$ , which explains the name of Kaluza's assumption<sup>1</sup>. If the radius of this extra dimension is small it provides a natural explanation for why we haven't seen it yet. An analogy can be drawn to an ant walking on a wire:

You stand far off and observe an ant walking along an apparently 1-dimensional wire. Suddenly the ant disappears and you have no idea where it has gone. You are confused. The confusion only lasts till you get close enough and discover that the ant can move around the wire as well as along it. By getting closer you have unveiled the extra dimension.

This curling up of dimensions is called Kaluza-Klein compactification. The radius of compactification was taken to be around the Planck length, where gravity effects were expected to become non-negligible. The circular topology of the extra dimension, means that any function of the extra dimension is  $2\pi R$  periodic<sup>2</sup> in the  $y$  coordinate (i.e  $f(y) = f(y + 2\pi R)$ ). This theory results in three fields that can be expanded in a Fourier series in the periodic coordinate  $y$ :

$$g_{\mu\nu}(x, y) = \sum_{n=-\infty}^{n=+\infty} g_{\mu\nu n}(x) e^{\frac{iny}{R}} \quad (7.3)$$

$$A_{\mu}(x, y) = \sum_{n=-\infty}^{n=+\infty} A_{\mu n}(x) e^{\frac{iny}{R}} \quad (7.4)$$

$$\phi(x, y) = \sum_{n=-\infty}^{n=+\infty} \phi_n(x) e^{\frac{iny}{R}} \quad (7.5)$$

---

<sup>1</sup> $R$  is the degree of freedom corresponding to moving along the "height" of the cylinder, while  $S$  represents that we can move around it

<sup>2</sup>If you go around a cylinder you end up where you started after having moved a distance equal to the circumference

## 7. KALUZA-KLEIN THEORIES AND THE GRAVITON

---

The equations of motion for each of these fields become:

$$(\partial_\mu \partial^\mu - \partial_y \partial^y) g_{\mu\nu}(x, y) = \sum_{n=-\infty}^{n=+\infty} \left( \partial_\mu \partial^\mu + \frac{n^2}{R^2} \right) g_{\mu\nu n}(x) = 0 \quad (7.6)$$

$$(\partial_\mu \partial^\mu - \partial_y \partial^y) A_\mu(x, y) = \sum_{n=-\infty}^{n=+\infty} \left( \partial_\mu \partial^\mu + \frac{n^2}{R^2} \right) A_{\mu n}(x) = 0 \quad (7.7)$$

$$(\partial_\mu \partial^\mu - \partial_y \partial^y) \phi(x, y) = \sum_{n=-\infty}^{n=+\infty} \left( \partial_\mu \partial^\mu + \frac{n^2}{R^2} \right) \phi_n(x) = 0 \quad (7.8)$$

The three fields that appear represent the graviton  $g_{\mu\nu}$ , the photon  $A_\mu$  and a scalar  $\phi$ . We recognize the equations as Klein-Gordon equations with particles of mass  $\frac{n}{R}$ . For different values of  $n$ , there are different values of the mass. These mass states are called Kaluza-Klein excitations. Different values of  $n$  yield different mass states and all the mass states are collectively referred to as a Kaluza-Klein tower of states.

The extra-dimensional theories we'll consider use the compactification scheme in Kaluza-Klein theories. One difference is that they consider different kinds of spaces than  $S^1$  to be compactified. On a historical note: Pauli actually considered compactifying  $S^2$  in  $R^4 \times S^2$ . He did not publish anything since he didn't know what to do with the resulting massless vector fields from the  $S^2$  compactification. [33]

In addition the theories use the concept of “branes” (mathematically speaking a manifold) from string theory. The branes are embedded into some higher dimensional space. The full space (brane + higher dimensions) is referred to as the bulk. The branes effectively localize particles in different parts of the universe. The basic idea in both scenarios is that we live on a four-dimensional manifold (brane) where all SM particles and interactions take place. The mediator of gravitational interactions, the graviton, is free to propagate throughout the extra dimensions.

The motivation behind such models is that gravity has not been probed on small scales (presently about 0.1 mm). Originally, the rationale behind taking the compactification scale  $R \sim \frac{1}{M_{\text{Planck}}}$  in KK theories was dimensional analysis involving Newton's gravitational constant. The fundamental mass and length scales of the EW theory and

gravitation obtained this way are:

$$\begin{aligned}
 M_{\text{Planck}} &= \sqrt{\frac{\hbar c}{G_N}} \simeq 10^{19} \frac{\text{GeV}}{c^2} \\
 M_{\text{EW}} &= \sqrt{\frac{\hbar^3}{c G_{\text{EW}}}} \simeq 300 \text{ GeV} \\
 l_{\text{Planck}} &= \sqrt{\frac{\hbar G_N}{c^3}} \simeq 10^{-35} \text{ m} \\
 l_{\text{EW}} &= \sqrt{\frac{G_{\text{EW}}}{\hbar c}} \simeq 10^{-19} \text{ m}
 \end{aligned}
 \tag{7.9}$$

The widely different mass-scales (or length if you'd like) are problematic when trying to unify the SM forces with gravitation. If one assumes that no new physics arises in-between these scales, the masses one calculates for the Higgs boson shoot up to the Planck mass. This constitutes the hierarchy problem (explained in more detail in section 8.1). If the extra-dimensional models are true, the Newtonian gravitational potential would be modified at small scales and the hierarchy problem could be circumvented.

## 7.2 ADD, Large Extra Dimensions

The ADD model [4] is named after Arkani-Hamed, Dimopoulos and Dvali, which first proposed it. They suggest that there is only one fundamental scale in nature, the experimentally well documented  $M_{\text{EW}}$ . The reason for the apparent weakness (i.e. large mass scale) of gravitational interactions are  $n$  extra compact spatial dimensions of radius  $R$ . The total space (universe) has the topology  $R^4 \times M_n$ , with  $M_n$  denoting the space to be compactified. If one places two test masses  $m_1, m_2$  at a distance  $r \ll R$ , the gravitational potential as decided by Gauss' law of flux conservation (in  $4+n$  dimensions) is:

$$V(r) \sim \frac{m_1 m_2}{M_{\text{Pl}(4+n)}^{n+2}} \frac{1}{r^{n+1}}, \quad r \ll R
 \tag{7.10}$$

At a distance  $r \gg R$ , the flux lines do not penetrate the extra dimensions and we get the ordinary potential:

$$V(r) \sim \frac{m_1 m_2}{M_{\text{Pl}(4+n)}^{n+2}} \frac{1}{R^n r}, \quad r \gg R \quad (7.11)$$

The constant  $M_{\text{Pl}(4+n)}$  is the “real” Planck mass. It is postulated to be of the same order as the electroweak mass (i.e.  $M_{\text{Pl}(4+n)} \sim M_{EW}$ ). The value we observe is the effective one  $M_{\text{Pl}}^2 \sim M_{\text{Pl}(4+n)}^{n+2} R^n$ . If  $R$  is chosen to reproduce the Planck scale, choosing  $n = 1$  gives an extra dimension  $R \sim 10^{13}$ , which is in the original paper, quite dryly, commented to be “empirically excluded”. For larger values of  $n$  (i.e. more dimensions) the extra dimensions are smaller, in particular for  $n = 2$ , it is of the order of  $R \sim 100\mu\text{m} - 1\text{mm}$ . Since  $1\text{mm} \gg l_{\text{planck}}$ , the theory is often referred to as a theory of Large Extra Dimensions.

SM particles live on the brane and have the characteristic interaction energy  $M_{EW}$ . The characteristic interaction energies of the ordinary particles are related to the thickness ( $\delta$ ) of the brane in the extra dimensions ( $M_{EW} \sim \frac{1}{\delta}$ ). The phenomenological consequence of this will be among other things KK-modes of the graviton and mini-black holes. In fact, these mini black holes have a very real possibility of being observed at the LHC. This is because the strengthening of gravitational interactions at small distances (see (7.10)) could lead to an abundance of mini black hole formation. Let us now go on to consider another popular extra-dimensional theory, namely the RS model. Here, the extra dimensions need not be as ‘large’ as in the above theory.

### 7.3 RS, a warped geometry

The Randall-Sundrum (RS) model [5] inherits its name from the creators, Lisa Randall and Raman Sundrum. There are two versions of the theory, namely RS1 and RS2. In RS1 (which we will deal with) there is a bounded, extra dimension, while the RS2 has an unbounded dimension. It is an extra-dimensional theory using the same theoretical concepts as in ADD<sup>1</sup>, but differs from ADD in three main aspects:

1. It has only *one* extra dimension
2. The dimension need not be ‘large’

---

<sup>1</sup>That is, branes and KK compactification

3. It has *two* branes, namely the “Planck brane” and the “TeV brane”
4. The geometry of the extra dimension is “warped”<sup>1</sup>

In the paper [5], Randall and Sundrum argue that although the hierarchy problem is solved in Large Extra Dimensional theories, it is replaced by another difficulty. The tuning of the thickness of the brane (i.e. the  $M_{EW}$  scale) versus the size of the extra dimensions  $R$ . This has a natural explanation in the RS models, which is related to the “warped” geometry.

In the RS1 model two branes are placed in a new dimension with coordinate  $y$ . The space is bounded by  $y = 0$  and  $y = \frac{1}{kW}$ . The constant  $k$  is around the Planck scale and  $W$  multiplied by  $k$  is around the TeV scale. In this set-up the constant  $W$  is referred to as the “warp factor”. This is because its value says something about how the geometry of spacetime changes as one moves in the new dimension. The two branes are placed at the points  $y = \frac{1}{k}$  (Planck brane) and  $\frac{1}{kW}$  (TeV brane). In this scenario they obtain a new metric (which “measure” the distance between to points infinitesimally close to each other) as a solution of Einstein’s equations. The new metric is the ordinary Minkowski metric multiplied by a function of the extra dimension  $y$ . It looks like:

$$ds^2 = \frac{1}{k^2 y^2} (dy^2 + g_{\mu\nu} dx^\mu dx^\nu) \quad (7.12)$$

If we make the coordinate change

$$\phi \equiv -\pi \frac{\ln(ky)}{\ln(W)}, \quad 0 < \phi < \pi \quad (7.13)$$

and define  $r_c$  through  $W = e^{\pi k r_c}$  we get:

$$ds^2 = e^{-2kr_c\phi} g_{\mu\nu} dx^\mu dx^\nu + r_c^2 d\phi^2 \quad (7.14)$$

This coordinate representation shows more clearly what happens as we wander out through the extra dimension. The spacetime part of the metric ( $g_{\mu\nu} dx^\mu dx^\nu$ ) is multiplied by a rapidly changing number. This changes the measure which we (ordinary

---

<sup>1</sup>In contrast to the flat geometry of ADD

## 7. KALUZA-KLEIN THEORIES AND THE GRAVITON

---

mortals confined to the TeV brane) use to decide the geometry of spacetime and effectively “warps” the geometry at one point in  $y$ -space relative to another. In contrast to the ADD model the four-dimensional planck mass in this scenario is[34]:

$$M_{\text{Pl}(4)}^2 = \frac{M_5^3}{k} \left[ 1 - e^{-2kr_c\pi} \right] \quad (7.15)$$

where  $M_5$  is the five-dimensional planck mass. For a small warp factor we see that

$$kM_{\text{Pl}(4)}^2 = M_5^3 \quad (7.16)$$

so that  $k$ ,  $M_{\text{Pl}(4)}$  and  $M_5$  are comparable in magnitude. This means that warp factor can effectively generate a low energy scale on the TeV brane from a high energy scale on the Planck brane, which solves the hierarchy problem. We can in fact generate an energy scale of 1 TeV (weak scale)[34]

$$\Lambda_{EW} = M_{\text{Pl}(4)} e^{-kr_c\pi} \quad (7.17)$$

by choosing  $kr_c \sim 12$ .

Having gained a basic understanding of the two extra dimensional theories we move on to the phenomenology section.

### 7.4 Phenomenology

Firstly we should say that the models described above are presented in their most basic form. Extensions of both of these models exist, which can produce phenomenological signatures of a wide variety[34]<sup>1</sup>. For instance, in the ADD scenario one can let some or all of the SM fields propagate throughout the bulk. Allowing this leads to problems with renormalization. This can again be fixed by multiplying the fields by a rapidly vanishing function of the extra dimension (e.g. a gaussian). In effect this gives SM fields that, to a certain extent, are allowed to propagate in the extra dimension. Upon compactifying the extra dimensions these fields also have KK excitations. Since particle signatures are dependent on the particular choices made in the model it is hard to give a brief and concise overview of all of them. We will therefore stick to the characteristic signatures of extra dimensions, namely the KK excitations of the graviton.

---

<sup>1</sup>RS-type models can produce some of the  $Z'$  gauge bosons of chapter 5

For our experimental situation the prime candidate for enhancing the cross section are the KK excitations of the spin-2 Graviton. Luckily the ADD and RS model have certain characteristic differences in this regards, which is related to the flat vs. warped geometry. There are two main differences [35]:

1. The spectrum of the Graviton KK states in ADD are evenly spaced and can effectively be treated as continuous, while the RS scenario predicts unevenly spaced states that must be treated as discrete
2. The couplings to matter in ADD comes from the collective strength of the whole KK tower and is of order 1 TeV, while in the RS model each resonance has a coupling of order 1 TeV

Let us make a comment on the relation of spacing of states to the extra dimensions. The even spacing of the KK excitations in ADD simply result from the fourier expansion (7.8), which gives particles of mass  $\frac{n}{R}$ . In the RS scenario this is more complicated because of the geometry of the space<sup>1</sup>. Mathematically the KK-modes of RS are given by a linear combination of Bessel functions<sup>2</sup>. The consequence of this is the uneven spacing mentioned above and mass modes given by  $x_n = ke^{-kr_c\pi}$ , where  $x_n$  are the roots of the Bessel functions.

At the LHC a KK Graviton in the ADD scenario could be produced in association with a jet from quarks or gluons, together with a  $\gamma$  or a  $Z$ . This leads to signals with either jet  $+\gamma$ + missing energy or  $Z$ + missing energy, where the missing energy is the elusive Graviton. There are sizable production cross sections for this, which in the ADD scenario are directly related to the number of extra dimensions and the energy scale of the theory[34] Another possibility is indirect search through production of fermion or boson pairs. This is the situation we find ourselves in. In this situation the fundamental scale of the theory are not directly related to increasing the production cross sections[34] and could, possibly, be hard to adjust to a sizable value.

<sup>1</sup>Technically called an Anti-de-Sitter space[5]

<sup>2</sup>Bessel functions are the solutions of a particular differential equation. Since differential equations often appear in physics they are common. Examples include the radial schrödinger equation, heat conduction, vibration modes etc.

## 7. KALUZA-KLEIN THEORIES AND THE GRAVITON

---

Within the confines of RS, Gravitons are resonantly produced and decay predominantly into two jets. Excesses can then be found in for instance diboson channels[34]. In other words an RS graviton suits our situation well.

If a KK Graviton were the decaying particle, it would be important to distinguish this spin-2 particle from a spin-1 resonance. In the study [35] they look at a method of distinguishing the spin-1 case from the spin-2 case at Hadron Colliders in both the RS and ADD scenarios.

I would like to make an additional comment on the black-hole production discussed in section 7.2. In a study published in late 2010 from the CMS collaboration at the LHC [36], they investigate this possibility within the framework of ADD. They demand that black hole formation should occur if the impact parameter is less than the Schwarzschild radius<sup>1</sup>. Lower mass bounds for the black holes are set to about 3.5 to 4.5 TeV for a wide variety of parameters.

Leaving the extra-dimensional scenarios here, we go on to look at Technicolor and the possibility of a composite Higgs.

---

<sup>1</sup>The radius where some amount of non-rotating mass collapses into a black hole in GR

## Chapter 8

# Technicolor

The Standard Model Higgs is assumed to be a fundamental scalar particle. It is responsible for SSB and for generating particle masses. In Technicolor one imagines that the Higgs is a composite object or what is termed a fermion condensate. Instead of being fundamental, the Higgs is some bound fermion state. This does not make the Higgs mechanism obsolete since the fermion state would effectively be the scalar responsible for SSB in the EW sector. Symmetry breaking is now caused by some interacting fermions and is therefore referred to as “Dynamical Electroweak Symmetry Breaking” (DEWSB).

The idea of bound fermion states acting as scalars can be compared with pions in QCD and indeed early Technicolor models were essentially scaled up versions of QCD. The phenomenon of asymptotic freedom, exhibited by non-abelian gauge theories, can be used to describe such a bound fermion state<sup>1</sup>. Theoretical aspects and phenomenological consequences of this theory, will be laid out more plainly in the next section. First I would like to give some motivation for taking this approach.

The Technicolor approach is mostly motivated by the principle of naturalness. Naturalness means that the theoretical predictions of a theory should be stable under small variations of the input parameters (e.g. the mass of a particle shouldn't be changed significantly upon varying the input slightly). In the Standard Model the assumption of a fundamental scalar field (Higgs field) gives rise to such a problem. It is termed the

---

<sup>1</sup>As is the case for QCD and pions

hierarchy problem. To explain the hierarchy problem we must get a bit technical.

### 8.1 Hierarchy problem

The SM can be considered as a low-energy effective field theory, meaning that it's only valid up to some cut-off energy  $\Lambda$ . Grand Unified Theories predict a unification of forces at about  $10^{16}$  GeV. Assuming that the SM is valid up to this scale (a.k.a. the “big desert” assumption) introduces a problem concerning quantum corrections to the squared Higgs mass ( $m_h^2$ ). Corrections involve calculations with loops and different loops give rise to different contributions to the squared Higgs mass. The contributions are typically proportional to the square of the cut-off energy. If the different  $\Lambda^2$  corrections do not cancel out it means that the Higgs mass should be of order  $\Lambda$  (remember that  $\Lambda \sim 10^{16}$  GeV). The fine-tuning problem that arises can be thought of in the following way:

1. The corrections ( $\Delta m_h^2$ ) are proportional to  $\Lambda^2$
2. We remove them at the one-loop level by choosing (tuning) the parameters such that the different contributions cancel
3. Calculate corrections at the two-loop level
4. Realize that we have to tune the parameters again to simultaneously cancel the one and two loop corrections
5. Calculate corrections at the three-loop level
6. ....

This behaviour goes on in all orders of perturbation theory and is hard to get rid of. Of course many physicists (e.g. promoters of Technicolor and Supersymmetry) remain skeptical about the big desert assumption. A concrete example of this fine-tuning is found in the diagrams 8.1 and 8.2.

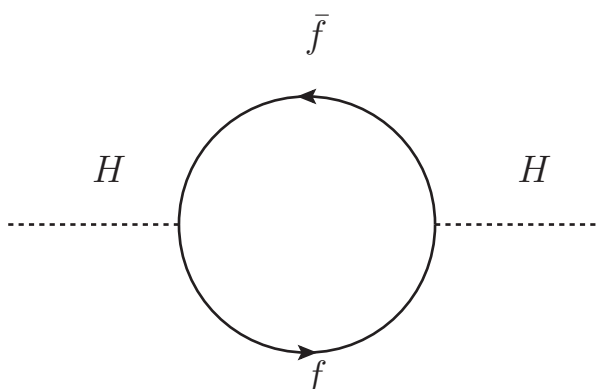


**Figure 8.1:** Higgs mass correction through fermion loop

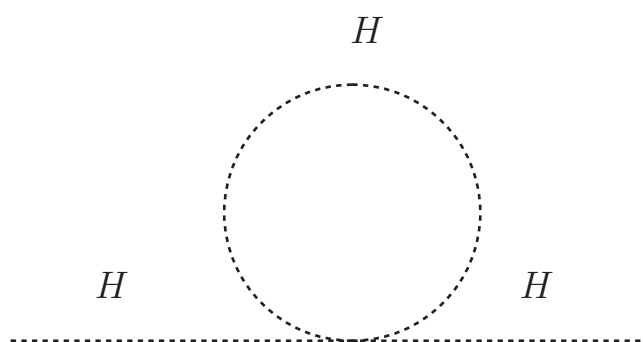


**Figure 8.2:** Higgs mass correction through self-coupling

## 8. TECHNICOLOR

---

The corrections to the squared Higgs mass that emerge are calculated in [11]. They are

$$\Delta m_{h1}^2 = \frac{\Lambda^2}{16\pi^2}(-2g_f) \quad (8.1)$$

$$\Delta m_{h2}^2 = \frac{\Lambda^2}{16\pi^2}(\lambda) \quad (8.2)$$

where  $g_f$  is the Yukawa coupling constant and  $\lambda$  is the quartic coupling of the Higgs. If we naively choose  $\lambda = 2h_f$ , the sum of the corrections disappears. This relation does not make the  $\Lambda^2$  term disappear in the next order of perturbation theory. Here the gauge-boson contributions are neglected, but the situation is similar when they are included.

Instead of trying to relate  $\lambda$  to different parameters to cancel the terms, this quadratic divergence can be absorbed in a redefinition of the bare mass (renormalization). One still has a residual term from the fermion loop causing problems [11]. Supersymmetry is a scheme which cancels out these divergences by relations as above. They do this by introducing new particles and therefore new loops. It is not an entirely successful procedure as new heavy particles push the mass corrections up.

Taking the SM as given and valid up to some energy cut off, we can now understand why the ADD and RS models fix the hierarchy problem.

### 8.2 Composite Higgs and Dynamical Electroweak Symmetry Breaking

Now we will look more closely at the DEWSB mechanism.<sup>1</sup> In this scenario we do not have any fundamental scalar field that acquires a non-zero VEV. Instead we will introduce a new strong force called Technicolor (TC), which acts on new fermions. Technicolor is responsible for the bound fermion-antifermion pair, which acts as the effective Higgs. Before introducing the minimal Technicolor model, we will go through a toy model that Susskind looked at in 1978 [38]. This will hopefully make the mechanism of DEWSB more transparent.

---

<sup>1</sup>These following sections follow closely the development in [3] with some material from [37]

## 8.2 Composite Higgs and Dynamical Electroweak Symmetry Breaking

---

### 8.2.1 Toy model

Starting with the SM we remove the Higgs doublet, all leptons and the two heaviest families of quarks. The only fermions in the theory are now the lightest quark doublet. In this model the quarks  $(u, d)$  remain massless down to the QCD confinement scale 250 MeV. They then combine with gluons into hadrons with masses round 1 GeV. [3]. An interesting thing happens to the pions, they act like the Goldstone bosons of the Higgs model. They get eaten by the  $W$  and  $Z$  and give the gauge bosons their masses. Let's examine this mechanism more closely. The first thing we do is to turn off the EW  $SU(2)_L \times U(1)$  interaction. The fermions are still massless, because the Higgs field isn't there. With  $\bar{\Psi} = (\bar{u}, \bar{d})$ , the fermionic lagrangian is

$$L_f = \bar{\Psi} i \not{D} \Psi \tag{8.3}$$

This is invariant under  $SU(2)_V$  (inserting two by two constant unitary matrices between doublets). Invariance under  $SU(2)_V$  is called isospin or isotopic spin symmetry. Using the chiral projection operators we can write this as

$$L_f = \bar{\Psi}^L i \not{D} \Psi^L + \bar{\Psi}^R i \not{D} \Psi^R \tag{8.4}$$

This expression is equivalent to the other and invariant under the group  $SU(2)_L \times SU(2)_R$  (Inserting two by two constant unitary matrices between left and right handed doublets). This symmetry is often referred to as chiral symmetry. We now choose the VEV's

$$\langle 0 | \bar{u} u | 0 \rangle = \langle 0 | \bar{d} d | 0 \rangle \neq 0 \tag{8.5}$$

This spontaneously breaks the symmetry from  $SU(2)_L \times SU(2)_R$  to  $SU(2)_V$ . To see this more clearly observe that:

$$\langle 0 | \bar{\Psi} \Psi | 0 \rangle = \langle 0 | \bar{u} u + \bar{d} d | 0 \rangle \neq 0 \tag{8.6}$$

$$\bar{\Psi} \Psi = \bar{\Psi}^L \Psi^R + \bar{\Psi}^R \Psi^L \tag{8.7}$$

Here,  $\Psi^L$  and  $\Psi^R$  transform differently under  $SU(2)_L \times SU(2)_R$ , implying that (8.7) is not invariant under this transformation. It is invariant under the  $SU(2)_V$  operation though. This is a spontaneous breakdown of the symmetry  $SU(2)_L \times SU(2)_R \rightarrow SU(2)_V$ . The parameter  $\langle 0 | \bar{\Psi} \Psi | 0 \rangle$  is a so-called order parameter, that are used to characterize

## 8. TECHNICOLOR

---

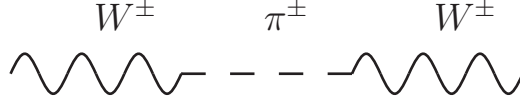


**Figure 8.3:** Pion-W coupling

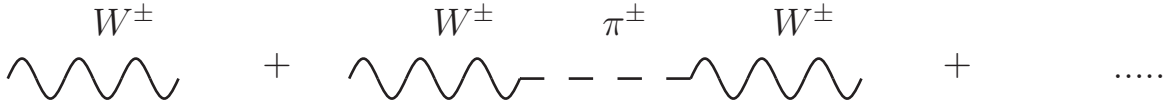


**Figure 8.4:** Higgs contribution

a spontaneous breakdown of symmetry<sup>1</sup>. Accompanying this SSB are three massless Goldstone bosons<sup>2</sup>, which we identify with the pions. The pions are associated with the axial currents [3]:

$$j_{Aa}^\mu = f_\pi \partial^\mu \pi_a = \bar{q} \gamma^\mu \gamma^5 \frac{\sigma^a}{2} q \quad (8.8)$$

where the  $\sigma^a$  are the Pauli matrices and  $f_\pi$  the pion decay constant. The pion fields are taken to be

$$\pi^\pm = \frac{1}{\sqrt{2}}(\pi_1 \mp i\pi_2) \quad (8.9)$$

When we switch on the Electroweak interactions the pions get eaten by the  $W$  and  $Z$  bosons. This happens through the kinetic terms for the quarks in (8.4). The resulting couplings between pions and gauge bosons are [3]:

$$\frac{1}{2}g(f_{\pi^+}W_\mu^+ \partial^\mu \pi^+ + f_{\pi^-}W_\mu^- \partial^\mu \pi^- + f_{\pi^0}W_\mu^0 \partial^\mu \pi^0) + \frac{1}{2}g'f_{\pi^0}B_\mu \pi^0 \quad (8.10)$$

The  $W_\mu^\pm - \partial^\mu \pi^\pm$  couplings give rise to diagrams as in 8.3.

If we make a geometric series out of this diagram as in Figure 8.4, we will modify the  $W$  propagator by

---

<sup>1</sup>Analogous to the VEV of the SM

<sup>2</sup>Goldstone's theorem: The number of goldstone bosons are equal to the number of broken generators. Effectively if the group  $G$  with  $N$  free parameters is broken down to the group  $H$  with  $M$  free parameters we get  $N - M$  free parameters.

## 8.2 Composite Higgs and Dynamical Electroweak Symmetry Breaking

---

$$\frac{1}{p^2} \rightarrow \frac{1}{p^2 - \left(\frac{gf_{\pi^\pm}}{2}\right)^2} \quad (8.11)$$

This implies that the  $W$  particle has gained a mass  $M_W = \frac{gf_{\pi^\pm}}{2}$ . Similarly, the  $Z$  boson gets a mass through the  $W^0$  and  $B$  couplings. This gives a mass-squared mixing matrix in the  $(W_0, B)$  basis [3]:

$$\frac{f_{\pi^0}^2}{4} \begin{pmatrix} g^2 & gg' \\ gg' & g'^2 \end{pmatrix} \quad (8.12)$$

As in the Standard Model, we identify the eigenvectors and corresponding eigenvalues

$$Z = \frac{gW_3 - g'B}{\sqrt{g^2 + g'^2}} \quad (8.13)$$

$$A = \frac{g'W_3 + gB}{\sqrt{g^2 + g'^2}} \quad (8.14)$$

$$M_Z = \frac{(g^2 + g'^2)f_{\pi^0}^2}{4} \quad (8.15)$$

$$M_A = 0 \quad (8.16)$$

The tree-level relation

$$\frac{M_W}{M_Z} = \frac{f_{\pi^\pm}}{f_{\pi^0}} \cos \theta_W \quad (8.17)$$

is the same as in the Standard Model since  $f_{\pi^\pm} = f_{\pi^0}$ . The problem is that the pion decay constant is  $\approx 93$  MeV and is too small to account for the gauge boson masses. If we could enhance this constant up to  $v \approx 246$  GeV, we would get the value for gauge boson masses. Technicolor does exactly this job.

### 8.2.2 Minimal Technicolor

In the minimal technicolor model that Susskind and Weinberg introduced, one expands the gauge group of the SM with a QCD like group  $SU(N)_{TC}$ , with a coupling that grows strong around  $\Lambda_{TC} = 500$  GeV.

$$SU(3)_C \times SU(2)_L \times U(1)_Y \rightarrow SU(N)_{TC} \times SU(3)_C \times SU(2)_L \times U(1)_Y \quad (8.18)$$

In addition to the new gauge interactions there are new fermions that feel this force. They are called technifermions. In the minimal model one adds a techniquark doublet.

## 8. TECHNICOLOR

---

The techniquarks will carry Technicolor, but not ordinary color. SM particles do not carry Technicolor. The new doublet is as denoted in [3]:

$$\begin{pmatrix} p_L \\ m_L \end{pmatrix}^\alpha \sim (N, 1, 2, 0) \quad (8.19)$$

Here, the three first numbers in the parenthesis describe which  $k$ -plets particles are under various forces. The numbers describe Technicolor, color and EW force respectively. The last number is the hypercharge. The index  $\alpha = 1, 2, 3 \dots N$  labels the techniquark representation and the subscript  $L$  refers to the fact that only the left-handed part of the fields are included. To have a working example the quark doublet

$$\begin{pmatrix} u \\ d \end{pmatrix} \quad (8.20)$$

has the numbers ( $TC = 1, C = 3, EW = 2, Y = \frac{1}{6}$ ). Quarks do not carry Technicolor so they are singlets under TC. They form a triplet under color, doublet under EW and this doublet has hypercharge  $\frac{1}{6}$ .

One also adds right-handed electroweak singlets:

$$p_R \sim (N, 1, 1, \frac{1}{2}) \quad (8.21)$$

$$m_R \sim (N, 1, 1, -\frac{1}{2}) \quad (8.22)$$

From the hypercharge of the electroweak singlets we see that  $p$  and  $m$  have electric charge  $\pm\frac{1}{2}$ .

The Technicolor dynamics is just a scaled-up version of QCD with the technipion decay constant set to  $F_\pi = 246$  GeV. The symmetry will be spontaneously broken as in the toy model above. When the EW force is turned on, an approximate picture is that three technipions will be eaten by the  $Z$  and  $W^\pm$  and three pions will acquire mass. In reality it's a linear combination of technipion and pion states that get eaten or appear as physical pions.

$$|\text{eaten pion}\rangle = \frac{F_\pi |\text{technipion}\rangle + f_\pi |\text{QCD pion}\rangle}{\sqrt{F_\pi^2 + f_\pi^2}} \quad (8.23)$$

$$|\text{physical pion}\rangle = \frac{F_\pi |\text{QCD pion}\rangle - f_\pi |\text{technipion}\rangle}{\sqrt{F_\pi^2 + f_\pi^2}} \quad (8.24)$$

### 8.3 Beyond the minimal Technicolor model

---

Since  $F_\pi \gg f_\pi$ , technipions constitute the majority of the meson and QCD pions appear in the physical spectrum. Analogous to the toy model we get mass for the  $W^\pm$  and  $Z$ :

$$M_W = \frac{1}{2}gF_\pi \tag{8.25}$$

$$M_Z = \frac{gF_\pi}{2 \cos \theta_W} \tag{8.26}$$

With  $F_\pi = v = 246$  GeV, the  $W$  and  $Z$  bosons have the right mass. This is a nice way of generating the gauge boson masses, but now we must explain the quark and lepton masses. The minimal Technicolor scheme only introduces couplings between SM particles of the same chirality (i.e.  $\bar{u}_L$  couples to  $u_L$  and  $\bar{u}_R$  couples to  $u_R$ ). A mass term would be a mixture of right and left handed fields:

$$\bar{u}u = \bar{u}_L u_R + \bar{u}_R u_L \tag{8.27}$$

There are different approaches to giving the fermions their masses in Technicolor. A typical feature they have in common is that they all run into phenomenological problems of some kind. The phenomenological problems are highly model dependent and therefore also the ways of getting rid of them. One of these approaches is Extended Technicolor (ETC). We will focus on this and briefly its extension to Walking Technicolor.

### 8.3 Beyond the minimal Technicolor model

Discussing ETC, Walking TC and their associated particle spectrum is a rather technical one. A complete treatment is beyond the scope of this thesis. An attempt at a non-technical discussion is made. Hopefully, enough theoretical concepts will be introduced to understand the following points:

1. Roughly what ETC and walking TC are about
2. Some phenomenological problems these kinds of theories encounter
3. Some theoretical basis for the phenomenological signatures to be discussed in the following section

## 8. TECHNICOLOR

---

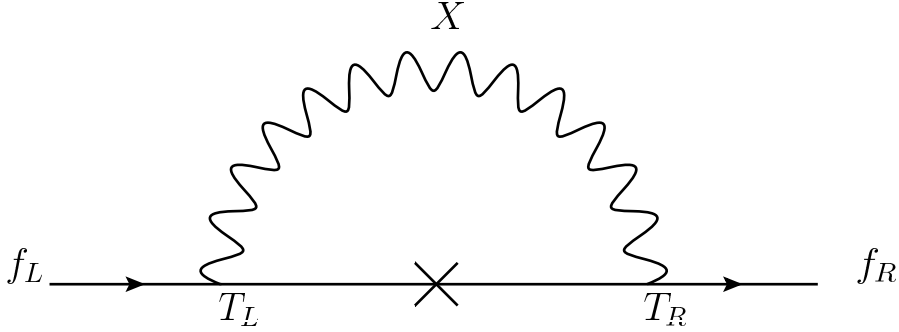


**Figure 8.5:** Fermion mass generated by a heavy ETC gauge boson  $X$

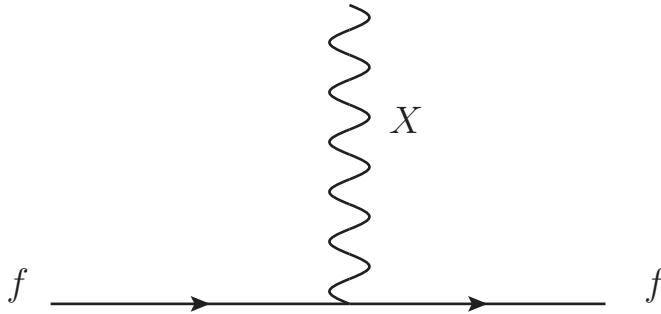


**Figure 8.6:** fermion-fermion couplings in ETC

### 8.3.1 Extended Technicolor

Throughout this subsection one should keep in mind that ETCs objective is giving fermions mass. In technicolor this mass is generated the technifermions. In ETC theories one extends the TC gauge sector in such a way that fermions can couple to technifermions. The way one does this it can be summarized as follows:

1. Embed  $G_{TC}$  in a larger gauge group  $G_{ETC}$ , symbolically represented by  $G_{TC} \subset G_{ETC}$
2. Break  $G_{ETC}$  to  $G_{TC}$  at the scale  $\Lambda_{ETC} > \Lambda_{TC} \sim 500$  GeV, symbolically represented by

$$G_{ETC} \xrightarrow{\Lambda_{ETC}} G_{TC} \times SU(3)_C \times SU(2)_L \times U(1)_Y$$

In general this enlargement of the gauge group gives couplings between fermion-fermion, technifermion-fermion and technifermion-technifermion as in Figures 8.6, 8.7 and 8.8. The technifermion-fermion coupling allows the fermion masses to be generated through

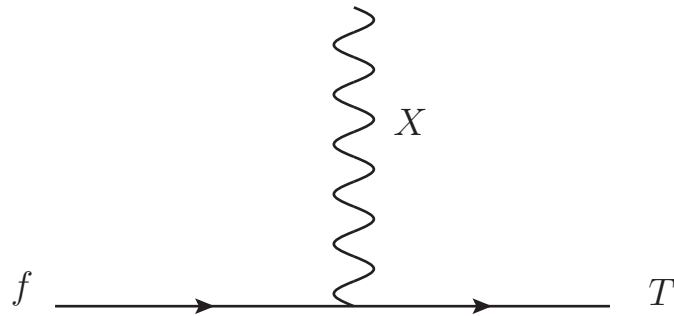


**Figure 8.7:** fermion-technifermion couplings in ETC

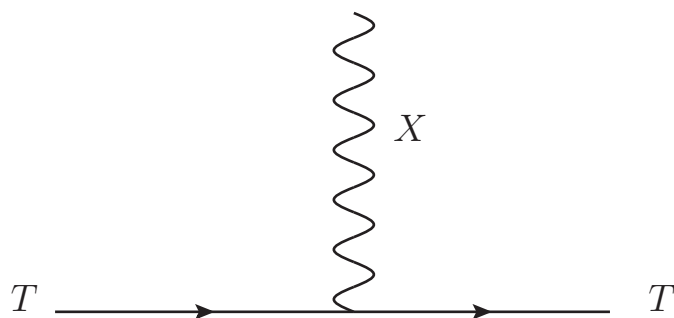


**Figure 8.8:** technifermion-technifermion couplings in ETC

## 8. TECHNICOLOR

---

radiative corrections shown in Figure 8.5. This diagram gives the fermion a mass given by[3]:

$$m_f \sim \frac{\langle \bar{T}T \rangle_{\Lambda_{ETC}}}{\Lambda_{ETC}^2} \quad (8.28)$$

$\langle \bar{T}T \rangle_{\Lambda_{ETC}}$  is the technifermion condensate. A naive estimate based on dimensional analysis gives:

$$\langle \bar{T}T \rangle_{\Lambda_{ETC}} \sim \Lambda_{TC}^3 \quad (8.29)$$

It's here that ETC runs into its first phenomenological troubles. The fermion-fermion couplings illustrated in Figure 8.6 introduce Flavour Changing Neutral Currents (FCNC). There are experimental restrictions on these FCNCs. An example is the well studied  $K_L$ ,  $K_S$  mesons, which provide one of the strongest constraints [3]. These mesons are linear combinations of the states  $\bar{d}s$  and  $\bar{s}d$  which are composed of strange and down quarks (and their anti particles). In the ETC scheme operators of the form

$$\frac{1}{\Lambda_{ETC}^2} \bar{s}d\bar{s}d \quad (8.30)$$

appear. These operators give diagrams such as 8.9. The difference in the mass of  $K_L$  and  $K_S$  gives the constraint:

$$\Lambda_{ETC} > 500 \text{ TeV} \quad (8.31)$$

Combining this constraint with (8.28) and  $\Lambda_{TC} \sim 500 \text{ GeV}$  leads to a fermion mass bound of  $m_f < \frac{1}{2}\text{MeV}$  (which is rather small compared to e.g. the top quark mass). The theories of Walking Technicolor and strong ETC are attempts to remedy this restriction. In the next subsection, we'll go through walking technicolor somewhat briefly.

### 8.3.2 Walking Technicolor

As we saw in (8.28), the fermion mass is proportional to the technifermion condensate. The quark-mass bound  $m_f < \frac{1}{2}\text{MeV}$  was estimated from dimensional analysis,

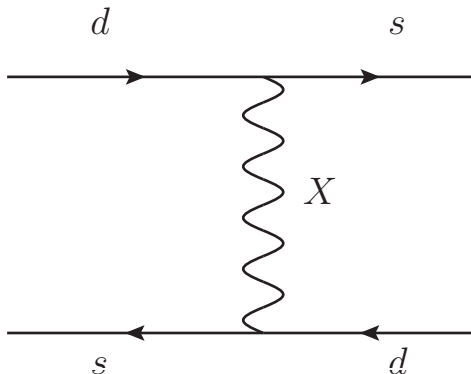


**Figure 8.9:** Example of flavour changing neutral currents in ETC,  $M_X \sim \Lambda_{ETC}$

$\langle \bar{T}T \rangle_{\Lambda_{ETC}} \sim \Lambda_{TC}^3$ . If one had a greater value for the technifermion condensate this bound could be changed. In the end the condensate will take the values[3]:

$$\langle \bar{T}T \rangle_{\Lambda_{ETC}} \sim \Lambda_{TC}^3 \left( \frac{\Lambda_{ETC}}{\Lambda_{TC}} \right)^\gamma \quad (8.32)$$

Here,  $\gamma$  is a real number with values between 0 and 2. Putting  $\gamma = 0$ , reproduces the estimate  $\langle \bar{T}T \rangle_{\Lambda_{ETC}} \sim \Lambda_{TC}^3$ . An approximate picture is that Walking Technicolor gives  $\gamma \approx 1$  and strong ETC theories  $\gamma \approx 2$ . This can produce fermion masses of the desired magnitude. As an example, consider  $\gamma = 1$ . Using  $\Lambda_{ETC} \sim 500$  TeV and  $\Lambda_{TC} \sim 500$  GeV results in an enhancement factor  $\frac{\Lambda_{ETC}}{\Lambda_{TC}} \sim 10^3$

To get a glimpse of why it's called walking Technicolor we will look at how the technifermion condensate is calculated. Using the diagram 8.5 together with the propagator approximation

$$\frac{-g^{\mu\nu} + \frac{p^\mu p^\nu}{M_X^2}}{M_X^2 - p^2 + i\epsilon} \longrightarrow \frac{-g^{\mu\nu}}{M_X^2} \quad (8.33)$$

results in a fermion mass of[3]:

$$m_f = \frac{g_{ETC}^2}{M_X^2} \frac{N}{4\pi^2} \int_0^{\Lambda_{ETC}^2} d^2 p^2 \frac{\Sigma(p^2)}{p^2 + \Sigma^2(p^2)} \quad (8.34)$$

Here,  $g_{ETC}$  is the ETC coupling at the scale  $\Lambda_{ETC}$ ,  $N$  the number of Technicolors and the upper limit of the integral is a UV cut-off energy. Comparing (8.34) with (8.28) we

## 8. TECHNICOLOR

---

can understand the convention of defining

$$\langle \bar{T}T \rangle_{\Lambda_{ETC}} = \frac{N}{4\pi^2} \int_0^{\Lambda_{ETC}^2} dp^2 p^2 \frac{\Sigma(p^2)}{p^2 + \Sigma^2(p^2)} \quad (8.35)$$

The function  $\Sigma(p^2)$  is important for the final value of the fermion mass. In particular its behaviour for large  $p$  influences the value of the condensate. For instance, if one assumes that  $\Sigma(0) \approx \Lambda_{TC}$  and that  $\Sigma(p^2)$  falls off as  $\frac{1}{p^2}$  or  $\frac{1}{p}$ , one reproduces (8.32) with  $\gamma = 0$  and  $\gamma \sim 1$  respectively [3]. The  $\frac{1}{p}$  result is, as alluded to earlier, what happens in walking Technicolor.

To get to the bottom of the walking in Walking Technicolor we have to investigate the function,  $\Sigma$ . This function may be estimated from what is called the Schwinger-Dyson equation. This equation involves an integral with a running coupling constant  $\alpha_{TC}(p^2)$ . The behaviour of  $\Sigma$  turns out to be sensitive to how the coupling changes for high-values of  $p$  (i.e.  $p > \Lambda_{TC}$ ). In QCD the coupling “runs” (i.e. decreases fast) above the QCD scale  $\Lambda_{QCD} \sim 200$  MeV and we get the  $\Sigma \sim \frac{1}{p^2}$  case with  $\gamma \approx 0$ . Walking Technicolour is the suggestion that the coupling “walks” (i.e. decreases more slowly) instead of “running”. This gives the  $\Sigma \sim \frac{1}{p}$  case and  $\gamma \approx 1$ .

Leaving this rather technical non-technical discussion of the walking coupling to more qualified men (and women), we proceed to pseudo-Goldstone bosons (PGB), which are candidates for observation in TC theories.

### 8.3.3 Pseudo-Goldstone bosons

In ETC theories one typically adds more than one technidoublet as is done in the minimal Technicolor doublet. When the chiral symmetry is spontaneously broken one gets more Goldstone bosons than are eaten. In the toy model, the symmetry breaking  $SU(2)_L \times SU(2)_R \rightarrow SU(2)_V$  were accompanied by  $2^2 - 1 = 3$  massless Goldstone bosons (MGB), which were eaten by the gauge bosons. Naively, if one has two doublets that break in the same fashion, we’ll have 6 MGBs out of which 3 will be eaten and 3 left. Massless Goldstone bosons are not observed so one does not want this in a theory. The resolution is that they appear as what is called pseudo-Goldstone bosons.

In the toy model and the minimal Technicolor model the MGBs that appear are massless only because the quarks are massless. When one generates fermion masses via ETC this is no longer true. A quark mass term explicitly breaks the chiral symmetry since it can be written:

$$\bar{\Psi}\Psi = \bar{\Psi}^L\Psi^R + \bar{\Psi}^R\Psi^L \quad (8.36)$$

As a result of this we get pseudo-Goldstone bosons. A familiar example of PGBs is the pions of ordinary QCD. We will not go into further detail concerning how they appear theoretically (through explicit chiral symmetry breaking), but instead state a way of thinking about them: A pseudo-Goldstone boson is associated with a chiral-symmetry breaking and appear in the physical spectrum as massive particles.

## 8.4 Phenomenology

Since there is no generally accepted version of ETC, we give the phenomenology of a minimal TC theory as presented in[3]. Here the TC group is taken to be  $SU(3)$ , this means that it is easy to list the phenomenological signatures as it is basically just a scaled up version of QCD. Of course there are some differences:

1. There is a scalar resonance at the TeV scale instead of the Higgs
2. The masses of the techniparticles are higher
3. They have techni-isospin instead of isospin

Even though such a model can not be a realistic one, it introduces enough particles for our sake. The ones we could be interested in are the analogues of the vectormesons, specifically the technirho ( $\rho_T$ ) could provide us with a spin-1 resonance of 200 GeV. In the above model this is not the case. Since it is just a scaled up version of QCD the mass of the rho is also scaled up, which gives about 3.5 TeV, this is too large for us. This could perhaps be adjusted to fit with our situation in some versions of Walking and Running Technicolor theories. For instance In [39], the recently reported bump in the Tevatron experiment was attributed to a  $\rho_T$  of mass 290 GeV decaying.

## 8. TECHNICOLOR

---

## Chapter 9

# Conclusion

In this thesis a hypothetical, experimental observation was analysed. The experimental observation concerned an unknown particle  $X$  of mass 200 GeV that decayed through the mode  $X \rightarrow ZZ \rightarrow 4l$ , which is also known as the “Higgs golden channel” for masses above 200 GeV. There was assumed to be an excess in the production cross section. The further analysis centered on how we could enhance the production cross section of two  $Z$ s, relative to the SM Higgs contribution, with beyond the Standard Model effects.

In chapter five we investigated the possibility that the particle  $X$  was a new, neutral gauge boson  $Z'$ . We calculated production cross sections for both  $Z'$  and  $ZZ$  production. The result was that experimental constraints seem to make enhancement difficult. With an overestimate on the  $Z'$  coupling to fermions in a ‘leptophobic’ scenario we could enhance the cross section to about the same order of magnitude as the SM Higgs.

In chapter six we looked at the possibility that the next to lightest Higgs of a 2HDM(II) could be the perpetrator. We took into account constraints from B physics on the charged sector and the LEP non-observation. The result was that enhancement of the production cross section seems feasible. The enhancement was most easily obtained through gluon fusion, with a top quark present in the loop diagram. Compared to the previous case of  $Z'$ , an order-of-magnitude enhancement is easier to accommodate. In chapters 7 and 8 a review of theoretical concepts and some phenomenological signatures were presented. Chapter 7 dealt with two extra-dimensional theories. ‘Large

## 9. CONCLUSION

---

extra dimensions' of Arkani-Hamed, Dimopoulos and Dvali and the Randall-Sundrum model. In particular, the treatment emphasized the theoretical foundations of the two models and their different characteristic phenomenological signature as regards the Graviton. Chapter 8 dealt with the theory of Technicolor. The treatment emphasized somewhat the development of theoretical concepts as the theory is highly technical. A small summary was also included on phenomenology.

# References

- [1] WAI-YEE KEUNG, IAN LOW, AND JING SHU. **On Decays of  $Z'$  into Two  $Z$  Bosons and the Landau-Yang Theorem.** *Phys. Rev. Lett.*, **101**:091802, 2008. 1, 42, 47, 58
- [2] GORDON KANE JOHN F. GUNION, HOWARD E. HABER AND SALLY DAWSON. *The Higgs Hunter's Guide*. ADDISON WESLEY, 2007. 1, 8, 66, 67
- [3] STEPHEN F. KING. **Dynamical electroweak symmetry breaking.** *Rept. Prog. Phys.*, **58**:263–310, 1995. 1, 94, 95, 96, 97, 98, 102, 103, 104, 105
- [4] NIMA ARKANI-HAMED, SAVAS DIMOPOULOS, AND G. R. DVALI. **The hierarchy problem and new dimensions at a millimeter.** *Phys. Lett.*, **B429**:263–272, 1998. 1, 85
- [5] LISA RANDALL AND RAMAN SUNDRUM. **A large mass hierarchy from a small extra dimension.** *Phys. Rev. Lett.*, **83**:3370–3373, 1999. 1, 86, 87, 89
- [6] F. MANDL AND G. SHAW. *Quantum Field Theory - Second Edition*. John Wiley and Sons, 2010. 3, 11, 17, 19, 27, 29, 62, 63
- [7] LONDON HIGH ENERGY PHYSICS GROUP, IMPERIAL COLLEGE. **Picture of Higgs branching ratio and Higgs potential.** <http://www.hep.ph.ic.ac.uk/cms/physics/higgs.html>. 5
- [8] GUIDO ALTARELLI AND MARTIN W. GRUNEWALD. **Precision electroweak tests of the standard model.** *Phys. Rept.*, **403-404**:189–201, 2004. 11, 27, 31, 32
- [9] ABDELHAK DJOUADI. **The Anatomy of electro-weak symmetry breaking. I: The Higgs boson in the standard model.** *Phys. Rept.*, **457**:1–216, 2008. 11, 27
- [10] J. BAEZ AND J. P. MUNIAN. *Gauge Fields, Knots and Gravity*. World Scientific, 2007. 14
- [11] GAUTAM BHATTACHARYYA. **A Pedagogical Review of Electroweak Symmetry Breaking Scenarios.** *Rept. Prog. Phys.*, **74**:026201, 2011. 27, 29, 30, 31, 32, 94
- [12] ABDUL WAHAB EL KAFFAS, WAFAA KHATER, ODD MAGNE OGREID, AND PER OSLAND. **Consistency of the Two Higgs Doublet Model and CP violation in top production at the LHC.** *Nucl. Phys.*, **B775**:45–77, 2007. 32, 65, 66, 68, 71, 72, 73, 74, 78

## REFERENCES

---

- [13] MICHAEL E. PESKIN AND TATSU TAKEUCHI. **A New constraint on a strongly interacting Higgs sector.** *Phys. Rev. Lett.*, **65**:964–967, 1990. 32
- [14] E. M. HENLEY AND A. GARCIA. *Subatomic Physics*. World Scientific, 2007. 35
- [15] V.D BARGER AND R.J.N PHILLIPS. *Collider Physics*. Addison-Wesley Pub. Co., Redwood City, Calif. :, 1987. 35, 37, 38
- [16] C. N. YANG. **Selection Rules for the Dematerialization of a Particle into Two Photons.** *Phys. Rev.*, **77**(2):242–245, Jan 1950. 42
- [17] G AAD ET AL. **The ATLAS Experiment at the CERN Large Hadron Collider.** *Journal of instrumentation*, 2008. 54
- [18] N. KAUER. % bf Narrow-width approximation limitations. *Physics Letters B*, **649**(5-6):413 – 416, 2007. 56
- [19] K NAKAMURA AND PARTICLE DATA GROUP. **Review of Particle Physics.** *Journal of Physics G: Nuclear and Particle Physics*, **37**(7A):075021, 2010. 57, 59, 62
- [20] SM WANG. **Gauge Couplings at the LHC.** Technical Report ATL-PHYS-PROC-2010-094, CERN, Geneva, Oct 2010. 58
- [21] MARCELA S. CARENA, ALEJANDRO DALEO, BOGDAN A. DOBRESCU, AND TIMOTHY M. P. TAIT. **Z-prime gauge bosons at the Tevatron.** *Phys. Rev.*, **D70**:093009, 2004. 59
- [22] THOMAS APPELQUIST, BOGDAN A. DOBRESCU, AND ADAM R. HOPPER. **Nonexotic neutral gauge bosons.** *Phys. Rev.*, **D68**:035012, 2003. 59, 60
- [23] HOWARD GEORGI AND SHELDON L. GLASHOW. **Decays of a leptophobic gauge boson.** *Physics Letters B*, **387**(2):341 – 345, 1996. 60
- [24] MATTHEW R. BUCKLEY, DAN HOOPER, JOACHIM KOPP, AND ETHAN NEIL. **Light Z' Bosons at the Tevatron.** 2011. 60
- [25] S. DITTMAYER ET AL. **Handbook of LHC Higgs Cross Sections: 1. Inclusive Observables.** 2011. 62, 63, 64
- [26] JOHN F. GUNION AND HOWARD E. HABER. **The CP-conserving two-Higgs-doublet model: The approach to the decoupling limit.** *Phys. Rev.*, **D67**:075019, 2003. 64, 65, 66
- [27] SACHA DAVIDSON AND HOWARD E. HABER. **Basis-independent methods for the two-Higgs-doublet model.** *Phys. Rev.*, **D72**:035004, 2005. 65, 66, 67, 68

- 
- [28] AARON K. GRANT. **The Heavy top quark in the two Higgs doublet model.** *Phys. Rev.*, **D51**:207–217, 1995. 67, 73, 79
- [29] WAFAA KHATER AND PER OSLAND. **CP violation in top quark production at the LHC and Two-Higgs-Doublet Models.** 2003. 68, 71
- [30] ABDUL WAHAB EL KAFFAS, PER OSLAND, AND ODD MAGNE OGREID. **Constraining the two-Higgs-doublet-model parameter space.** *Phys. Rev. D*, **76**(9):095001, Nov 2007. 71, 72
- [31] W KILIAN, M KRAMER, AND P. M. ZERWAS. **Higgs-strahlung and  $WW$  fusion in  $e^+e^-$  collisions.** *Phys. Lett.*, **B373**:135–140, 1996. 73
- [32] V. H. SATHEESH KUMAR AND P. K. SURESH. **Gravitons in Kaluza-Klein theory.** 2006. 82
- [33] M. SHIFMAN. **LARGE EXTRA DIMENSIONS: Becoming acquainted with an alternative paradigm.** *Int. J. Mod. Phys.*, **A25**:199–225, 2010. 84
- [34] MARC BESANCON. **Models and signatures of extra dimensions at the LHC.** 2010. 88, 89, 90
- [35] E. W. DVERGSNES, P. OSLAND, A. A. PANKOV, AND N. PAVER. **Center edge asymmetry at hadron colliders.** *Phys. Rev.*, **D69**:115001, 2004. 89, 90
- [36] VARDAN KHACHATRYAN ET AL. **Search for Microscopic Black Hole Signatures at the Large Hadron Collider.** *Phys. Lett.*, **B697**:434–453, 2011. 90
- [37] J. R. ANDERSEN ET AL. **Discovering Technicolor.** 2011. 94
- [38] LEONARD SUSSKIND. **Dynamics of spontaneous symmetry breaking in the Weinberg-Salam theory.** *Phys. Rev. D*, **20**(10):2619–2625, Nov 1979. 94
- [39] ESTIA J. EICHTEN, KENNETH LANE, AND ADAM MARTIN. **Technicolor at the Tevatron.** 2011. 105